

**Numerical studies on prototype CHS and open sections  
welded joints for steel truss girders with the use of laser  
cutting technology**

**João Pedro Mineiro Serralha**

Thesis to obtain the Master of Science Degree in  
**Civil Engineering**

Supervisors

Professor Jorge Miguel Silveira Filipe Mascarenhas Proença

Professor Luís Manuel Calado de Oliveira Martins

**Examination Committee**

Chairperson: Professor António Manuel Figueiredo Pinto da Costa

Supervisor: Professor Jorge Miguel Silveira Filipe Mascarenhas Proença

Member of the Committee: Professor Pedro António Martins Mendes

**October 2017**



# Acknowledgements

I would like to start by expressing my deep and sincere gratitude to my thesis' supervisors, Professor Jorge Proença and Luís Calado for the opportunity to be part of LASTEICON project, for trusting in my work until the last minute, for their incentive and availability shown during all year. This work revealed to be really challenging during some periods and one of the most intense experiences in my life, which was fundamental for my development as a professional and as a human being. Additionally, thank them for giving me the opportunity to join one of the LASTEICON project meetings, in Dusseldorf, which turned to be a completely new experience to me and where I had the possibility to see and learn from very interesting people in this field.

For the big support with SolidWorks software I would like to thank Professor Luís Sousa, from the Mechanical Engineering Department of Instituto Superior Técnico, who was always available to help me despite not being part of the project.

To engineer Mário Arruda, thank for all the help with Abaqus software and FEM modelling.

In general, I thank to all my friends and family who have been close to me during this present year, for their friendship and support in many ways and at many levels. To my close friends Manuel Ferreira and Madalena Silva as they always gave enthusiasm and strength to move forward. Concerning the development of the present work, I thank João Petinga Almeida for his constant interest and patience showed during the years spent together in the university.

My most expressive thank goes to my parents, for all the unconditional support and understanding, to whom I owe the person I am today. For this and much more, I dedicate them this dissertation.



# Abstract

In the era of technology, construction industry has changed very little in the past few years and, when compared to others, it is performing poorly in areas like project delivery, life cycle performance and sustainability. In order to achieve more efficient and optimized solutions in steel structural construction, innovative design connections on truss girders pretend to be developed making use of laser cutting advanced technology. These connections consist of performing laser cutting slots in the chord's faces so that brace members can pass through and be welded on both top and bottom faces.

The structural performance of these connections was assessed based on the results provided by a finite element numerical analysis in two different types of truss girders specimens. Several innovative geometries were studied considering the powerful capabilities of laser cutting and different parameters were tested to prove the viability of this technology. Results showed that these joints are able to minimize deformations and stresses' concentration as well as to reduce the design dimensions with no losses in performance.

Although the main focus is on the outstanding structural and architectural properties of hollow structural section profiles, the additional study of open section joints showed the extendibility potential of this technology in other applications.

**Keywords:** laser cutting, hollow structural sections, connections, truss girders, steel detailing, numerical modelling



# Resumo

Numa era em que a tecnologia tem revolucionado o nosso dia-a-dia, é de constatar o pouco avanço que a indústria da construção tem tido, comparativamente com outras indústrias, em áreas como gestão de projeto, sustentabilidade e ciclo de vida útil. De forma a desenvolver este sector, foi proposta a possibilidade de estudar a influência da tecnologia de corte laser na eficiência, otimização e conceção de novos tipos de ligações de estruturas metálicas, mais especificamente em vigas-treliça. Estas ligações consistem em criar aberturas nos perfis das respetivas cordas, com corte laser, que permitam a passagem dos perfis de contraventamento pelo seu interior de modo a poderem ser soldados em ambos os topos da corda.

Para tal, foi realizado um estudo sobre o comportamento estrutural das ligações através da análise numérica de dois tipos de treliças, nomeadamente Pratt e Warren. Esta análise foi feita num programa de elementos finitos (Abaqus). De entre as diferentes ligações criadas, um conjunto de parâmetros foi escolhido de modo a poder comparar o seu comportamento e desta forma provar a viabilidade desta tecnologia. Os resultados obtidos demonstraram que as novas ligações testadas permitem diminuir as deformações e tensões criadas nestes elementos assim como diminuir a secção das mesmas, sem causar perdas de resistência.

Por fim, apesar de este projeto se focar essencialmente em ligações tubulares devido às suas inúmeras propriedades arquitetónicas e estruturais, a aplicação desta tecnologia na conceção e posterior estudo de secções abertas permitiu provar que existem mais áreas com potencialidade para serem investigadas.

**Palavras-chave:** Corte laser, secções fechadas, ligações, treliças, modelação numérica





# Content

- Acknowledgements..... iii**
- Abstract..... v**
- Resumo ..... vii**
- Content..... ix**
- List of Tables ..... xi**
- List of Figures..... xiii**
- List of Symbols..... xvii**
- List of Acronyms ..... xix**
- 1. Introduction..... 1**
  - 1.1. Scope ..... 1
  - 1.2. Objectives and structure of the dissertation ..... 2
- 2. Laser cutting technology in steel truss girders joints..... 5**
  - 2.1. Overview..... 5
  - 2.2. Laser cutting process ..... 5
  - 2.3. Laser cutting in steel construction ..... 9
    - 2.3.1. Fabrication and full-scale drawings ..... 9
    - 2.3.2. Sustainability and economical aspects..... 10
  - 2.4. Hollow structural sections..... 12
    - 2.4.1. Truss girders..... 12
    - 2.4.2. Hollow structural section profiles ..... 13
    - 2.4.3. Hollow structural section joints ..... 14
  - 2.5. State-of-the-art ..... 18
    - 2.5.1. Previous developments in the research of numerical analysis ..... 18
    - 2.5.2. Previous developments related to LASTEICON project..... 20
  - 2.6. Fabrication tolerances ..... 23
- 3. Truss specimens analysed ..... 25**
  - 3.1. Introduction..... 25
  - 3.2. Description of truss specimens ..... 25
  - 3.3. Description of joints ..... 27
- 4. Numerical analyses ..... 31**
  - 4.1. Introduction..... 31
  - 4.2. Welding simulation ..... 31
  - 4.3. Numerical Modelling..... 32
    - 4.3.1. Material Properties..... 32
    - 4.3.2. Geometry of the truss specimens..... 34
    - 4.3.3. Model assembly..... 38

4.3.4.	Loading and boundary conditions.....	39
4.3.5.	Mesh definition.....	40
4.3.6.	Type of analyses.....	42
4.3.5.1.	First Analysis Approach .....	42
4.3.5.2.	Sensitivity analysis.....	43
4.3.5.3.	Design of truss specimens.....	43
4.3.5.4.	Analysis of joints .....	44
<b>5.</b>	<b>Numerical results.....</b>	<b>47</b>
5.1.	Analysis of the results .....	47
5.1.1.	First analysis approach.....	47
5.1.2.	Sensitivity analysis.....	48
5.1.3.	Design of truss specimens .....	48
5.1.4.	Results of numerical model on joints.....	51
5.1.4.1.	Substructure type I.....	51
5.1.4.2.	Substructure Type II.....	56
<b>6.</b>	<b>Parametric analyses .....</b>	<b>63</b>
<b>7.</b>	<b>Conclusions and future developments.....</b>	<b>69</b>
7.1.	General conclusions .....	69
7.2.	Numerical tests.....	70
7.3.	Future developments.....	70
	<b>Bibliography .....</b>	<b>73</b>
<b>A.</b>	<b>Appendix .....</b>	<b>75</b>

# List of Tables

Table 2.1: Comparison between cutting methods..... 6

Table 2.2: Type of joint model – classification. .... 14

Table 4.1: Abaqus software units. .... 34

Table A.1: Design of axial resistance of welded joints between CHS brace members and CHS chords.  
..... 75

Table A.2: Range of validity for welded joints between CHS brace members and CHS chords. .... 75

Table A.3: Description of numerical tests performed for CHS and Open section profiles. .... 76

Table A.4: Truss type I – profile dimensions and number of tests. .... 76

Table A.5: Failure modes for joints between CHS members. .... 77



# List of Figures

Figure 2.1: Laser cutting process detail of a circular hole.....	6
Figure 2.2: Laser cutting process detail of a CHS profile.....	6
Figure 2.3: Specimens worked exploiting different technologies: a) plasma; b) laser; c) drill and saw. .....	6
Figure 2.4: Schematic image of the laser cutting mechanism. ....	7
Figure 2.5: Variation of surface roughness with cutting speed under different laser powers. ....	8
Figure 2.6: Heat affected zone analysis on a laser cut surface, divided in three zones through the thickness of the cutting kerf. ....	8
Figure 2.7: Example of a hollow section joint materialised with stiffeners and bolting. ....	9
Figure 2.8: Steelwork made with CHS elements processed by laser cutting technique.....	9
Figure 2.9: Breakdown of costs of the steel frame of a typical multi-storey commercial building....	11
Figure 2.10: Scheme of the benefits of LASTEICON during the life cycle of a building project. ....	11
Figure 2.11: Comparison between spatial trusses with open and circular sections to show the aesthetical advantage of tubular sections. ....	13
Figure 2.12: Classification of joints by rotational stiffness. ....	15
Figure 2.13: Detail of model connection for lattice girders.....	15
Figure 2.14: Failure modes. ....	17
Figure 2.15: Truss modelling detail with beam and shell elements. ....	19
Figure 2.16: Diagram force vs relative displacement for different models.....	20
Figure 2.17: Traditional and pre-cut method for CHS joints.....	20
Figure 2.18: Ways of connecting the weld to the chord and diagonal. ....	21
Figure 2.19: Types of laser cuts. 1) perpendicular to its axis; 2) parallel to the diagonal; 3) a combination of both. ....	21
Figure 2.20: Joint detail made through laser cutting. ....	22
Figure 2.21: Deformation parameters of a K-joint.....	22
Figure 2.22: Half section view of the analysed joint; Embedded RHS brace member going inside the RHS chord. ....	23
Figure 2.23: LASTEICON I-beam-to-CHS-column joint specimen. ....	23
Figure 3.1: Substructure type I - Pratt truss. ....	26
Figure 3.2: Substructure type II - Warren truss.....	26
Figure 3.3: Traditional N-joint, substructure type I (without eccentricity). ....	27
Figure 3.4: Traditional K-joint, substructure type II (without eccentricity). ....	27
Figure 3.5: Joint New_1 (embedded vertical), substructure type I.....	28
Figure 3.6: Joint New_2 (embedded diagonal), substructure type I. ....	28
Figure 3.7: Different views from the CHS Joint New_3, substructure type I.....	28
Figure 3.8: Joint New_1, substructure type II.....	29
Figure 3.9: Joint New_2, substructure type II.....	29
Figure 3.10: Joint New_3, substructure type II.....	29

Figure 3.11: Traditional open section joint, substructure I. ....	29
Figure 3.12: New Open Section Joint, substructure type I. ....	29
Figure 3.13: Traditional open section joint, substructure type II. ....	30
Figure 3.14: New open section joint, substructure type II. ....	30
Figure 4.1: Welding of a tubular connection. ....	32
Figure 4.2: Steel material properties. ....	33
Figure 4.3: $\sigma - \epsilon$ diagram. ....	33
Figure 4.4: CHS substructure type I. ....	34
Figure 4.5: CHS substructure type II. ....	35
Figure 4.6: OPEN section substructure type I. ....	35
Figure 4.7: OPEN section substructure type II. ....	35
Figure 4.8: Open section bracing members detail. ....	36
Figure 4.9: Beam element profile creation. ....	36
Figure 4.10: Design sections geometry. ....	36
Figure 4.11: Spaced models composed by beam and solid elements. ....	37
Figure 4.12: Forces directions of the analysed joints, for each truss specimen. ....	37
Figure 4.13: Beam OPEN section orientation of substructure type I. ....	38
Figure 4.14: Beam OPEN section orientation of substructure type II. ....	38
Figure 4.15: Kinematic coupling constraint between beam's node and joint's surface nodes. ....	39
Figure 4.16: Boundary conditions and action load. ....	39
Figure 4.17: Detail of mesh arrangement with tetrahedral elements. ....	41
Figure 4.18: Detail of mesh arrangement with hexahedral elements. ....	41
Figure 4.19: Truss girder with 8m span. ....	42
Figure 4.20: Two types of simplified models for joints analyses. ....	42
Figure 4.21: Simplified T-joint solid model used for sensitivity analyses. ....	43
Figure 4.22: Calculation of vertical deformation on chord's face for N and K-joints. ....	45
Figure 4.23: Calculation of brace members deformation for N and K-joints. ....	45
Figure 5.1: Von Mises stresses on N-joints, through a simplified model analysis. ....	47
Figure 5.2: Comparison between coupling constraints. ....	48
Figure 5.3: Load – displacement, CHS substructure type I. ....	49
Figure 5.4: Load – displacement, OPEN section substructure type I. ....	49
Figure 5.5: Load – displacement, CHS substructure type II. ....	49
Figure 5.6: Load – displacement, OPEN section substructure type II. ....	50
Figure 5.7: Von Mises stresses on deformed substructure type I. ....	50
Figure 5.8: Von Mises stresses on deformed substructure type II. ....	50
Figure 5.9: Global behaviour of CHS models - substructure type I. ....	51
Figure 5.10: Global behaviour of OPEN section models - substructure type I. ....	51
Figure 5.11: Chord surface deformation on CHS N-joints (A). ....	52
Figure 5.12: Chord surface deformation on CHS N-joints (B). ....	52
Figure 5.13: Effective plastic strain on traditional connection (A), truss type I. ....	53

Figure 5.14: Vertical brace deformation of CHS N-joints (A & B). .....	54
Figure 5.15: Von Mises stresses on CHS N-joints (A). .....	54
Figure 5.16: Von Mises stresses on OPEN section N-joints (A). .....	55
Figure 5.17: Vertical deformation of the upper flange of OPEN sections N-joints (A & B). .....	55
Figure 5.18: Vertical brace deformation of OPEN sections N-joints (A & B). .....	56
Figure 5.19: Global behaviour of CHS models – substructure type II.....	56
Figure 5.20: Rotation deformation of CHS truss specimen type II.....	57
Figure 5.21: Global behaviour of OPEN section models - substructure type II. ....	57
Figure 5.22: Lateral displacements variation on CHS K-joints (z-direction). .....	58
Figure 5.23: Lateral expansion deformation on chord's face of CHS K-joints (A & B).....	58
Figure 5.24: Lateral tightening deformation on chord's face for CHS K-joints (A & B). .....	59
Figure 5.25: Vertical distortion in the upper flange of the chord for OPEN section K-joints (A & B).60	
Figure 5.26: Longitudinal deformation in diagonal members for OPEN section K-joints (A & B). ...	60
Figure 5.27: Lateral expansion of chord's face on CHS connection (A), for trusses type I & II. ....	61
Figure 5.28: Vertical distortion in the upper flange of the chord for OPEN section connection (A), truss type I & II.....	61
Figure 6.1: Global deformation of CHS profiles for different thicknesses, truss type I. ....	63
Figure 6.2: Global behaviour of CHS profiles for different thicknesses, truss type II.....	64
Figure 6.3: Lateral displacements in CHS N-joint (A) with 4mm thickness, truss type I. ....	64
Figure 6.4: Lateral displacements in CHS N-joint (A) with 6,3mm thickness, truss type I. ....	64
Figure 6.5: Vertical chord surface deformation on CHS N-joints (connection A) for both chord thicknesses, truss type I. ....	65
Figure 6.6: Vertical chord deformation on CHS N-joints (connection B) for both chord thicknesses, truss type I. ....	66
Figure 6.7: Displacement diagram “New_1 (4mm)” (connection A), truss type II. ....	66
Figure 6.8: Displacement diagram “New_3 (4mm)” (connection A), truss type II. ....	66
Figure 6.9: Lateral tightening deformation of CHS K-joints (connection A) for different chord thicknesses, truss type II. ....	67
Figure 6.10: Lateral expansion of chord's face on CHS K-joints (connection A), for truss type II. ...	68
Figure A.1: Detail to understand the compatibility in the positioning of angle profiles. ....	79
Figure A.2: Deformed shape of a CHS T-joint without external stiffeners. ....	79
Figure A.3: Von Mises stresses for OPEN section K-joints, truss type II.....	80
Figure A.4: Von Mises Stresses for CHS N-joints with 4mm chord thickness (region under the compression brace), truss type I. ....	81
Figure A.5: Von Mises stresses for CHS K-joints with 4mm chord thickness (region under diagonal tension member), truss type II.....	82
Figure A.6: Von Mises Stresses for CHS K-joints with 4mm chord thickness (region under the compression brace), truss type II. ....	83





# List of Symbols

## Chapter 2

$d_1$  - brace diameter

$d_0$  - chord diameter

$l_0$  - chord length

$l_1$  - brace length

$t_0$  - chord wall thickness

$t_1$  - brace wall thickness

$\alpha$  - chord length parameter  $2l_0/d_0$

$\beta$  - diameter ratio between brace and the chord  $d_1/d_0$

$\gamma$  - half-diameter to thickness ratio of the chord  $d_0/(2t_0)$

$\tau$  - brace wall-to-chord wall thickness ratio  $t_1/t_0$

$N_{Rd \text{ PRECUT}}$  – failure load of the pre-cut joint

$N_{Rd \text{ Traditional}}$  – failure load of the traditional joint

$f(p)$  – reduction factor formula

## Chapter 3

$f_u$  - ultimate tensile strength

$f_y$  – yield strength

## Chapter 4

$I_{xx}$  – moment of inertia in the x-direction

$I_{yy}$  – moment of inertia in the y-direction

$A$  – section area

$x_c$  – x position of the centre of mass

$y_c$  – y position of the centre of mass

$\epsilon_y$  – yield strain

$\epsilon_u$  – ultimate strain

$\nu$  – poisson's ratio



## List of Acronyms

**CHS** – Circular Hollow Sections

**FE** – Finite Element

**FEA** – Finite Element Analysis

**FEM** – Finite Element Method

**LASTEICON** – Laser Technology for Innovative Connections in Steel Construction

**LCT** – Laser Cutting Technology

**RFCS** – Research Fund for Coal and Steel

**RHS** – Rectangular Hollow Section

**HAZ** – Heat Affected Zone

**HSS** – Hollow Structural Section

**SW** - SolidWorks



# 1. Introduction

## 1.1. Scope

Adapting on shaping the future of construction, the importance of innovating and adopting formal processes, with rigor and consistency, getting knowledge from other industries and having a less conservative company culture are aspects that construction industry must establish to keep up with the labour productivity improvement of other industries (BUEHLER 2017). The possibility of creating standardized and prefabricated components with automatic and efficient processes in a smart life-cycle assessment pretends to transform the construction industry. However, the drivers of change are several and demanding (technique, economy, sustainability, society, politics, regulation, etc).

The LASTEICON project comes hand to hand with this purpose by adopting laser cutting technology (LCT), used already in other industries (e.g. automobile industry), to improve the quality and performance of steel structures, with emphasis on hollow structural sections' (HSS) connections. The use of HSS in steel construction is much smaller when compared with the use of open structural sections. In fact, structures composed by circular hollow sections (CHS) have much more complex detailing, more fabrication and erection requirements and more steelwork in terms of connections, resulting in higher global costs.

Therefore, taking advantage of the developed laser cutting technology, the innovative project called LASTEICON – Laser Technology for Innovative Connections in Steel Construction, appeared to solve this issue and be the key turning point in the market position of hollow structural sections. The major intention is to promote these sections as an industry standard approach in building frames, by simplifying joint solutions with emphasis in the steel connection type I-beam-to-CHS-column. Additionally, an extra study of LCT application in other structural systems, in particular truss girders, pretends to demonstrate the extendibility and potential of this technology (CASTIGLIONI, et al. 2015).

The advantages of this type of technology are well known for a long time but its applications in the construction industry are still reduced. In fact, the use of laser cutting on structural joints' fabrication might lead to the possibility of designing new connection's configurations.

Included in the Europe 2020 strategy for the construction sector, this project focuses mainly on smart and sustainable growth with green and competitive economy. LASTEICON investigations aim to achieve:

- High precision, increased quality and reduced costs of joint fabrication
- High structural performance
- Increased reliability
- Energy efficient and sustainable fabrication process

- Eco-friendly joint fabrication
- Safer workplace
- Contribution to Eurocodes, with new connection types
- Better market position for hollow sections.

The LASTEICON project is carried out with the financial grant of the Research Fund for Coal and Steel of the European Commission (RFCS-2015-709807). With a prospect duration of 42 months, it is formed by a consortium which covers different expertise areas from five EU countries. The group is composed by five research centres, a design office specialized in steel and composite structural design, a world-wide company specialised in the production of laser cutting machines, a steel construction company with more than 50 years of experience in the sector and one of the largest tubular solution provider of the world, in a total of 9 partners:

Participant no.1: RWTH Aachen, Germany

Participant no.2: Università di Pisa (UNIFI), Italy

Participant no.3: Universiteit Hasselt, Belgium

Participant no.4: Instituto Superior Técnico (IST), Portugal

Participant no.5: INSA Rennes, France

Participant no.6: FINCON CONSULTING ITALIA SRL, Italy

Participant no.7: ADIGE-SYS SPA, Italy

Participant no.8: OCAM SRL + Officina Carpenteria Metallica, Italy

Participant no.9: Vallourec Deutschland GmbH (VALL), Germany

## **1.2. Objectives and structure of the dissertation**

The present dissertation aims at presenting the research undertaken on steel truss' joints, fabricated making use of laser cutting technology, and to study its structural performance based on the analysis of the results provided by a refined analytical model developed with a finite element software (ABAQUS). The results taken will represent the basis to design truss specimens and to perform a sensitivity analysis to assess the most influencing parameters.

Additionally, it is pretended that this work can be a benchmark analysis to define details and suggestions for further numerical studies on these types of joints. In conclusion, the main objectives of this dissertation can be summed up in the following points:

- Design of new joints configurations
- Execution and analysis with numerical models using Finite Element Method (FEM) software
- Sensitivity and parametric analyses on the studied joints

## 1.2. Objectives and structure of the dissertation

Regarding the structure of this document, it is organised in 7 chapters, as follows.

The present chapter (Chapter 1) begins to present an overview of the LASTEICON project as well as the scope and objectives of this dissertation. Additionally, it summarily describes the structure of the document and the content of each chapter.

In Chapter 2, an introduction to laser technology is firstly done to explain its process, advantages and particularities. Then, an introduction to the design of truss girders and hollow section' connections is performed, in terms of their characteristics, behaviour and normative guidelines. Finally, the most relevant work done on this field is presented in the form of a state-of-the-art literature review.

In Chapter 3, presents the description of the type of truss specimens studied and the geometry detail of the innovative designed connections.

The methodology used to perform numerical analyses is made in Chapter 4, together with the description of all the considered assumptions to create the simplified models. Additionally, the types of analyses made are specified along with the analyses parameters used on numerical models' simulations.

In Chapter 5, the numerical results obtained from models' simulations are presented as well as drafting explanations and interpretation of the results. Additionally, the most influent parameters on these investigation field are identified.

From the results and main conclusions drafted from numerical studies, a parametric analysis will be performed in Chapter 6 where the influence of that parameter in the behaviour of truss specimens will be considered.

Finally, Chapter 7 presents the main conclusions achieved based on the investigations undertaken, a discussion about this work and some recommendations for future developments on the project.





## 2. Laser cutting technology in steel truss girders joints

### 2.1. Overview

The existing market around the fabrication of steel truss girders is already considerably experienced and advanced, where several solutions can be found to solve most structural challenges. However, much of these solutions have been based on the application of external stiffeners such as plates and rings and no extensive changes were made on the types of joints used. Concerning the welded connections, several similarities are found between failure modes and mostly due to important factors as the quality of the welding metal and the execution process. In this way, by focusing on these aspects, better structural behaviour could be achieved resulting in a reduction on costs and external stiffeners.

Despite the complexity of laser cutting, the progress in fields like automation and modelling software allowed the implementation of this technology into the fabrication of steel structural connections. This chapter will focus mainly on hollow structural sections, following the project goal of creating innovative joint's typologies making use of the potential of technology and those profile sections.

### 2.2. Laser cutting process

The activity of fabrication and cutting represents a big portion of steel industry and moreover of steel construction. The metal cutting methods existing today can be divided into three major categories: mechanical, thermal and chemical. Mechanical cutting covers all the traditional techniques using saw, shear, abrasive water jet, etc., whereas thermal and chemical correspond to techniques as the oxy-fuel (chemical), plasma and laser cut (thermal). There is still an extra technique, which combines thermal and chemical methods, where plasma and laser cutting techniques use an assisting gas. The non-conventional methods represent a more streamlined technique as there is no contact between the device and the material, which reduces the chance of contamination and marking (IVARSON, POWELL and SILTANEN 2015).

Laser cutting technology process (Figure 2.1) is a well-established profiling method in manufacturing industry with many applications (cutting, welding, drilling, heat treatments, and engraving). A variety of materials, from wood to super alloys, can be cut through this process although it is more efficient for small thickness materials comparing with other non-conventional techniques (Figure 2.2). According to (BURSI, et al. 2017), "In agreement with the EN ISO 9010 standard (CEN, EN ISO 9013:2002 Thermal Cutting. Classification of Thermal Cuts. Geometrical Product Specification and Quality Tolerances, 2002) the high-quality surface in terms of angularity tolerance, mean height and the great precision and possibility to process 3D geometries render the laser cutting an appealing technique for steel structures with complex geometries."

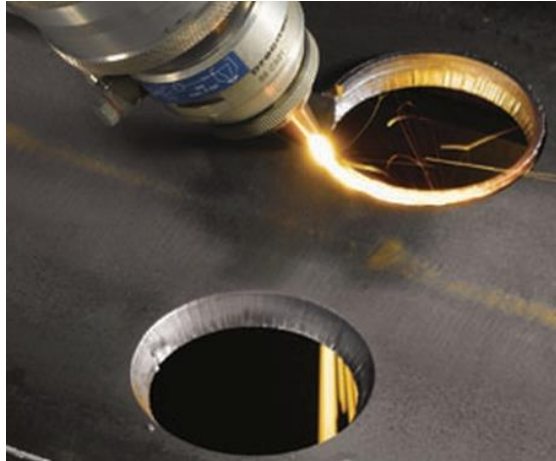


Figure 2.1: Laser cutting process detail of a circular hole (LASTEICON 2016).



Figure 2.2: Laser cutting process detail of a CHS profile (CASTIGLIONI, et al. 2015).

It is possible to find a lot of research on this field because laser machining offers an attractive alternative among all but also due to the several parameters that influence the cutting process. In Figure 2.3, excepting to plasma cut solution (a) which presents the worst result, it is possible to observe that the precision of the hole obtained by means of the laser technology (b) is comparable with the one performed by drill (c), however, with considerable time savings. In addition, Table 2.1 compares the characteristics of different cutting techniques for parameters such as precision, noise, cleaning process and initial investment.

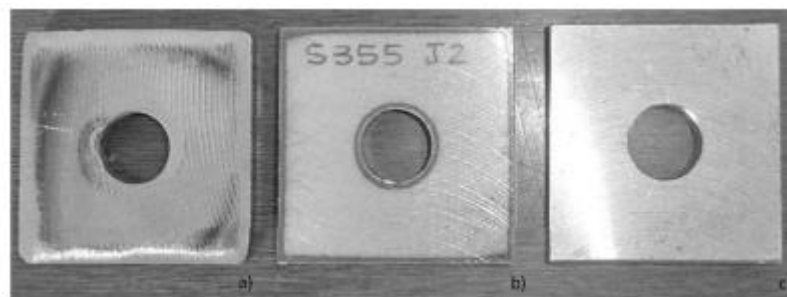


Figure 2.3: Specimens worked exploiting different technologies: a) plasma; b) laser; c) drill and saw (ZANON, et al. 2014).

Table 2.1: Comparison between cutting methods (CASTIGLIONI, et al. 2015).

	Laser CO2	Water Jet	Plasma	Flame
<b>Precision (mm)</b>	0.05	0.2	0.5	0.75
<b>Noise, pollution and danger</b>	Very low	Unusually high	Medium	Low
<b>Machine cleaning due to process</b>	Low	High	Medium	Medium
<b>Initial capital investment (1000 US \$)</b>	300	300+	120+	200-500

The laser cutting process can be divided into four different cutting mechanisms: fusion cutting, oxidation cutting, chemical degradation and vaporization. The cut is executed by a powerful laser beam through the melting of the material. Mentioning (IVARSON, POWELL and SILTANEN 2015), “the heat generated by the oxidation of iron contributes approximately half of the energy input to the cut zone, and the laser supplies the remaining half. The cutting process can be described as a laser initiated oxidation reaction the products of which are ejected from the cut zone by the incident gas jet.”. By using this assisting pressurized jet gas (normally CO<sub>2</sub>), the molten oxides produced in the cut zone do not adhere to the surrounding solid steel and therefore a clean-cut edge is generated. The following Figure 2.4 shows a schematic image describing this cutting process.

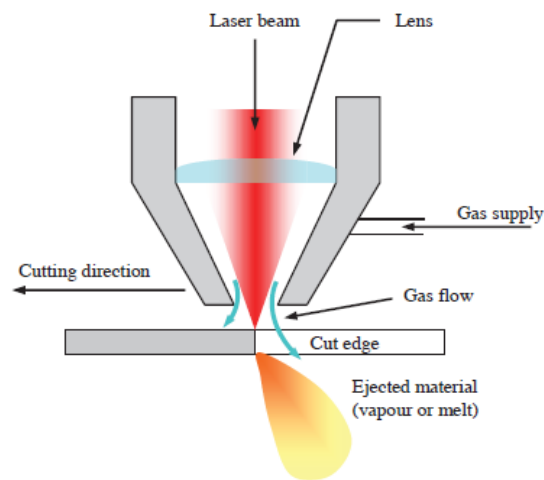


Figure 2.4: Schematic image of the laser cutting mechanism (IVARSON, POWELL and SILTANEN 2015).

To take full advantages and benefits from this technology and obtain an optimal cut surface in terms of quality and productivity, the appropriate parameters must be chosen, such as: workpiece conditions and characteristics (material properties, geometry, thickness), cutting speed, laser power, assist gas pressure and kerf width. According to (MADIĆ, et al. 2017), “the main difficulty is the fact that optimal combination of laser cutting parameter values for one performance characteristic is not even near optimal for other performance characteristics. Therefore, determination of laser cutting process conditions for multi-performance (multi-criteria) optimization is of prime importance.”.

The main phenomena to take place on laser cutting surfaces are: surface roughness, heat affected zone (HAZ), surface striation and residual stresses. Starting by surface roughness, Figure 2.5 shows how the parameters “cutting speed” and “laser power” influence this phenomenon and how an optimal point can be achieved.

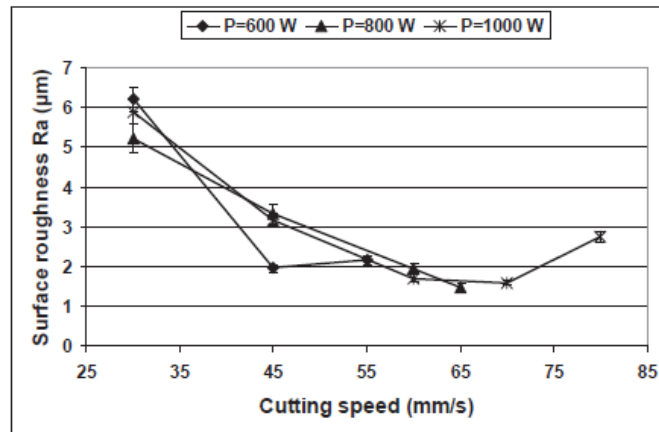


Figure 2.5: Variation of surface roughness with cutting speed under different laser powers (LI, SOBIH and CROUSE 2007).

Additionally, Figure 2.6 shows the description of laser cutting process with SEM (scanning electron microscopy) micrographs taken on cross-sections perpendicular to the kerf along the in-depth direction of a S355N piece of steel, labelled as IN, MID, OUT. Looking at the three different scans it is possible to see how the HAZ increases, almost linearly, along the direction of the laser pulse penetration, however, with minimal effects. Nevertheless, there are no cracks or significant defects, which shows the quality of this technology in the processing of steel (BURSI, et al. 2017).

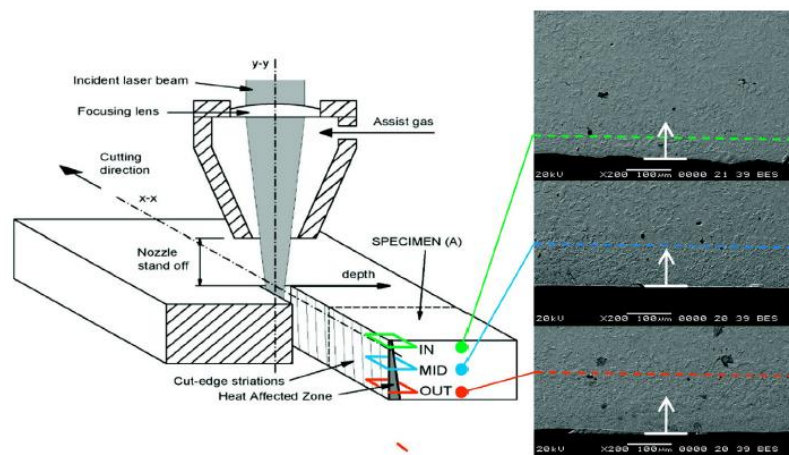


Figure 2.6: Heat affected zone analysis on a laser cut surface, divided in three zones through the thickness of the cutting kerf (BURSI, et al. 2017).

Concerning the striation phenomenon, it corresponds to periodic lines appearing on the cut surface as result of small fluctuations in laser power and gas flow which initiates hydrodynamic instabilities on the molten front. Finally, it is argued that thermal cutting processes can influence residual stresses and therefore have an important effect on the structural performance of systems subjected to extreme loads or high-cycle fatigue (BURSI, et al. 2017) & (ZANON, et al. 2014).

## 2.3. Laser cutting in steel construction

### 2.3.1. Fabrication and full-scale drawings

From a structural point of view, the potential of LCT promises to revolutionize steel construction. Comparing both Figure 2.7 and Figure 2.8, it is possible to understand the advantage of LCT in steel construction as it dispenses stiffener elements and bolted connections to produce a much more clean and aesthetical structure.



Figure 2.7: Example of a hollow section joint materialised with stiffeners and bolting (EXPO 2015 Construction).



Figure 2.8: Steelwork made with CHS elements processed by laser cutting technique (Piazza Garibaldi roofing in Naples, Italy).

The fabrication phase of HSS structures represents a big fraction of total construction costs. As a consequence, fabrication processes such as design drawings, cutting, assembly of the members and edge preparation for welds should be as efficient as possible. The procedure starts with the drawings made by the designer and draughtsman after pre-design and previous considerations (e.g. the equipment and the technology available in the workshop). Connection's drawings should be made in detail and in full-scale, depending on their level of complexity. The drawings should also include material properties, dimensions and fabrications procedures to avoid discrepancies. In the end, it should be checked by an inspector, who can mediate any controversy between the designer and the fabricator. During fabrication phase, the assembling procedure (order and sequence) is the key to a technical and economic production of structures. Moreover, the creation of a jig or assembling frame may become necessary and efficient since it offers a precise welding position and faster work for the welder.

When the structure arrives to the construction site, ready to be erected, the need for any type of temporary stiffeners should have been already studied once this operation might create unexpected stresses in the designed trusses. In this situation, hollow sections reveal big advantages comparing to open sections once they have superior torsional properties, which give them higher efficiency for out-of-plane stability, and therefore, no transverse stiffeners or lifting cradles might be needed (WARDENIER 2000).

During maintenance phase is important to verify and guarantee the designed behaviour of the structure but also the correct protection against corrosion and fire. With regard to corrosion, only the external surface of HSS requires protection, which can be solved with painting or metal coatings methods. To guarantee fire safety requirements, several materials can be applied to steel: insulating boards or panels; spray coating or plaster; intumescent paint. In this matter, hollow sections have, again, a major advantage because they can easily be filled with concrete or by circulating water. Fire protection requirements represent a significantly additional cost for steel structures when comparing with concrete. Thus, a strong effort must be made to apply them as economic and competitive as possible (WARDENIER 2000).

### **2.3.2. Sustainability and economical aspects**

To meet this project targets and considering the importance of sustainability in manufacturing industry, which is responsible for consuming 25% of the total energy in Europe, a life cycle assessment is essential to analyse this technology from an environmental performance perspective of energy and resources efficiency. The process uses electrical energy, assisting gas and generates waste material. These three impacts should be controlled, and sustainable measures should be adopted, such as recycling, machine tools and process control optimization. In comparison with other methods, laser cutting operations release much less noise and pollution, easy demount ability and re-use. By creating more precise solutions (accuracy around 10  $\mu\text{m}$ ) with less raw material and welding, CO<sub>2</sub> emissions during fabrication phase might be reduced and the ecological footprint of steel process can be minimized. In addition, the technology evolution and new generations of fibre laser promise to bring significant improvements and efficiency (KELLENS, et al. 2014).

In terms of automation, this process is definitely innovative and almost independent of human labour. Starting by CAD programming, which reduces the human error and increases quality, the cutting operation is entirely programmed and fully achieved by the laser beam which creates a safer environment.

According to partner ADIGE-SYS, “their costumers obtained production improvements in the range from 70% to 80% through LCT, with respect to conventional processes. This was mainly thanks to more stringent machining tolerances resulting in improved quality of joints, fittings, easier fastenings, process efficiency and vast flexibility”. Although the use of these powerful machines in construction industry requires a big capital investment (Table 2.1), the life-cycle manufacturing and reduced time in cutting

will decrease the overall costs. In a more open strategy, the improved design and simpler fabrication with reduced costs will increase the competitiveness of steel solutions in Europe and worldwide.

An analysis of the competitiveness of HSS structures against conventional open sections is difficult to make in an international way since the costs of material, labour and protection differ from country to country. In steel construction, fabrication costs represent approximately between 30-40% of the overall project cost (Figure 2.9). Due to joints increasing complexity this rate is likely to increase.

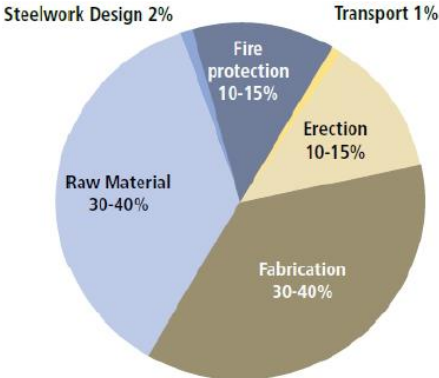


Figure 2.9: Breakdown of costs of the steel frame of a typical multi-storey commercial building (CASTIGLIONI, et al. 2015).

According to a preliminary estimation of two LASTEICON partners (OCAM in collaboration with FINCON), by applying LCT on an existing steel construction project, consisting of CHS profile as columns and I-profile as beams, fabrication costs of steel structures can be reduced by 8-9%. The savings can even be optimised if the sections are chosen to optimize the fabrication costs with LCT. Nevertheless, the benefits of this technology comprise all the life cycle of building project, as shown in Figure 2.10.



Figure 2.10: Scheme of the benefits of LASTEICON during the life cycle of a building project (CASTIGLIONI, et al. 2015).

## 2.4. Hollow structural sections

### 2.4.1. Truss girders

Truss girders represent a rational and facilitate construction making with minimum material expenditure and high degree of efficiency regarding construction elements. It is especially suitable for large-span structures and load transfer which is definitely useful in a broad category of man-made structures such as bridges, cranes, roofs, building skeletons and temporary construction frameworks (scaffoldings). This structure consists of rigid-beams, which exert mainly axial forces, that are usually connected by welded or bolted joints (SMITH, et al. (n.d.)).

The design is always a compromise between various requirements, such as static or fatigue strength, stability, economy in material usage, fabrication and maintenance. Thus, the designer should be aware of the implications of his solution since these requirements may sometimes conflict with each other. When designing these structures, a design optimization process falls into three broad categories: geometry, topology and cross-sectional optimization (KIRSCH 1989). Topology and geometry aim to find the best shape that will, in terms of mass and stiffness, support a given set of loads according to existing conditions. Cross-sectional optimization takes care of the designed variables concerning the profile section and is usually the most heavily researched (SMITH, et al. (n.d.)). Nowadays, categories as economy and sustainability gained more importance and therefore must also be considered in the design optimization.

One of the main characteristics of truss girders is their depth, which is determined in relation to span, loads, maximum deflection, etc. The ideal span to depth ratio for a simply supported truss is between 10 and 15. However, a ratio nearer to 15 will represent an optimized value if the total costs of the building are considered.

When loaded, truss girders may reach the collapse due to the failure of its members, joints or supports. In case the structure is statically indeterminate, then a combination of different failures may lead to collapse. Under compression, elements may be subjected to a mode of failure known as Euler's buckling where forces can cause a beam to bend out and ultimately fail. This effect depends on the effective length of the member ( $L$ ), its moment of inertia ( $I$ ) and the Young's Modulus ( $E$ ). The formula which determines the minimum axial force that creates buckling for an ideal column is represented in equation (1).

$$\begin{array}{l} \text{Critical Buckling} \\ \text{Load:} \end{array} \quad P_{CR} = \frac{\pi^2 \cdot EI}{L^2} \quad (1)$$

From this equation it is observed the considerable influence of the effective length parameter on the described load. This dimension is related to the rotational stiffness of beam's boundary conditions which, in the context of lattice girders, are represented by their end connections. Taking in account simplified



rules, given by (EN1993-1-8 2005), for the effective length of a compression member in a truss it should be considered, approximately, a factor of  $0,9*L$  for CHS chord members in plane and  $0,75*L$  for CHS brace members, in both planes.

On the other hand, when looking at LASTEICON innovative joints, these solutions are expected to be stiffer than the conventional ones which will decrease the effective length up to a minimum of  $0,5*L$  (fully constrain boundary conditions) and consequently increase the critical buckling load.

In sum, it is pretended to demonstrate that laser technology benefits can be extended to the enhancement of truss girders' structural performance.

### 2.4.2. Hollow structural section profiles

As already stated, this project is mainly focused on the use of circular hollow sections as a structural solution to perform the numerical studies on truss girders. Normally, these solutions are materialised by adopting local stiffeners, gusset plates or even by using open section profiles (Figure 2.11).

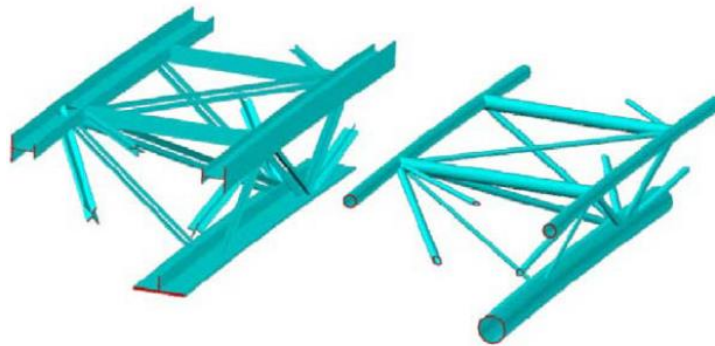


Figure 2.11: Comparison between spatial trusses with open and circular sections to show the aesthetical advantage of tubular sections (BURSI and KUMAR 2013).

Hollow section profiles have excellent mechanical and shape properties which can be resumed in the following points:

- The axial symmetric geometry gives them high axial, bending and torsional resistance;
- The inherent shape makes them have lighter overall weight and require smaller volume of fire and corrosion material;
- They are aesthetically more attractive and more efficient for elements subjected to wind, water and wave loading;
- From an architectural point of view, they offer more space and freedom to design new projects and services;
- They have reduced transport costs;
- It is easier to obtain a composite behaviour.

HSS can be manufactured as circular, square or rectangular. The market of laser cutting machines is very diversified and covers a wide range of available profiles dimensions. For round tubes, it is possible to cut from 10 to 508 mm in diameter with wall thicknesses up to 20mm and lengths up to 14m (CASTIGLIONI, et al. 2015).

### 2.4.3. Hollow structural section joints

In contrast to tubular members, which are mainly submitted to an axial loading condition, tubular joints are usually subjected to complex loadings and can become the weak points of a structure (KHODAIE, MOHAMADI-SHOOREH and MOFID 2012). Therefore, an appropriate type of joint should be determined from Table 2.2, depending on the classification of the joint and on the chosen method of analysis.

Table 2.2: Type of joint model – classification (EN1993-1-8 2005).

Method of global analysis	Classification of joint		
	Nominally pinned	Rigid	Semi-rigid
Elastic	Nominally pinned	Rigid	Semi-rigid
Rigid-Plastic	Nominally pinned	Full-strength	Partial-strength
Elastic-Plastic	Nominally pinned	Rigid and full-strength	Semi-rigid and partial-strength Semi-rigid and full-strength Rigid and partial-strength
Type of joint model	Simple	Continuous	Semi-continuous

Depending on the method of analysis used, joints should be classified according to their rotational stiffness (Elastic analysis), strength (Rigid-Plastic analysis) or both (Elastic-Plastic analysis). Considering an Elastic-Plastic analysis (the same that is going to be used in this work), the joints' rotational stiffness may be classified into three different groups by comparing their initial rotational stiffness with the classification boundaries of Figure 2.12.

- Nominally pinned joint - which should be capable to transmit internal forces without developing significant moments and to accept the resulting rotations under design loads;

- Rigid joint - which has sufficient rotational stiffness to justify analysis based on full continuity;

- Semi-rigid joint - which provides a predictable degree of interaction between members based on the design moment-rotation characteristics. It does not meet the criteria for a rigid or normally pinned joint;

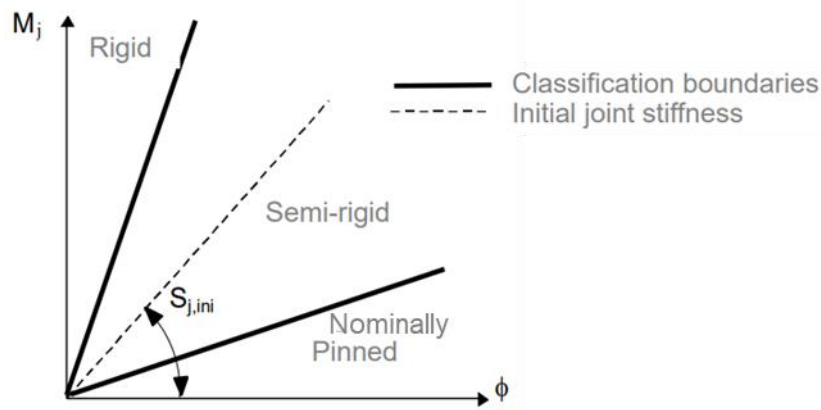


Figure 2.12: Classification of joints by rotational stiffness (EN 1993-1-8, 2005).

For rigid joints (Figure 2.12), where there is lower rotation capacity, an increasing of stresses might occur in addition to eventual imperfections, secondary moments and connecting eccentricities. Therefore, it is important to be aware of joint's classification although they can sometimes be tolerated regarding the ductile behaviour and plasticity of steel material.

When considering the application of HSS in the global analysis of lattice girders, the distribution of axial forces may be determined on the assumption that the members are connected by pinned joints. In fact, their connections shall present a ductile behaviour, so they can have enough rotation capacity which, especially for statically indeterminate structures, will provide an adequate redistribution of loads.

In Figure 2.13, three joint models' assumptions adopted for practical design situations are shown. In this case, brace members are connected to each other and the main chord is considered as continuous (rigid connection).

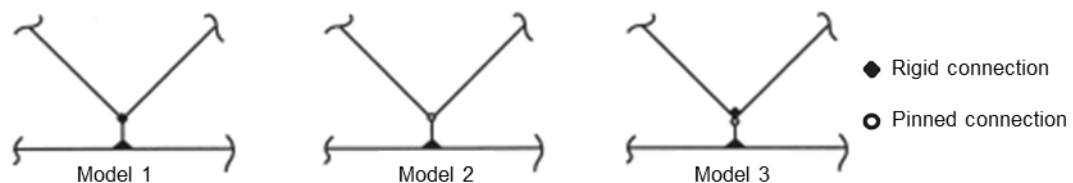


Figure 2.13: Detail of model connection for lattice girders (SAIDANI 1998).

Joints' geometry can also have substantial influence on the ultimate strength enhancement and in the provided ductility. To evaluate that, some parameters are used in research analysis of joints behaviour, as for example: chord and brace diameters ratio, wall thicknesses ratio, gap/ overlap between bracings, angle between bracing axes and brace-chord axes. According to (WARDENIER 2000), in terms of the design of CHS lattice girders connections, a good knowledge of the critical considerations that influence joints' efficiency is crucial to perform a solution without extensive and expensive reinforcement. Some of these considerations are described as a main guideline for designers and take into consideration some of the previous geometry parameters presented above:

1. Chords should generally have thick walls rather than thin walls. The stiffer walls resist loads from the brace members more effectively and the joint resistance thereby increases as the diameter to thickness ratio decreases. For the compression chord, however, a large thin section is more efficient in providing buckling resistance, thus, for this member the final CHS wall slenderness will be a compromise between joint strength and buckling strength, and relatively stocky sections will usually be chosen.
2. Brace members should have thin walls rather than thick walls (except overlap joints), as joint efficiency increases as the ratio of chord wall thickness to brace wall thickness increases. In addition, thin brace member walls will require smaller fillet welds for a pre-qualified joint (weld volume is proportional to the tension brace member thickness).
3. Ideally, CHS brace members should have a smaller width than CHS chord members, as this gives an easier weld situation for the joint at the saddle of the chord section.
4. Gap joints are preferred to overlap joints because the members are easier to prepare, fit and to weld. In the design process, a minimum gap  $g \geq t_1 + t_2$  ( $t_1$  and  $t_2$  represent the diameter of each brace member) should be provided such that the welds do not overlap each other.
5. An angle of less than  $30^\circ$  between a brace member and a chord creates serious welding difficulties at the crown heel location and it is not covered by the scope of "Comité International pour le Développement et l'Etude de la Construction Tubulaire" (CIDECT) recommendations (WARDENIER 2000).

When analysing the collapse of truss structures, if global failure is a consequence of joints failure, at least one of the following failure modes might have occurred.

- a) Chord face failure;
- b) Chord side wall failure by yielding, crushing or buckling under the compression of the brace member;
- c) Chord shear failure;
- d) Punching shear failure of a hollow section chord wall;
- e) Brace failure with reduced effective width (cracking in the welds or in the brace members);
- f) Local buckling failure of a brace member or of a hollow section chord member at the joint location.

For consultation, the respective failure modes due to axial loading and bending moment are graphically represented on Table A.6, Appendix.

However, for CHS welded joints within the range of validity of Table A.2, in Appendix A, only chord face failure and punching shear need to be considered. The two failure modes are shown in Figure 2.14,

respectively. The design axial resistance of these connections should be taken as the minimum value for these two failure modes, which can be calculated using the given formulas from Table A.1 in Annex, from (EN1993-1-8 2005, 109 & 113).

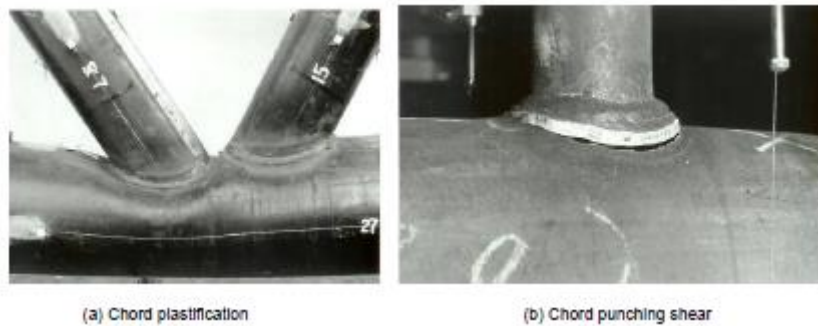


Figure 2.14: Failure modes (WARDENIER 2000).

According to (WARDENIER 2000), an ultimate deformation limit criterion results as a more efficient and satisfactory design procedure. Thus, when performing numerical analysis, a practical way to achieve the ultimate joint resistance corresponding to failure can be set as the lower of:

- a) Maximum load achieved on the force versus deformation (or displacement) diagram;
- b) The equivalent load level for a corresponding ultimate deformation limit, usually set as  $0,03 \times d_0$  ( $d_0$ = chord's diameter).

If necessary, it is always possible to consider reinforcement solutions to prevent any of the presented failure modes. Their main purpose is to increase the strength and rotational stiffness of joints. These solutions can either be external (bolted or welded plates, external rings, etc.) or internal (concrete filling, longitudinal stiffeners, internal-rings, etc.).

## 2.5. State-of-the-art

### 2.5.1. Previous developments in the research of numerical analysis

Concerning this dissertation purpose and the project goals, it is interesting to study previous research of other numerical analysis made on steel joints, especially on truss girders. Thus, some of the most relevant work found about this field is presented here and particular attention is given to:

- Methodology and FEM modelling
- Failure criteria
- Experimental & FEM results

Numerical analysis done in this area used FEM to model and simulate the behaviour of different truss girders joints, useful for engineering practice and saving the necessity to execute experimental tests. Additionally, some theoretical calculations were performed. Combining these results with experimental tests it is possible to calibrate models with considerable accuracy and use them for further model calculations.

Truss girders' modelling analyses should consider global as well as local behaviour of construction members and joints, depending on the requested accuracy and correctness pretended. Following (RADIĆ, MARKULAK and MIKOLIN 2010), the FE model can thereby be represented as:

- 1) Planar or space girder model made by beam elements with or without considering possible secondary influences (or influences due to joint eccentricity);
- 2) Space girder models made completely by 3D elements (shell or solid);
- 3) Space girder models combining beam and space elements;
- 4) Isolated truss girder joint models.

From these four approaches, the truss girder beam model application (1) is the simplest and most acceptable approach and it can conduct linear and non-linear analysis (material or geometrical). The joints can either be modelled as hinge links, where the result is only axial forces, or as rigid links. By choosing hinged links, it is recommended to consider additional influences from bending moments, such as: secondary bending moments, bending moments due to transverse load between truss nodes and bending moments due to eccentric member connection in joints.

On the other hand, by using rigid or semi-rigid links, a more realistic situation is studied, but as the model is only composed by beam elements it would not be possible to consider local effects on joints as consequence of their deformation characteristics. In fact, it would only be able to calculate stress redistribution caused by ductile behaviour of steel but not detail stress concentration in the joints. Alternatively, truss models composed completely by 3D shell (2), or solid elements, represent a more

complete model approach as it includes global and local system behaviour. Yet, these models are only used for research purposes due to their complexity and time-consuming during simulations (especially non-linear analysis).

An acceptable and more efficient modelling approach passes by combining beam with 3D shell or solid elements (3), in such a way that joints are modelled with 3D elements and the members are modelled with beam elements (Figure 2.15). In this case, the connection between those two elements is made through rigid links (called master-slave constraint) so joints are submitted to more realistic boundary conditions, which simulate the structural behaviour.

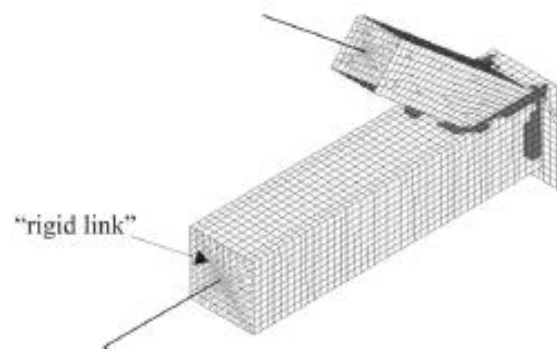


Figure 2.15: Truss modelling detail with beam and shell *elements* (RADIĆ, MARKULAK and MIKOLIN 2010).

According to (RADIĆ, MARKULAK and MIKOLIN 2010), the results from a load-displacement analysis allowed to verify that the results from those various calculation models were quite similar but there was significant difference in the limit load from the 3D space shell model (2) and the space beam model (1), possibly due to the inclusion of local joint detail in shell models. In contrast, when comparing the limit load results for a 3D shell model (2) and a 3D combined model (3), the results were almost identical. Moreover, a positive agreement was obtained between the 3D shell model (2) and an isolated 3D model of the critical joint (4), as it can be seen in the diagram of Figure 2.16.

In conclusion, the previous results point to the advantages of using combined models considering both global and local behaviour with great simplification in terms of complexity and calculations. Additionally, by comparing the results from Eurocode regulations with experimental results, it was possible to conclude that they lead to big conservativeness and so more experimental and analytical research should be made to achieve optimized results.

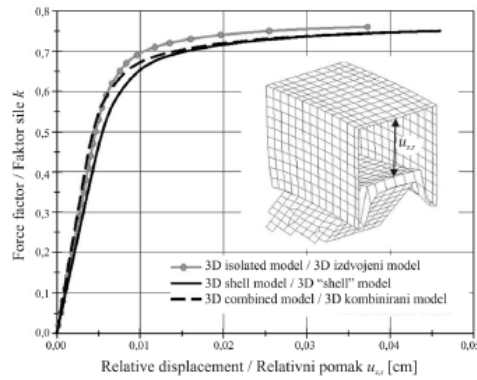


Figure 2.16: Diagram force vs relative displacement for different models.

Concerning the ultimate joint capacity estimation, the displacement measurement can be set depending of the expecting failure mode. According to (ZHU, et al. 2017), the analysed displacement was considered as the distance between the brace end and the chord centre to define the ovalisation of the joint.

### 2.5.2. Previous developments related to LASTEICON project

In a more extensive research, focus was put on investigated joints with similar configuration to the ones studied in this project.

The first article, from (P. BOERAEVE, et al. 2006) presents an alternative to the usual complex traditional steel joints by using laser technique to perform holes in the chords and then pushing the diagonal brace members into those holes before welding (Figure 2.17). With this approach no complex cuts need to be done in the brace members in order to guarantee good compatibility with the chord' surface.



Figure 2.17: Traditional and pre-cut method for CHS joints (P. BOERAEVE, et al. 2006).

To study these joints' behaviour, a FEM analysis was performed and a parametrical study was carried out to compare the new solution with the traditional ones. The final objective was to define correction



factors  $f(p)$ , to apply on regulated design formulas of conventional joints, as guidelines and good practice for the design of these new types of joints (Equation (2)).

$$N_{RD\_PRECUT} \approx f(p) \times N_{RD\_Traditiond} \tag{2}$$

In relation to FE analysis considerations, a bi-linear stress-strain material behaviour was chosen for the chords (elastic-plastic material). The failure of the diagonals and the weld was avoided artificially by adopting a perfectly elastic behaviour. In fact, weld material is usually stronger than the tubes material and it shall not be influenced by the cutting hole in the chord. The FEM study was performed in ABAQUS (FEM software) using shell elements and a simplified geometry (making use of joints' symmetry). A "Static General" analysis was executed considering geometric non-linearities.

To model weld contact, distinct ways can be accomplished in a FEM model. Through parametric analysis two optimized solutions were chosen, represented in Figure 2.18 by "Precut 3" and "Trad". All possibilities correspond to a chamfer solution, however, the first ones (Precut 1 and 2) consider an extension of the brace into the chord and that has a stiffening effect, which is not on the safer side.

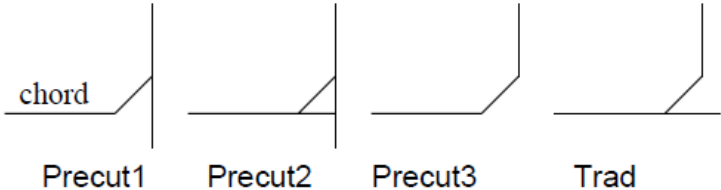


Figure 2.18: Ways of connecting the weld to the chord and diagonal.

The potentialities of laser cutting allow us to realize the cutting in different directions as shown in Figure 2.19.. Solution 2 (parallel to the diagonal) is faster and probably the one that requires less welding material, however, a minimum tolerance must be given to avoid possible tube imperfections and facilitate positioning.

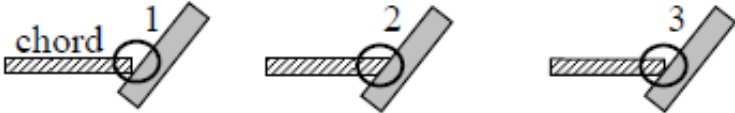


Figure 2.19: Types of laser cuts. 1) perpendicular to its axis; 2) parallel to the diagonal; 3) a combination of both.

Additionally, a concern was made about the thickness of the diagonals as it should be limited to 8mm otherwise weld would not be penetrating. A joint detail is shown in Figure 2.20, where it is possible to see the laser cutting, perpendicular to the chord axis, the tolerance given in chord's hole for better brace positioning. Figure 2.21 shows the deformation parameters set for a load - deformation analysis. In this case, the failure criterion was achieved for a deformation of 3%, consisting in the ratio between the maximum radial displacement ( $d1$  or  $d2$ ) and the chord's diameter.

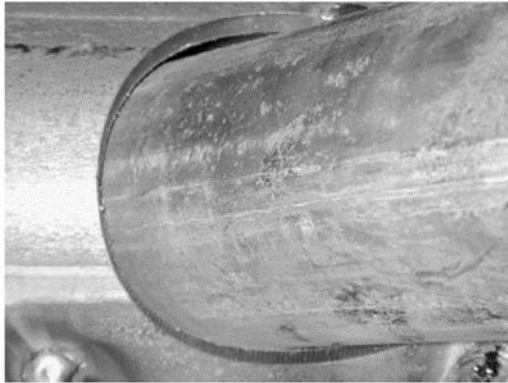


Figure 2.20: Joint detail made through laser cutting.

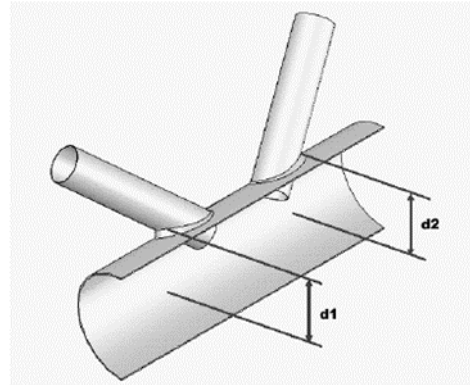


Figure 2.21: Deformation parameters of a K-joint.

After this first analysis and a validation of the numerical model, a parametric analysis was performed. The main parameters of the study, in agreement with the design considerations given in chapter 2.4.3, were:

- Width ratio between the diagonal and the chord ( $\beta = d_1/d_0$ );
- The width to thickness ratio of the chord ( $\gamma = d_0/t_0$ );
- The angles between the diagonals and the chord ( $\theta_1; \theta_2$ ).

These are some of the conclusions from these pre-cut joints analysis:

- Less preparation time is needed due to positioning as it simplifies the jig for the diagonal's welding;
- For fire resistance, it should be possible, with pre-cut joints to irrigate the structure from inside due to brace-chord internal connection;
- The greater the width ratio  $\beta$ , the greater the loss of strength in pre-cut joints. The study has shown that pre-cutting the chords lead, generally, to a decrease of the failure load (for width ratio  $\beta < 0,6$ , the loss of strength is less than 20%);
- Compression load in the chord is a significant parameter for K joints;
- A lot of applications from architectural buildings to mechanical applications could benefit from the present technique;
- Despite punching shear failure might not occur, the shell elements chosen for the mesh do not predict that failure mode and so this simplification should be considered.

(SZLENDAK and OPONOWICZ 2013) focus on a similar type of push-pull joint application in steel trusses, made with RHS profiles. The laser technology provides a new joint shape that creates more contact between the chord and the brace. Figure 2.22 shows in more detail the described joint. For these analyses, theoretical resistance formulas were used and compared with experimental and numerical analyses. Once more, a positive agreement was obtained between those models which proves the validity and potential to proceed with numerical analyses on further investigations in this field.

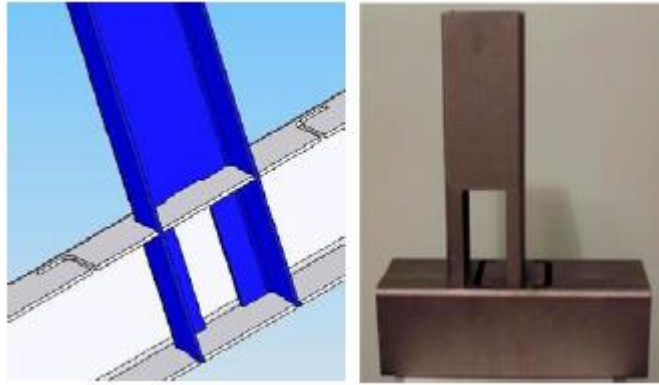


Figure 2.22: Half section view of the analysed joint; Embedded RHS brace member going inside the RHS chord (SZLENDAK and OPONOWICZ 2013).

## 2.6. Fabrication tolerances

The use of laser technology in steel cutting brings high cut accuracy (around 10 $\mu$ m (micro meters)) which will optimize welding quality, quantity and the assembling process (with minimized eccentricities). However, merchant steel bars produce profiles with small different dimensions from the nominal size and sometimes with imperfections. Because of that, some geometrical tolerances must be taken when performing laser cutting. In that way, a study was performed by other LASTEICON partners (FINCON 2016) to create rules and methods to eliminate the practical problems about this tolerance issue. The solution passes either by a first measurement of the profile dimensions with laser scanning or by a statistics investigation about the average tolerance of profiles. Even though this study has been performed only for I-beam-to-CHS-column joints (Figure 2.23), the results will be used accordingly for truss girders' joints.



Figure 2.23: LASTEICON I-beam-to-CHS-column joint specimen (FELDMAN 2016).

After the last project meeting in Dusseldorf (on July 2017), ADIGEYS reported the results from this study and has achieved an optimized tolerance of 1mm. Still, the consortium agreed that the best way to perform the slots was by measuring the beam cross-section dimensions automatically with a software, created by ADIGEYS. In conclusion, a first analysis will consider the slots to match the nominal section dimensions.



## 3. Truss specimens analysed

### 3.1. Introduction

To meet LASTEICON targets, IST is responsible for making a previous study on truss girders specimens with new joints typologies, and further experimental tests on “Laboratório de Estruturas e Resistência de Materiais (LERM)” in Instituto Superior Técnico, Lisbon. Once this study is finished and a final design of test specimens is achieved, IST should prepare and provide the shop drawings to send to partners, ADIGE-SYS and OCAM, which are responsible for the laser cutting and truss specimens’ fabrication, respectively. Despite the new analysed joints present a more complex shape than conventional ones, the use of LCT will allow the process to be highly simplified and structural behaviour might improve.

In order to study such complex and innovative connections, a powerful and appropriate software should be used for the 3D modelling. It is of great importance that joints’ geometries are sufficiently detailed once laser technology deals with high accurate precision and laser machines work automatically by reading from the technical drawings.

After some research, it was found that a software like SolidWorks or Autodesk Inventor were suitable to produce the pretended connections, however, SolidWorks revealed to be the most appropriate software as it has an associative interface with Abaqus which allows to transfer the models. In addition, this interface allows to subsequently modify the geometry in SolidWorks and propagate those modifications to Abaqus without losing any analysed features. This 3D modelling software came out to be much more practical and detailed when designing the connections’ geometry.

With respect to the 3D FEM analysis, the software used was ABAQUS/CAE v.6.13 once it was the one available in IST and proposed by the supervisors.

### 3.2. Description of truss specimens

This chapter will present the analysed truss specimens, with focus on CHS and OPEN sections. Two truss specimens are going to be studied first in order to understand joints’ behaviour. These two specimens represent two distinct types of trusses, such as: Pratt truss (TYPE I) and Warren truss (TYPE II).

The Pratt type girder consists of vertical and diagonal bracing members connected to the chords (Figure 3.1). Despite having more bracing members and joints comparing with Warren girders, in case

of having loading points in the chord, these additional vertical members will reduce chord's bending moments and effective length and will carry the vertical compression loads (WARDENIER 2000).

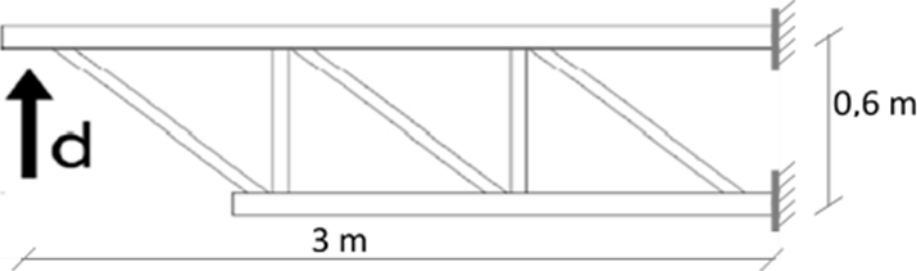


Figure 3.1: Substructure type I - Pratt truss (CASTIGLIONI, et al. 2015).

The Warren type girder, without verticals, is composed only by diagonal bracing members connected with the upper and bottom chords (Figure 3.2). From previous research, it is stated that the favourable angle between the chord and bracing lies in the range of 40° to 50° degrees. However, to decrease the number of joints, this angle may decrease to a minimum of 30°. For welded Warren trusses, the possibility of using gap joints brings a more economical solution in terms of fabrication costs. From an architectural point of view, this solution is more aesthetical and offers more open space for the arrangement of technical services (mechanical, electric, etc.). The efficient compression behaviour of CHS profiles generally provides the most economical solution when designing truss girders, specially Warren trusses (WARDENIER 2000).

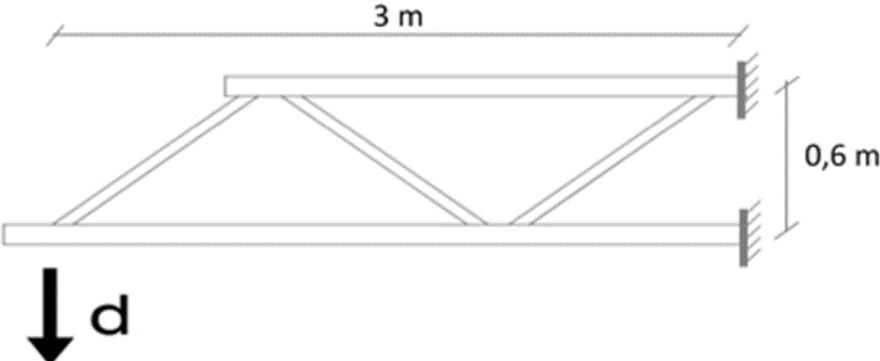


Figure 3.2: Substructure type II - Warren truss (CASTIGLIONI, et al. 2015).

### 3.3. Description of joints

New joints' configurations were designed according to the potentialities of LCT and the innovation purpose of LASTEICON project. All the joints are welded and composed by either hollow circular sections (CHS) or open sections (HEA and angle profiles). As already anticipated, the only difference of these conventional connections is that truss members are now laser-cut in order to better fit in the chord, with easier welding on the external surface.

From the presented truss specimens, two types of connections are going to be studied:

- N-joints (from TYPE I), Figure 3.3.
- K-joints (from TYPE II) [21], Figure 3.4.

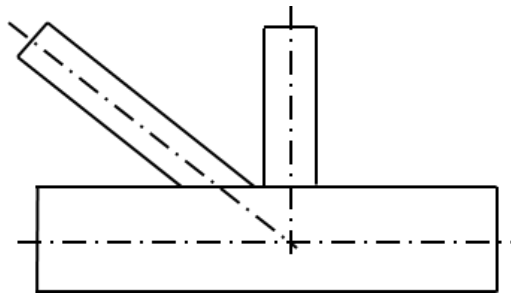


Figure 3.3: Traditional N-joint, substructure type I (without eccentricity).

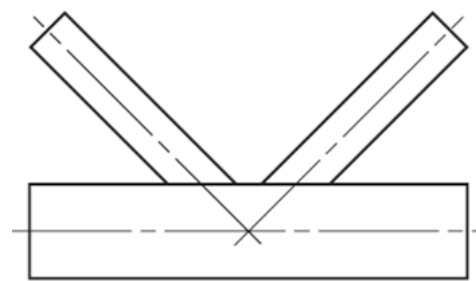


Figure 3.4: Traditional K-joint, substructure type II (without eccentricity).

The design of new connections is based on embedded brace members pushed inside the chords and welded on both top and bottom chord's surface. It is expected that these solutions turn out to be satisfactory in the way that brace members will work as internal stiffeners.

At a local perspective, the joint's strength will increase with the reinforcement on the chord and stresses will be distributed along its surface, avoiding the common failure modes. Subsequently, brace members' force will be spread along both chord's surfaces, decreasing stresses in the connection and giving the possibility to reduce section dimensions, for the same loading condition. Finally, sustainability can be optimized by creating solutions that enable to reduce the waste of steel and the weight of the structure.

All joints are designed with no overlapping bracing members and no eccentricity, which is going to avoid secondary stresses. In contrast, the reduction of the chord's face, by creating the slots, might decrease chord's strength.

For the truss specimen TYPE I, three types of new CHS N-joint configurations are going to be designed, plus the traditional configuration. Two of these new joints consider the possibility of having a vertical brace (new\_1) or a diagonal brace (new\_2) embedded inside the chord, as shown in Figure 3.5 and Figure 3.6, respectively.

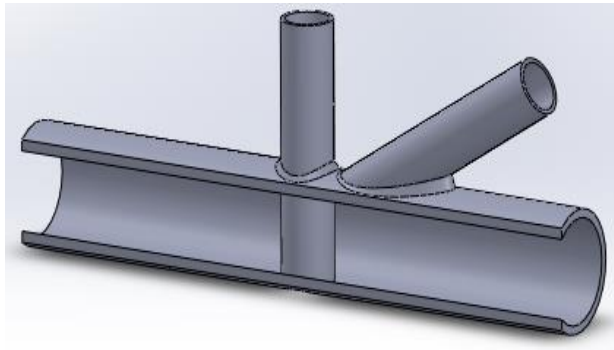


Figure 3.5: Joint New\_1 (embedded vertical), substructure type I.

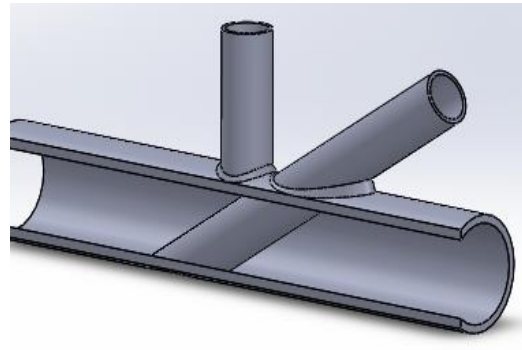


Figure 3.6: Joint New\_2 (embedded diagonal), substructure type I.

The third connection (new\_3) considers both vertical and diagonal braces embedded inside the chord. However, to accomplish that, only half of each brace section will enter through the chord, resembling on two half tube canes intersecting each other without touching. The following views, shown in Figure 3.7, describe in more detail this innovative joint.

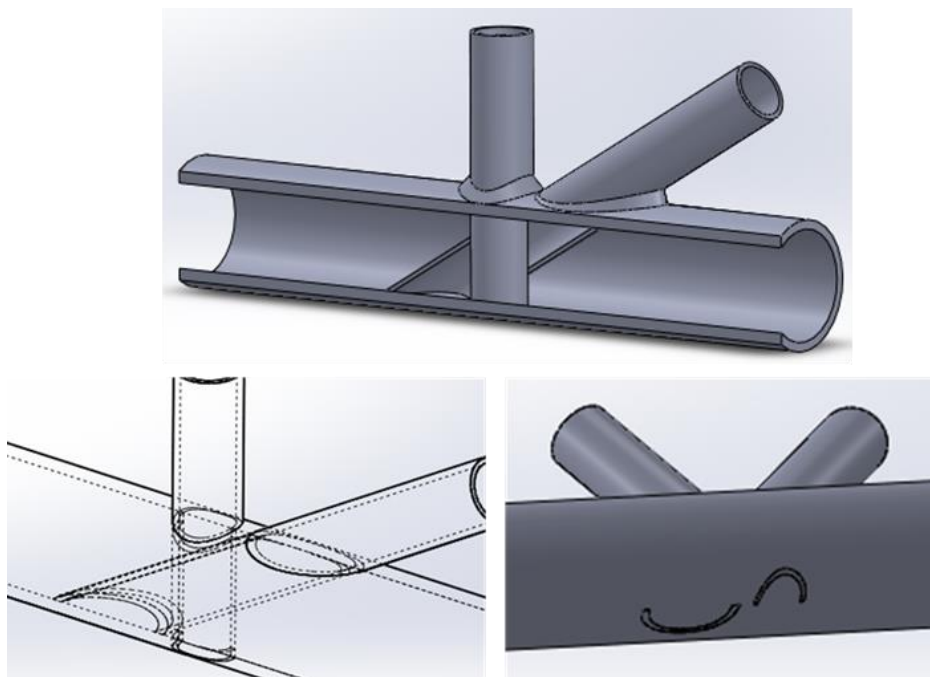


Figure 3.7: Different views from the CHS Joint New\_3, substructure type I.

In similarity with truss specimen type I, the designed joints in truss type II also consider the brace members embedded inside the chord with the only particularity that both members are in the diagonal direction. Figure 3.8, Figure 3.9 and Figure 3.10 show in detail the presented joints.



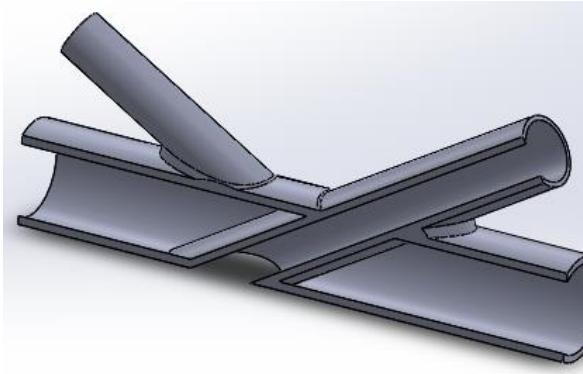


Figure 3.8: Joint New\_1, substructure type II.

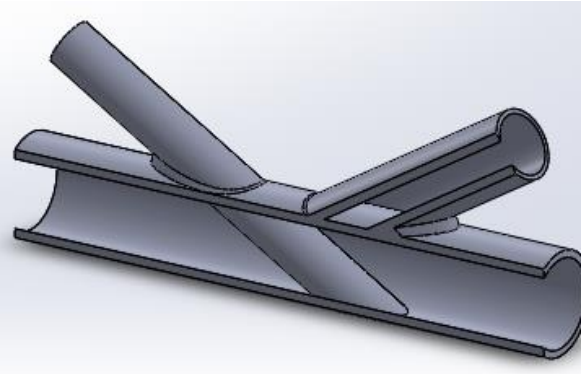


Figure 3.9: Joint New\_2, substructure type II.

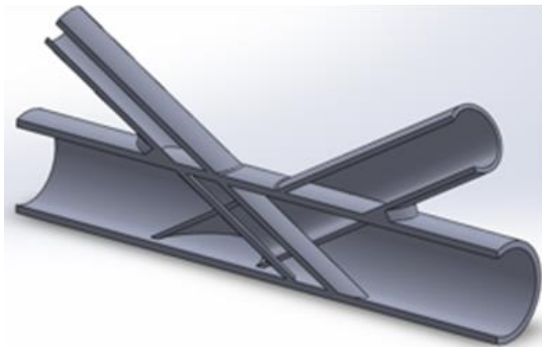


Figure 3.10: Joint New\_3, substructure type II.



As referred before, an extension of LCT to open section profiles pretends to prove the advantages of this technology in different applications. Therefore, the open section joints are also going to be designed considering bracing members passing through the chords. These joints are materialized with an HEA profile for the chords and two angle profiles for each brace. To guarantee no eccentricity in the joint, it was necessary to align the profiles trough their centre of mass. Also, the inside edges between the flange and the webs are usually rounded but for mesh simplification, these details were turned into live edges. Figure 3.11 and Figure 3.12 show the traditional and the new joint configurations, respectively, for a truss specimen type I.

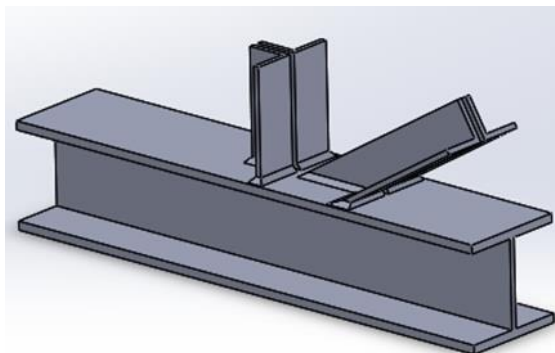


Figure 3.11: Traditional open section joint, substructure I.

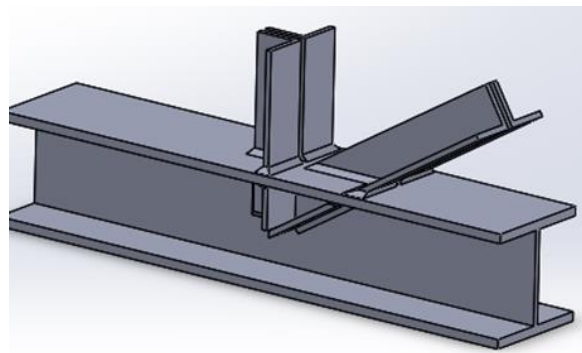


Figure 3.12: New Open Section Joint, substructure type I.

The same procedure was taken for the truss specimen TYPE II and the following joints, traditional and new, were modelled, as shown in Figure 3.13 and Figure 3.14.

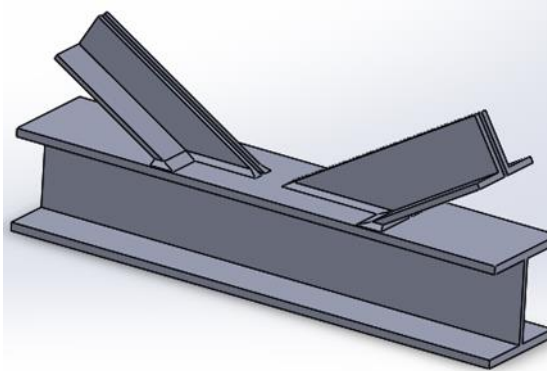


Figure 3.13: Traditional open section joint, substructure type II.

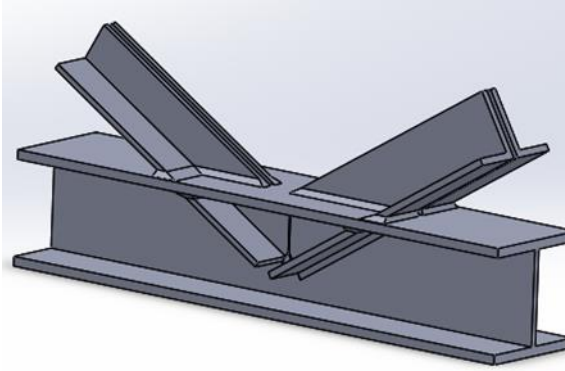


Figure 3.14: New open section joint, substructure type II.

For investigation on numerical analysis and future experimental tests it was decided to perform a total of ten models in which some of the joints configurations presented above would be tested. Table A.3, in Appendix, summarizes the models that will be tested in this work. The profiles' dimensions for CHS and OPEN sections were obtained from (VALLOUREC 2011) and (B2Bmetal.eu 2014), respectively.

Connection type New\_2 is not going to be submitted to numerical analyses neither experimental tests. As already explained, this connection is described by having one diagonal member embedded inside the chord and, for truss type II, this diagonal is the one with the smaller section. From the three new joints' configurations presented, this connection was the one that was discarded for further analyses because it is the solution where it is expected lower resistance in terms of rotational stiffness and strength. Additionally, this investigation always aims at considering the most potential and innovative connections that can bring advantages to LCT and sustainability to steel construction.

## 4. Numerical analyses

### 4.1. Introduction

To prove the extendibility of laser technology on new joints applications, previous FEM analyses must be made to assure their potential. In fact, much smaller investment is needed if previous numerical analysis can be performed, with accuracy, on an available software instead of through experimental tests.

The Finite Element Method (FEM) is a powerful and convenient technique for the computer solution of complex engineering problems. The method can find approximate solutions of the differential equations that describe the physical phenomena. For that, it is necessary to first idealize the real model into an analytical formulation, by splitting the geometry of the structure into smaller finite elements assigned with material properties, boundary conditions and imposed loads or displacements. These elements are then assembled together through their nodes, composing the finite element mesh. The equilibrium equation is solved through the definition of polynomial approximation functions that describe the displacement variation along each element. Therefore, the quality of the results depends largely on the number of elements adopted in the mesh and the order of the approximation functions.

As explained before, the software packages used for modelling were SolidWorks, for joints creation, and ABAQUS/CAE 6.13 for 3D FEM analysis.

In this chapter, the methodology used to perform FEM simulations will be presented as well as the detail of all the parameters chosen and assumptions made. This memory is essential in case it is intended to calibrate these models with upcoming experimental results.

### 4.2. Welding simulation

A life-cycle assessment pretends to be done to evaluate the performance of LCT and, based on that, one of the most influent parameters to be studied is the welding quantity used to perform each connection (Figure 4.1).

Despite welding being practical and commonly applied in steelwork, some issues must be considered once the applied forces are usually complex and the stiffness distribution along the welding perimeter is often non-linear. Additionally, residual stresses created by welding may have influence on the buckling strength of tubes and joints' fatigue behaviour.



Figure 4.1: Welding of a tubular connection (<https://www.i depot.ie/blog/inverter-welder/>).

In this dissertation, weld is being considered as part of the connection's geometry in a way to simulate the models as similar as possible to reality. Welding material will exhibit the same properties of the main members' material and it will be modelled, in SW, as a chamfer solution, in agreement with (P. BOERAEVE, et al. 2006). This solution is preferred to fillet welding to simplify mesh arrangement and avoid elements distortion. The size has been designed with approximately 4 millimetres of length although it presents some variations due to geometric characteristics of connections.

Having in reference the innovative joints presented in chapter 3.3, it was possible to observe that brace members which were embedded inside the chords were welded twice, in the top and bottom intersection with the chord's surface. At a first approach this will result in more wasted material when compared to the conventional joints, although the solution is predictably stiffer and with better structural performance.

### 4.3. Numerical Modelling

#### 4.3.1. Material Properties

The material properties of both chord and brace members were provided by Vallourec to be consistent with further experimental tests once this partner is responsible for the fabrication of the hollow section profiles. The material choice should be adequate to provide enough difference between the yield strength and the ultimate tensile strength so that the structure can act in a ductile manner (a minimum ratio for this difference is given by  $\frac{f_u}{f_y} \geq 1,2$ ). (WARDENIER 2000). The designation of steel is S355J2H (Figure 4.2) and is typically used for hot finished structural hollow sections with non-alloy steel properties.

Steel designation	Minimum yield strength $R_{eH}$ N/mm <sup>2</sup>			Minimum tensile strength $R_m$ N/mm <sup>2</sup>		Min. elong. % on gauge $L_0 = 5.65\sqrt{S_0}$ $t \leq 40 \text{ mm}^*$		Impact strength (10x10 mm)	
	$t \leq 16$ mm	$16 < t \leq 40$ mm	$t > 40$ mm	$t < 3$ mm	$3 \leq t \leq 65$ mm	Long.	Trans.	Temp. °C	J
S235JRH	235	225	215	360–510	340–470	26	24	20	27
S275J0H S275J2H	275	265	255	430–580	410–560	22	20	0 -20	27 27
S355J0H S355J2H	355	345	335	510–680	490–630	22	20	0 -20	27 27

Figure 4.2: Steel material properties (WARDENIER 2000).

The stress-strain relationship is elastic-plastic with linear kinematic strain hardening (Figure 4.3), for both tension and compression. Considering an isotropic material, the steel's elastic modulus ( $E_{modulus}$ ) and Poisson's coefficient ( $\nu$ ) were taken as 212 GPa and 0,285, respectively, according to Vallourec material's datasheet. The density of steel was also introduced, with approximately 7850 kg/m<sup>3</sup>. The strain hardening gradient was considered as 1% of the elastic modulus, which corresponds to 2,12 GPa.

In Figure 4.3 it is possible to see the bilinear material behaviour. The first point (1) corresponds to the yielding stress ( $f_y = 355$ MPa), where the yield strain ( $\epsilon_y$ ) was obtained from the constitutive material relation ( $E_{modulus} = \sigma/\epsilon$ ). The second and last point (2) corresponds to the ultimate tensile strength of steel which was obtained considering an ultimate deformation of about fifty times the yield strain ( $\epsilon_u = 50 \times \epsilon_y$ ). In fact, no failure criterion was defined on Abaqus material properties and consequently strain hardening will increase indefinitely above the ultimate limit strength specified, which is not true because the material should deform with simultaneous loss of strength. Therefore, when analysing models' results, the ultimate state (from equation (3)) will be considered as the failure criteria.

$$f_u = (\epsilon_u - \epsilon_y) \times \frac{E}{100} + f_y \quad (3)$$

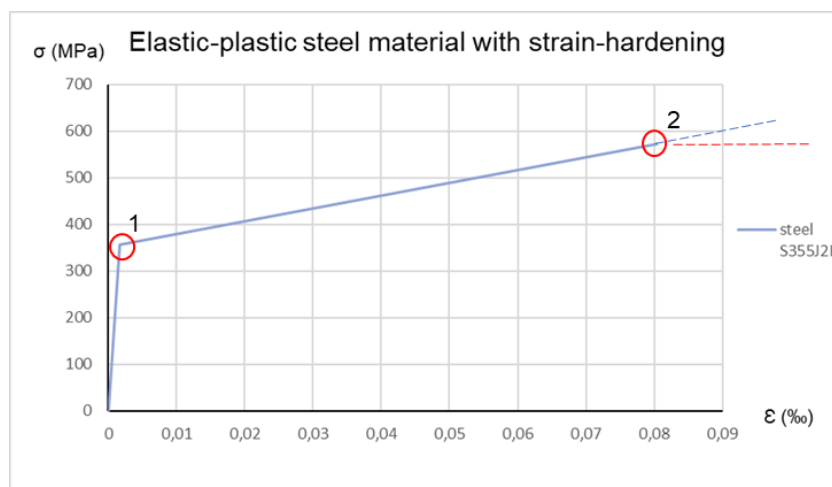


Figure 4.3:  $\sigma - \epsilon$  diagram.

As Abaqus doesn't identify the units to work on, it is important to choose the adequate ones and keep the consistency during the modelling. In Table 4.1, the units of the main variables used in these analyses are represented.

Table 4.1: Abaqus software units.

Variable	Units
Density	t/mm <sup>3</sup>
Force	N
Displacement	mm
Mass	t
Stress	MPa
Time	s
Rotation	rad

### 4.3.2. Geometry of the truss specimens

Before this dissertation has started, a pre-design of truss specimens was performed by the student Bernardo Pita Dias, also participating on LASTEICON project, and its dimensions were taken in the initial numerical analysis. This pre-design had special focus on IST laboratory capacity and requirements, such as hydraulic jacks loading capacity and stroke and size of the frames where the specimens were going to be tested.

Figure 4.4 and Figure 4.5 show the final designed dimensions of the CHS truss specimens after the pre-design and a subsequent preliminary study about trusses' ductile capacity, which will be explained later on.

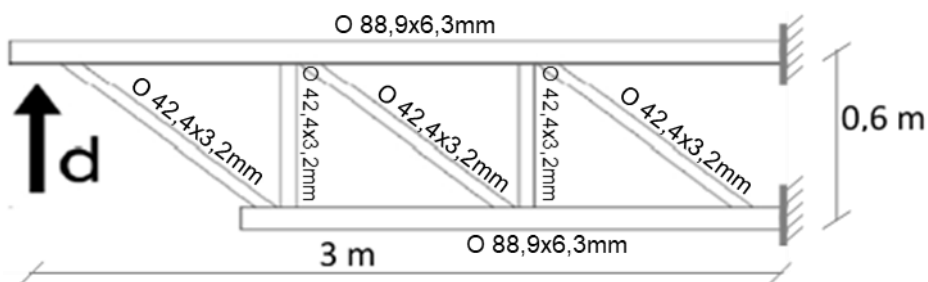


Figure 4.4: CHS substructure type I.

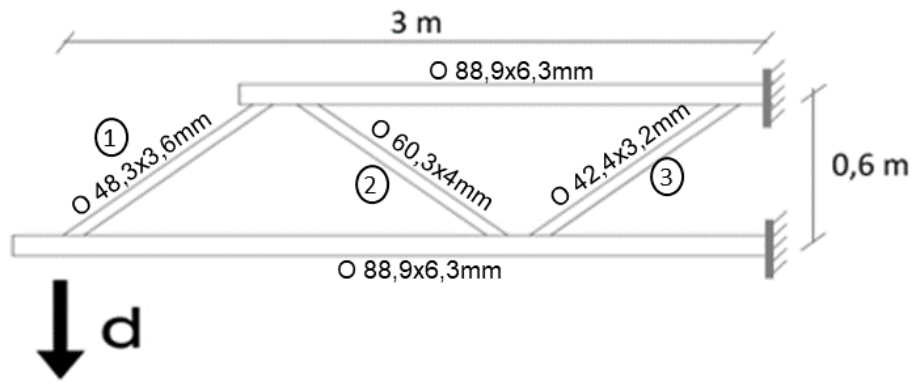


Figure 4.5: CHS substructure type II.

Finally, Figure 4.6 and Figure 4.7 show the final designed dimensions of OPEN section truss girder specimens.

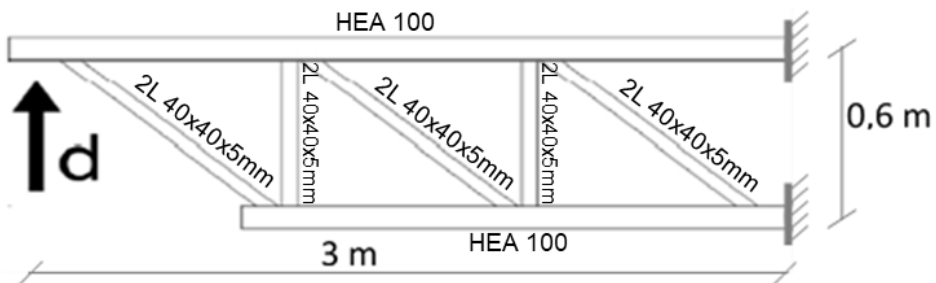


Figure 4.6: OPEN section substructure type I.

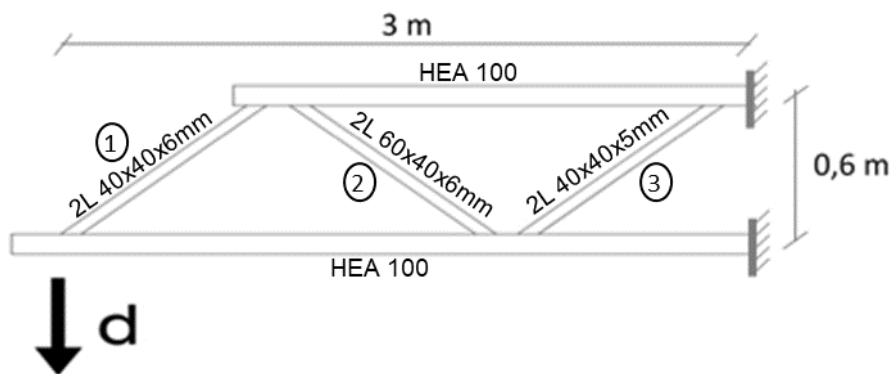


Figure 4.7: OPEN section substructure type II.

When modelling open section truss specimens as beam elements, a special detail was taken into consideration to model the bracing members, which are composed by two angle profiles, parallel to each other (see Figure 4.8). The model corresponds to a 2D planar truss and Abaqus only accepts one type of section for each beam element, therefore, it was not possible to introduce both angle profile sections separately. From the existing possibilities, as described in Figure 4.9, it was chosen a T-geometry to serve as the equivalent section.

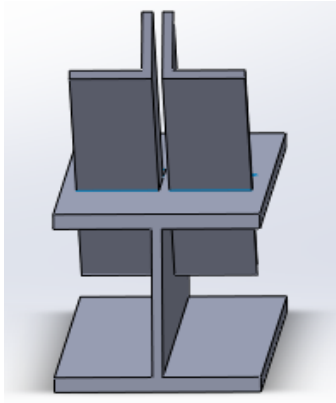


Figure 4.8: Open section bracing members detail (SOLIDWORKS n.d.).

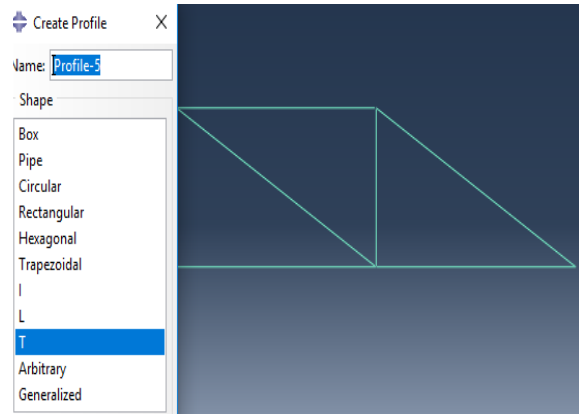


Figure 4.9: Beam element profile creation (Dassaul Systèmes 2013).

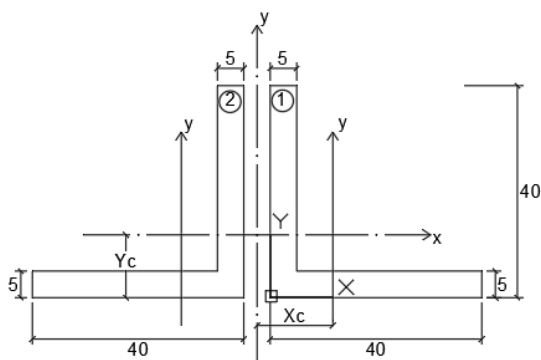
The T-section was designed in such a way so that the geometrical characteristics (such as the moment of inertia and the section area) were as similar as possible to the set of angle profiles. Using equations (4), (5) and (6), which relate the inertias and the areas (Figure 4.10), it was possible to find the requested dimensions for the equivalent T-section.

After simulating the trusses, to verify if enough ductility was obtained, and achieve the final design dimensions presented on Figure 4.6 and Figure 4.7, this process was repeated in the opposite direction. In the Appendix the respective geometrical properties of the several section profiles tested is also presented (Table A.7).

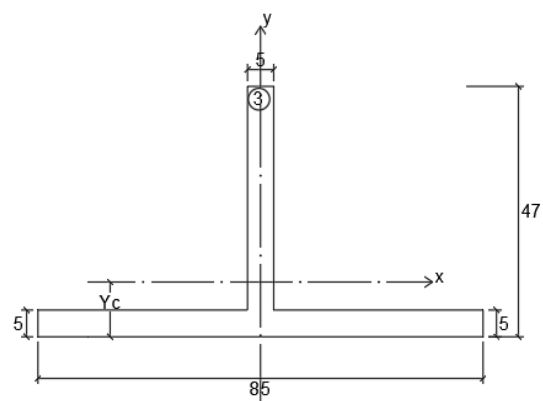
$$I_{xx}^3 = I_{xx}^1 + I_{xx}^2 \quad (4)$$

$$I_{yy}^3 = I_{yy}^1 + I_{yy}^2 + 2 \times [A \times (x_c)^2] \quad (5)$$

$$A^3 = A^1 + A^2 \quad (6)$$



a) Design section geometry



b) Equivalent section

Figure 4.10: Design sections geometry.

The set of angle profiles shown is positioned in a way that the moment of inertia is bigger in the y-direction, with exception to bar L 40x60x6. This means that the resistance to out-of-plane flexural buckling is higher than for in-plane buckling. Therefore, in addition to the extra support placed to restrict



lateral displacements, any possible deformation on the outside-of-plan direction is being prevented from happening.

Taking in reference (P. BOERAEVE, et al. 2006), the idea of creating a detailed solid model through SolidWorks and then transfer it to a FEM software might appear to solve both project goals (design joints configurations and numerical analysis). Therefore, a combination of beam and solid elements was created. In Figure 4.11, it is possible to view the final design model of trusses type I and II for CHS and OPEN section profiles.

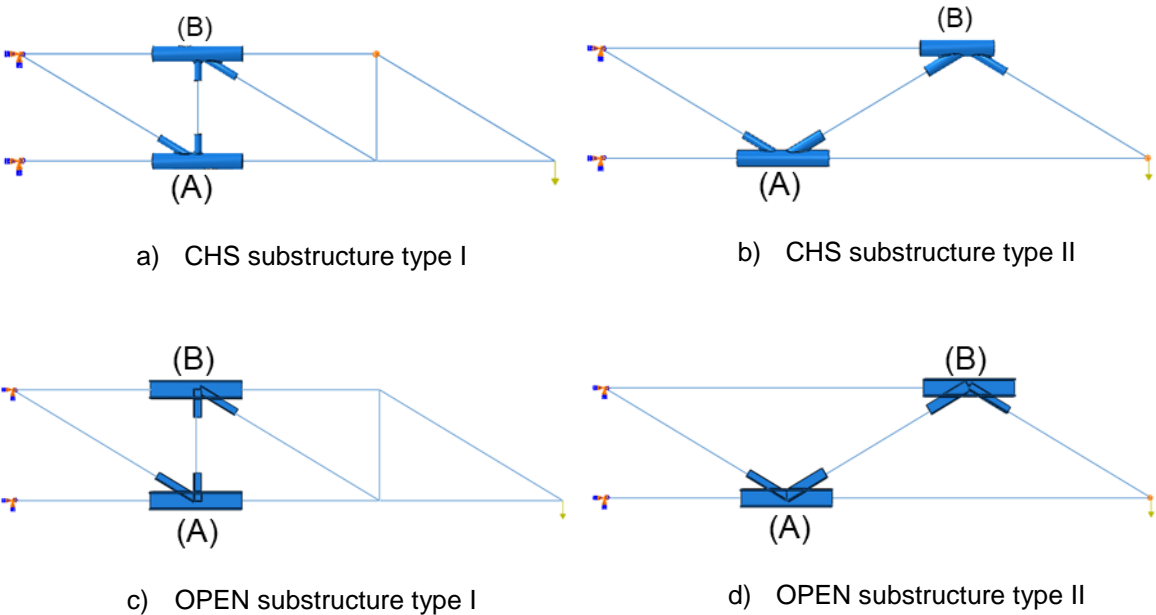


Figure 4.11: Spaced models composed by beam and solid elements.

Only two joints are going to be studied for each structure (A and B) to avoid too heavy models in terms of calculation duration. For truss type I, to get a more characteristic behaviour of this type of structures, the two joints near the supports will be studied. The length of each joint's member, measured from the central node, was considered as approximately a quarter of the respective total length. This value is related to the bending moment distribution and the fact that stresses in that zone are more uniform.

Connections A and B represent the same geometry and should behave very similarly as they are subjected to equivalent forces, from brace members, applied in the same direction (Figure 4.12). However, these connections are located, respectively, to bottom and top chords which means that for the loading condition in cause, the upper chord will be submitted to tension and the bottom one to compression. This aspect might influence the joints behaviour and, therefore, it will be considered in the future analyses.

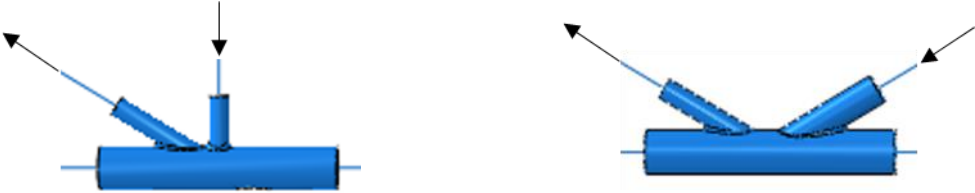


Figure 4.12: Forces directions of the analysed joints, for each truss specimen.

In contrast with CHS profiles, the beam section orientation for open sections is crucial and needs to be correctly introduced when modelling truss specimens. Therefore, special attention was given to the positioning of bracing members once they must be compatible between themselves and in agreement with the design of 3D models (see Figure A.1, in Appendix). In Figure 4.13 and Figure 4.14, the section orientation of OPEN profiles for each truss girder specimen is represented.

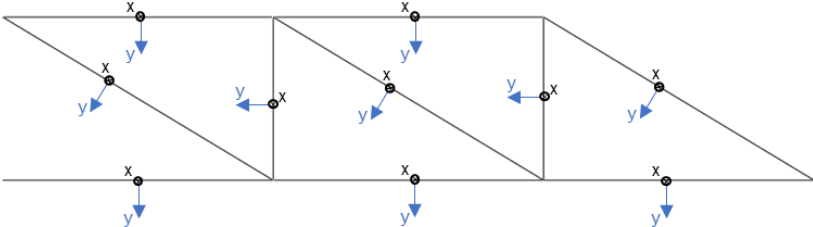


Figure 4.13: Beam OPEN section orientation of substructure type I.

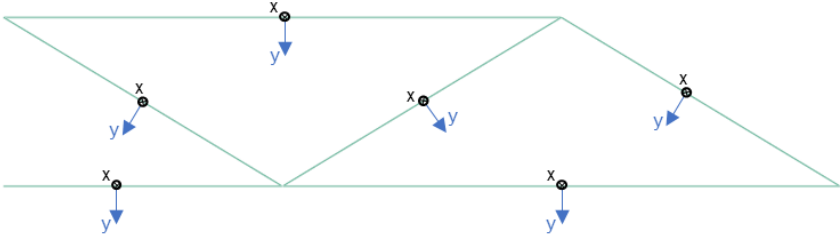


Figure 4.14: Beam OPEN section orientation of substructure type II.

In sum, Table A.4 and Table A.5, in Appendix, show the profiles’ dimensions and lengths that were manufactured by the partners. During the project, due to lack of stock from the partner Vallourec, some CHS profiles had to be changed. However, as the numerical analyses had already started, no change was done on the design models.

**4.3.3. Model assembly**

As the models are composed by two different element types (beam and solid), an interaction procedure was created. This interaction must be able to reflect the displacements and rotations between the beam end node and joint’s surface nodes by defining constraints on the analysis degrees of freedom. From the existing constraints, coupling allows to constrain the motion of a surface to the motion of a single point and, after testing the three types of coupling constraints, the kinematic was considered the appropriate one as it “couples the displacement and rotation of each attachment point (surface nodes) and constrains them to move with the rigid body motion of the reference node (beam node)” (Dassault Systèmes 2013). This constraint is represented in Figure 4.15.

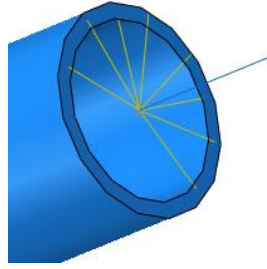


Figure 4.15: Kinematic coupling constraint between beam's node and joint's surface nodes.

Another assembly procedure that should be taken into consideration is the interaction between joint's members. In fact, when transferring the connections from SolidWorks to Abaqus, the models are considered as only one "part", which means that members are joined together like a unique solid. Even if the mesh on the interface regions may be dissimilar, the surfaces will work together so that there is no relative motion between them, like in a "tie constraint". This way, no contact or interactions needs to be created.

This assumption is a simplification of reality and a disadvantage of modelling with another software since it is not possible to specify the interaction between joints' members. However, when comparing this model with a butt welded joint, where the weld is in total contact with both interface regions, then it is correct to consider that steel bars are rigidly constrained to each other.

#### 4.3.4. Loading and boundary conditions

In LASTEICON's proposal, truss specimens' boundary conditions were set as simply supported to avoid that secondary moments created near the supports could affect joints' behaviour. However, higher displacements were obtained from this solution and it could affect laboratory requirements during the upcoming experimental tests. Therefore, the analyses were performed with fully constrained supports.

The boundary conditions are shown in the left side of Figure 4.16, with orange and blue colours, which restrain both displacement and rotation of the affected nodes. Additionally, a second boundary condition was set on the middle upper chord's node restraining trusses' displacement in the out-of-plane direction to avoid out-of-plane flexural buckling.

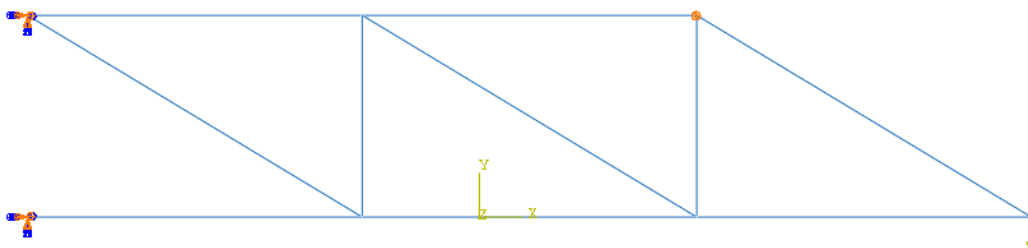


Figure 4.16: Boundary conditions and action load.

In Figure 4.16, it is also possible to see the applied load, with vertical direction, on the right end side of the truss, in the same location proposed by LASTEICON's proposal.

In this preliminary stage, a "General Static" analysis was chosen in the step module, considering geometric nonlinearity. This step analysis is defined by sequential events where the state of the model at the end of one step provides the initial state for the start of the next step (Dassaul Systèmes 2013). In this case, each step corresponds to an increment of load which is going to increase until it achieves the maximum value or until the model diverges and no solution is found. The non-linear geometry effects will be accounted for when large displacements occur.

Thereafter, it is necessary to introduce the time symbolizing the total period in which the load will be divided. Subsequently, an incremental procedure is specified, where Newton's method is used to solve the nonlinear equilibrium equations at each increment. If the increment size is too big, more iterations are necessary to reach the equilibrium and, as each iteration is computationally expensive, increments size should be kept small. During the first model analyses, the initial increment size was taken as default (equal to 1). However, the model failed after a small number of increments because the initial state was too far away from the radius of convergence for the equilibrium state. This means that the initial increment of load needed to be smaller in order to guarantee the convergence and the sequence of the simulation. As a solution, this value was decreased to 0,01 and sometimes even 0,001, due to geometry complexity of the model.

For the output requests, it was pretended to have an equal amount of data across the different models. In that way, it was requested to extract data "every x units of time", in which x had the value of 0,01, which means that for each total period, one hundred data values of each output parameter will be computed.

#### **4.3.5. Mesh definition**

Mesh quality (arrangement and size) is definitely important to the overall model accuracy of FEA results and can ultimately mean the difference between predicting that a design will or will not fail. The reduction of elements' size allows the mesh to be more uniform and capable to adapt to model's deformation. Therefore, in regions where large deflections and stress concentrations are expected, the mesh must be more refined whereas in non-crucial regions, to reduce the model size and the calculations duration, the mesh size can be larger.

Solid models can be meshed through alternative element types like tetrahedron (tet), hexahedron (hex), prims and pyramids. The difference remains essentially in the geometry and number of degrees of freedom. Tet elements are the default element type for most physic models because all them can be meshed, regardless of the shape or topology. On the other hand, hex elements are more demanding, as they require particular model geometry in order to be able to mesh. However, the significantly reduction on the number of elements often makes it more appealing.

In Figure 4.17 and Figure 4.18 it is shown one of the analysed joints meshed with tet and hex elements, respectively, and the adoption of a more refined mesh in crucial regions of the connection. In

this case, where the mesh size is similar in both models, the number of tetrahedron elements is almost four times bigger than hexahedron (45396 to 12168 elements). Additionally, the mesh detail along the thickness is shown, composed by two elements, which is the minimum number advised by (Abaqus v.6.13 2013) when components might present some flexural behaviour.

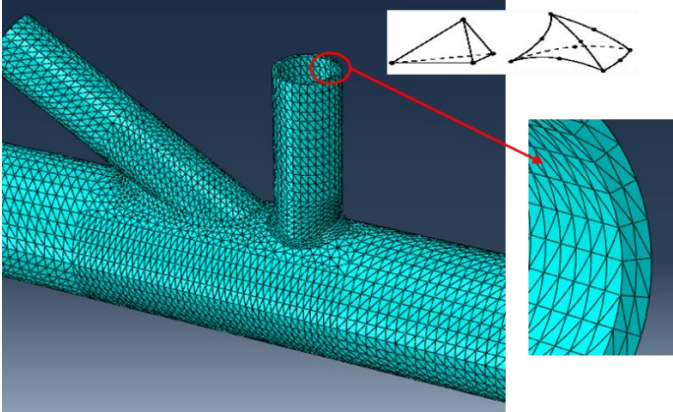


Figure 4.17: Detail of mesh arrangement with tetrahedral elements.

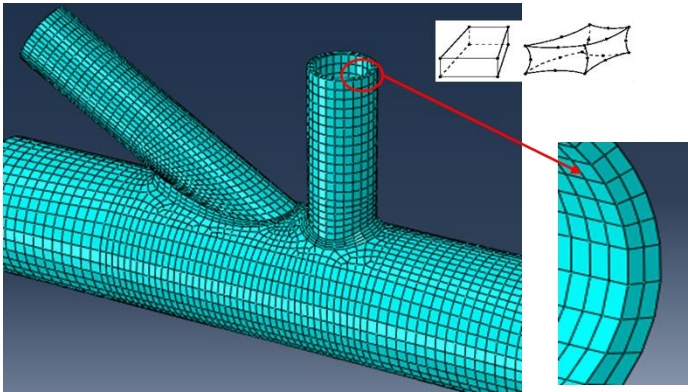


Figure 4.18: Detail of mesh arrangement with hexahedral elements.

When defining the element type properties, a secondary geometric order was chosen for the polynomial approximation functions (shape functions), where the error of the solution decreases with the third power of the size of the elements. Especially for tet elements, this assumption is considerably important once its linear geometric order represents a very stiff element, which may lead to inaccurate solutions. Therefore, a 10-node quadratic tetrahedron element (C3D10) and a 20-node quadratic hexahedron (C3D20R), with reduced integration, were chosen. Each node has 3 degrees of freedom.

The rest of the truss model, composed by beam elements, represents a more simplified mesh solution. For the analyses, a two-node linear beam in space (IB31) is going to be adopted.

In conclusion, whenever the geometry of the joint allows to mesh the model with Hex elements, they will be adopted instead of Tet elements, to reduce time calculations. Otherwise, the mesh will be performed with Tet elements.

## 4.3.6. Type of analyses

### 4.3.5.1. First Analysis Approach

The initial purpose of this dissertation was to study joints' behaviour without the context of the whole truss specimen and, in that way, a simplified model was created to simulate the connections. After being designed in SW and transferred to Abaqus, the created FEM model should be able to calculate forces, displacements and rotations on connection members with enough accuracy and in correlation with trusses girders behaviour. Therefore, the highlighted connections on Figure 4.19 were created and analysed based on a complete truss girder (simply supported, with 8m span).

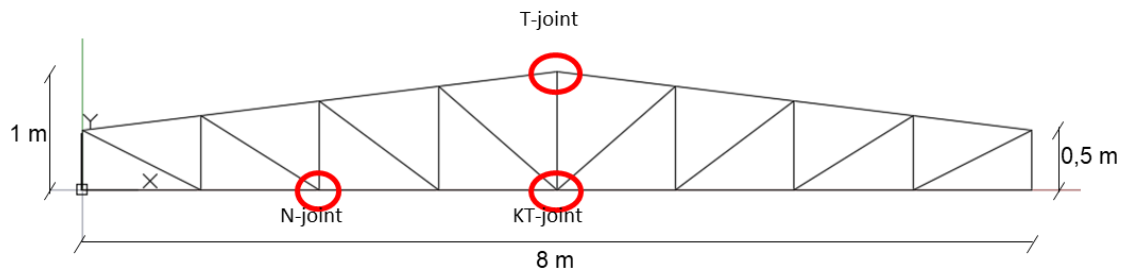


Figure 4.19: Truss girder with 8m span.

The two simplified K-joint models shown in Figure 4.20 represent two assumptions to study joints' behaviour. The model (a) is isostatic so reaction forces can be calculated directly from the input loads on the members. The model on the right side (b), from (P. BOERAEVE, et al. 2006), is statically indeterminate (hyperstatic) and gets a simplified version of truss behaviour by only considering axial load. During model analyses, input loads applied on the members shall be proportional between each other to simulate the transmission of forces through the structure. Numerical analyses were performed adopting model (b).

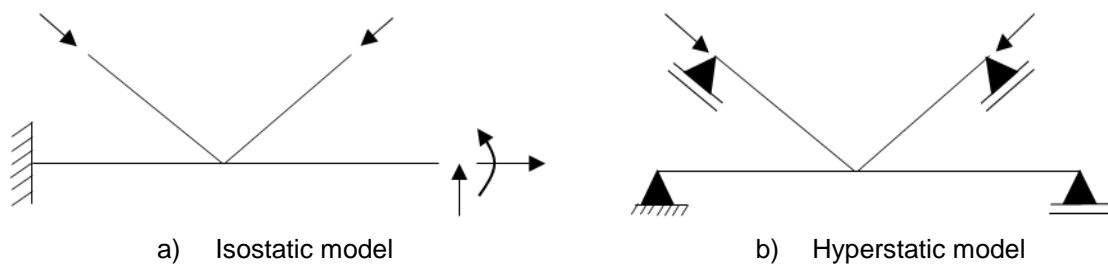


Figure 4.20: Two types of simplified models for joints analyses.

However, to meet LASTEICON proposal's targets, in which it is intended to prove the extendibility of laser cutting technology in truss girder applications by testing new solutions and compare them with conventional ones, it was requested to first have a qualitative validation of numerical results through the test of small truss specimens which should be representative of the full-scale truss described on Figure 4.19..

#### 4.3.5.2. Sensitivity analysis

The conversion of 3D geometric models (from SW) to 3D FEM models (Abaqus) required several numerical validation tests to fully understand the influence and meaning of the main parameters introduced.

In order to guarantee that SW models could be efficiently tested in Abaqus, a T-joint was reproduced in both programmes, with the same geometry and conditions. In SW, the modelling procedure used for solid joints was the same, which consists on creating each member in a “Part”, separately, and then assembling them to perform the weld through a chamfer geometry. In Abaqus, the model was built with a unique geometry because it is expected that the transferred model will behave like a unique solid where the interface regions are tied to each other.

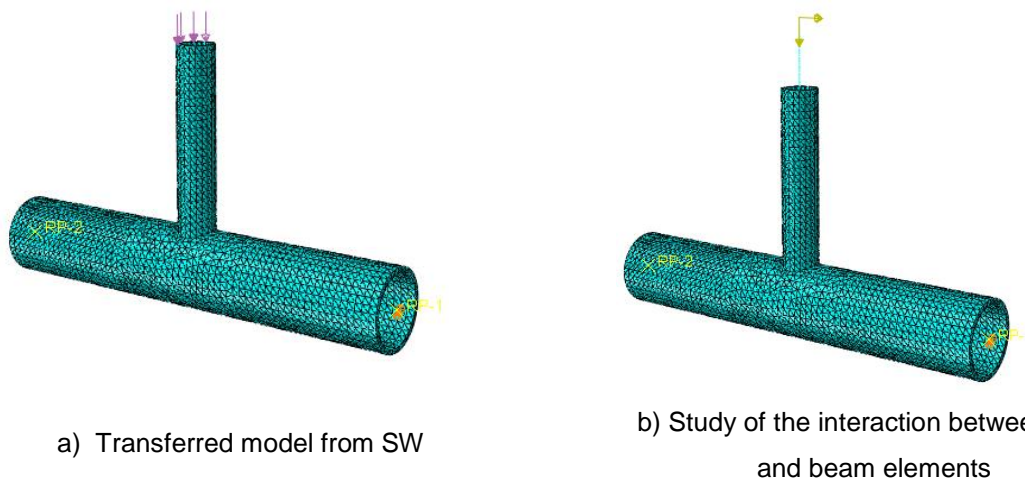


Figure 4.21: Simplified T-joint solid model used for sensitivity analyses.

The next study focused on the interaction between solid and beam elements where it was study the behaviour correspondent to the different types of constraints (kinematic, continuum and structural distributing couplings).

#### 4.3.5.3. Design of truss specimens

A first model of truss specimens, only composed by beam elements, was simulated on Abaqus to determine the final design for the section profiles. The base dimensions were taken from a pre-design study (which will correspond to the model “initial”), performed by another IST colleague. These simulations based their study on the ductile behaviour of truss specimens in order to evaluate if the maximum displacement was in agreement with IST laboratory requirements and if no buckling effect or collapse were occurring prematurely. In fact, as this work pretends to study and compare joint’s behaviour it is important to explore them above the yield limit, where high plasticity occurs. Moreover, the design must be efficient and optimized, which means that each bar must be explored to its maximum capacity.

In this regard, a “Static-Riks” analysis was performed instead of the initial “Static-General”. This analysis is suitable to study the buckling of the structure through the concept of arc-length (Abaqus v.6.13 2013). Therefore, by iteratively increasing the profiles’ sections, whenever there was buckling or not enough ductile response, it was possible to obtain the final trusses dimensions, which were already presented in section 4.3.2..

The results taken from these analyses will also help deciding which action load should be applied to study the final models. As explained already, the applied load must take the structure above the yield limit having in consideration the maximum displacement obtained.

#### **4.3.5.4. Analysis of joints**

After the simplified model, with only beam elements, has been analysed, it is time to introduce the 3D detailed solid models and proceed with the investigation on the behaviour of the new designed connections. In this work, it is pretended to establish the more efficient parameters to efficiently compare different joint’s configurations at local and global behaviour.

Starting by comparing different joints typologies, a first investigation was performed on the influence of each joint on the global behaviour of truss specimens. According to previous statements in this document, the introduction of innovative connections with increased stiffness might bring several advantages on global structural performance. This study will be conducted mainly on the determination of the maximum displacements and rotations of the structures.

Concerning the local deformations, according to EC3, for joints within the range of validity given in Table A.2 (Appendix), only chord face failure and punching shear failure needs to be considered.

To calculate the deformation on chord’s face along the increment of load, a set of nodes was created on the upper and bottom side of the chord to record vertical displacements. In that way, considering the initial diameter of the chord, it was possible to calculate the respective vertical deformation. In Figure 4.22, the location of the respective nodes for CHS joints is presented for substructures type I and II, where the deformation is calculated from the following equation (7):

$$\varepsilon = \frac{N_2 - N_1}{d_1} \quad (7)$$



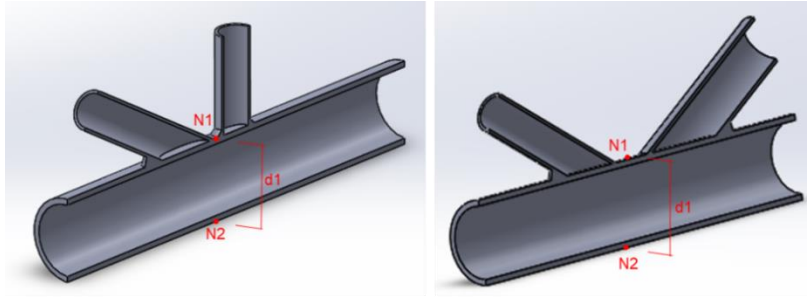


Figure 4.22: Calculation of vertical deformation on chord's face for N and K-joints.

Subsequently, the longitudinal deformation on brace members will also be determined. The fact that embedded members were considered as passing through the chord may predict that compression forces can be distributed along the upper and lower chord's face, minimizing the deformation and increasing joints' strength. Nodes were placed on the compression' side of the braces' face (Figure 4.23), due to some bending moment influence.

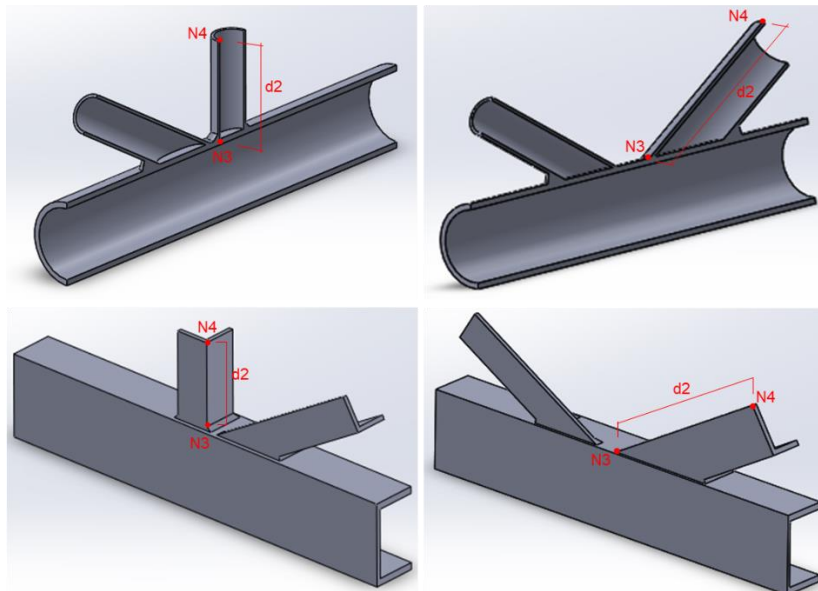


Figure 4.23: Calculation of brace members deformation for N and K-joints.

For OPEN sections, the determination of chord's deformation will be performed after a first observation of numerical models to find out the regions where maximum plastic strains, displacements and stresses occur.



# 5. Numerical results

## 5.1. Analysis of the results

### 5.1.1. First analysis approach

The first numerical models were performed on T, N and KT connections based on the truss girder with 8m span represented in Figure 4.19. These analyses represented a preliminary study where lower action loads were applied under linear elastic behaviour. From the observation of Von Mises stresses distribution on joint's deformed shape, some qualitative conclusions could be stated. Figure 5.1 represents one of the joints analysed.

The load combination applied on this joint induces equal axial compression in both brace members whereas the chord's extremity surfaces are constraint with simply supported boundary conditions, according to the simplified model (b) from Figure 4.20..

In first place, it is noted that stresses in the "traditional" joint are more concentrated in the top of chord's face than in the "New\_2" joint. On the other hand, the innovative joint contains small regions with high stress concentration (represented in MPa units), which may suggest that punching shear failure can occur on the bottom face of the chord. Moreover, a visual evaluation may predict that the chord's face in the traditional joint is more deformed than in joint New\_2. In contrast, the face of the embedded diagonal looks to be crushed by the deformation induced by the chord.

In conclusion, although the numerical analyses present some interesting effects, the load and boundary conditions set for the model, as well as the deformation shape indicated in Figure 5.1, do not agree with the natural conditions and deformations experienced in real structures like truss girders. Therefore, no parameters were analysed as this approach ended to be forgotten.

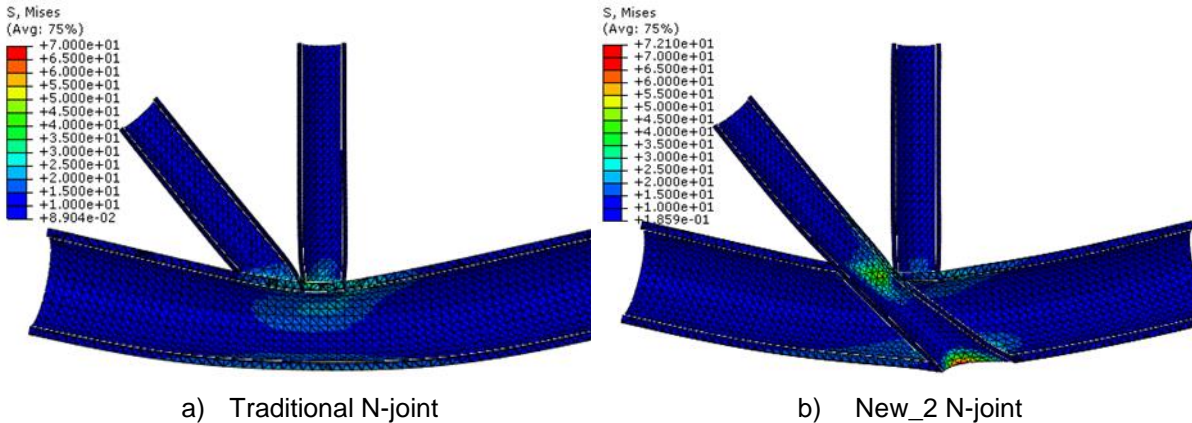


Figure 5.1: Von Mises stresses on N-joints, through a simplified model analysis (units in MPa).

### 5.1.2. Sensitivity analysis

Starting with the validation of the transferred models from SW to Abaqus, it is secure to say that the behaviour obtained from both models was completely identical, as expected.

In regard to the interaction between beam and solid elements, the analyses performed on the T-joint revealed that kinematic coupling was the pretended solution. In fact, kinematic coupling is restraining both displacements and rotations of the surface nodes with the reference point, whereas in the distributing solution only the rotations were being constrained, as shown in Figure 5.2..

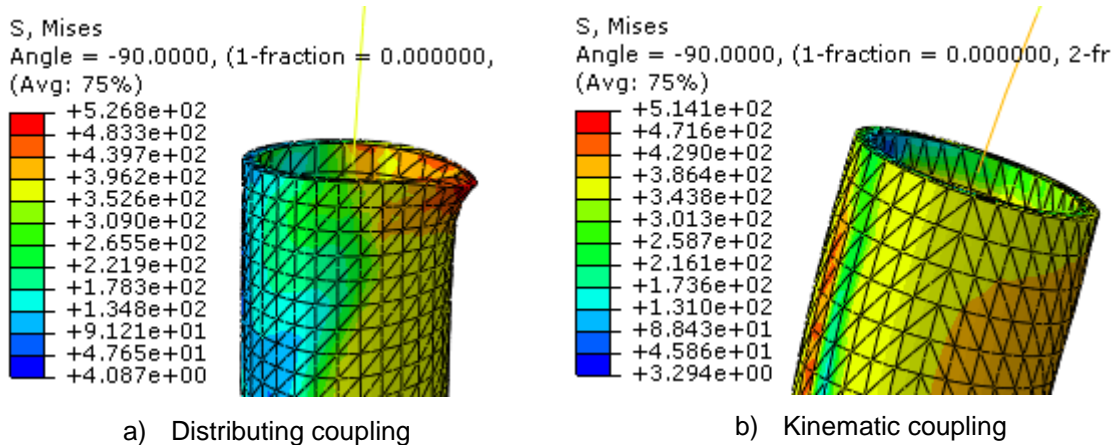


Figure 5.2: Comparison between coupling constraints (units in MPa).

### 5.1.3. Design of truss specimens

The results from the pre-design of truss specimen type I, for CHS and OPEN section profiles, are represented in Figure 5.3 and Figure 5.4 by a load vs displacement relation. Each of the curves shown in the graphics relate to a certain combination of profiles tested, which are described in Table A.8 on the Appendix.

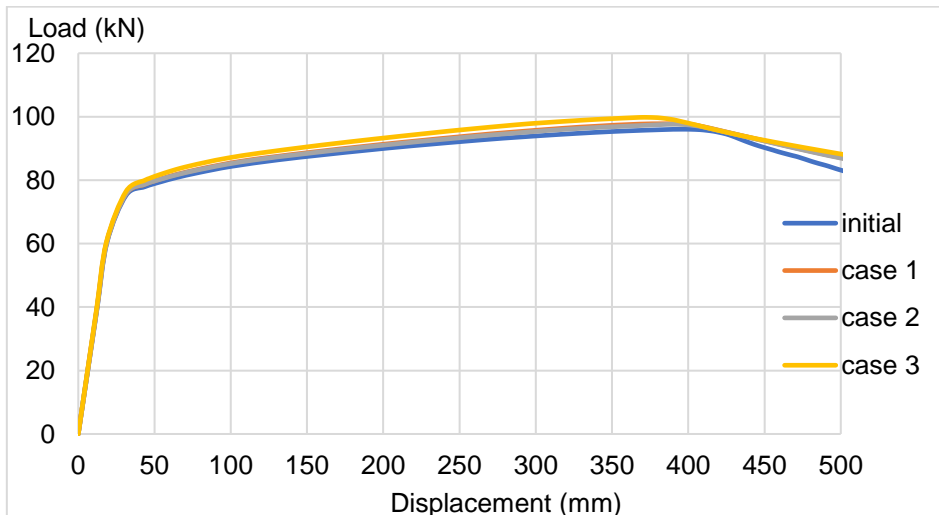


Figure 5.3: Load – displacement, CHS substructure type I.

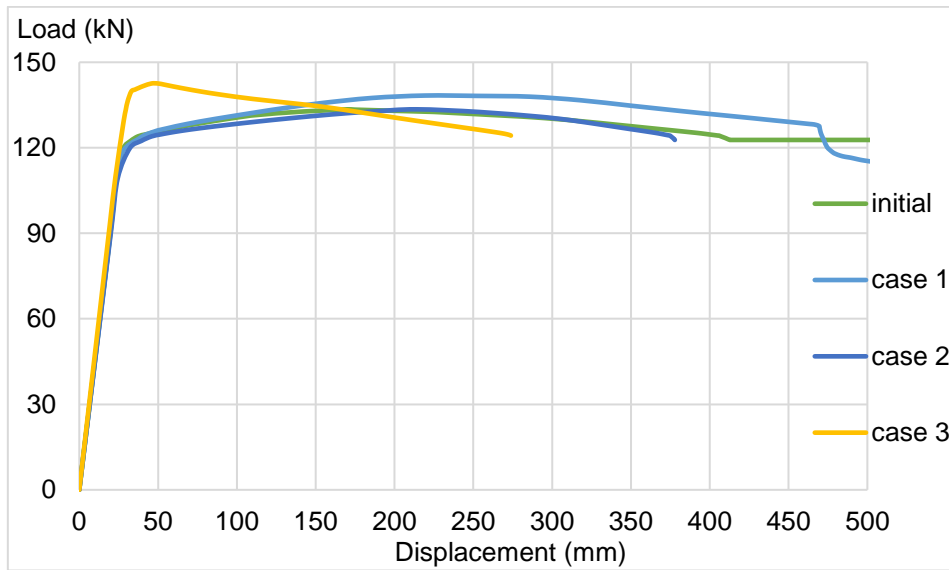


Figure 5.4: Load – displacement, OPEN section substructure type I.

The results obtained for CHS truss show that all tested combinations have similar behaviour in terms of displacement and ductility, with no buckling effect occurring prematurely. In that way, the “initial” pre-design was maintained. For OPEN sections, the situation was identical, with exception to “case 3”, and so the “initial” model was also maintained.

In extension, Figure 5.5 and Figure 5.6 describe some of the different profiles’ dimensions tested for truss specimen type II.

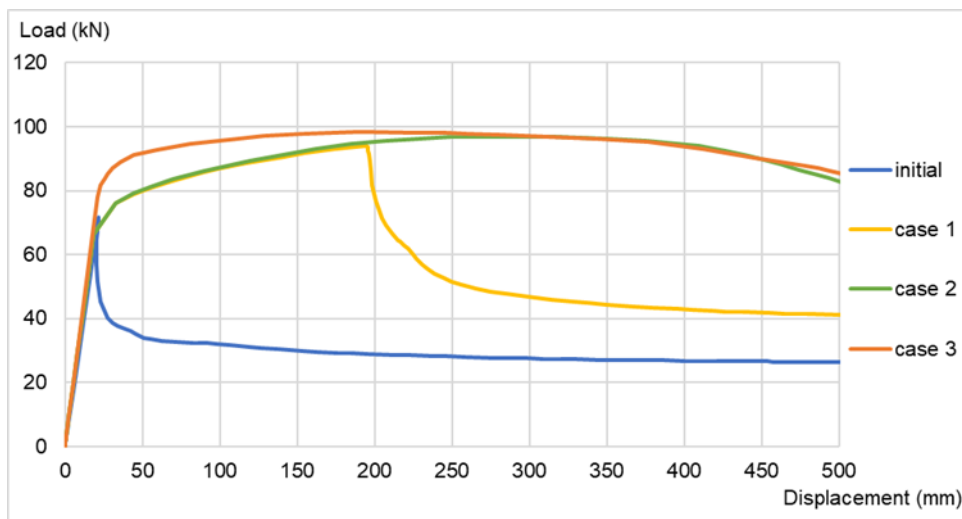


Figure 5.5: Load – displacement, CHS substructure type II.

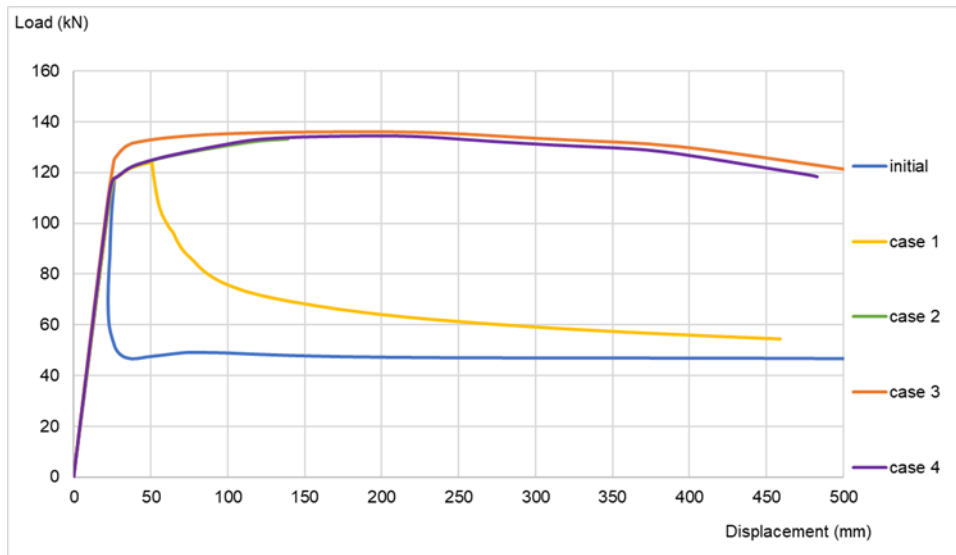


Figure 5.6: Load – displacement, OPEN section substructure type II.

In this pre-design, premature buckling was occurring on the compression brace “BAR 2” (according to Figure 4.7). In that way, by increasing the dimensions of this profile it was possible to obtain the desired ductile behaviour. In some situations, it was also considered an alternative section for brace “BAR 1” due to its large tension force. The final combination of profiles was chosen to be “case 3” for substructure type I and “case 4” for substructure type II.

These results also enabled to determine the action load that will be applied in final joints’ models. Therefore, forces of 90kN for CHS and 130kN for OPEN sections’ truss specimens were chosen.

Finally, when looking at trusses’ deformation shape with the final chosen dimensions, it was concluded that this pre-design presents a good result in terms of global behaviour as the critical point where buckling is going to occur is placed on the lower chord, near the supports.

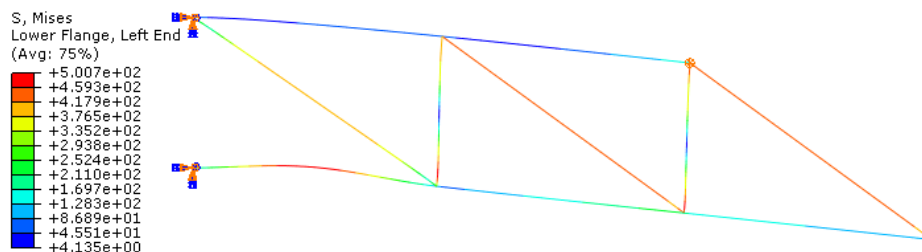


Figure 5.7: Von Mises stresses on deformed substructure type I (units in MPa).

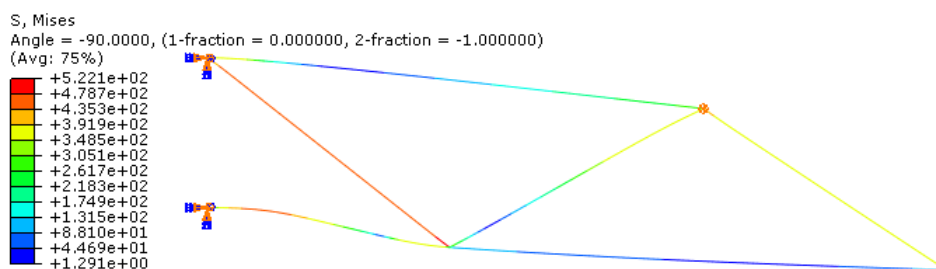


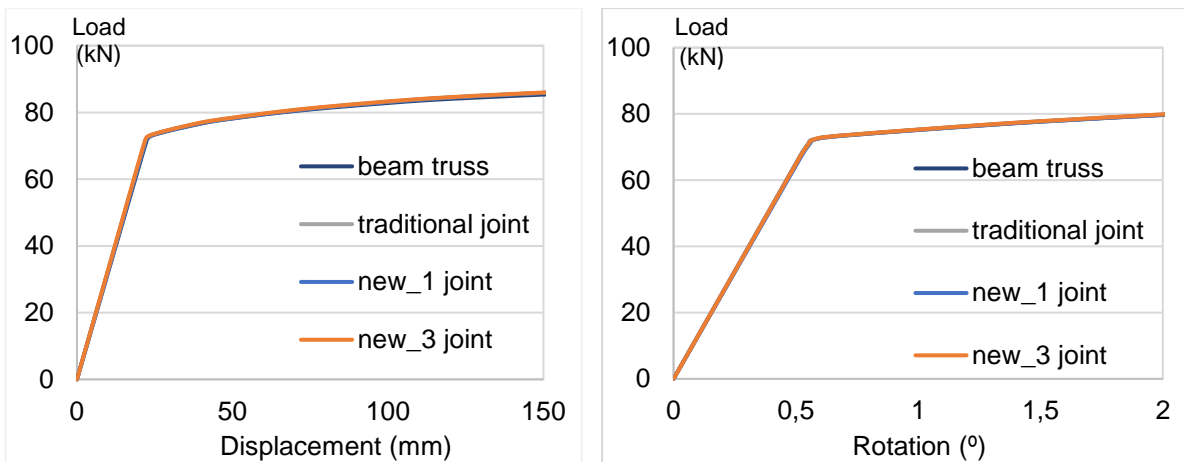
Figure 5.8: Von Mises stresses on deformed substructure type II (units in MPa).

### 5.1.4. Results of numerical model on joints

Concerning the joint's analyses, the results from all types of connections studied in truss type I (CHS and OPEN sections) are first shown as well as a comparison between them. Thereafter, the same procedure will be applied to truss type II. Finally, truss specimens will be compared and some conclusions will be draft.

#### 5.1.4.1. Substructure type I

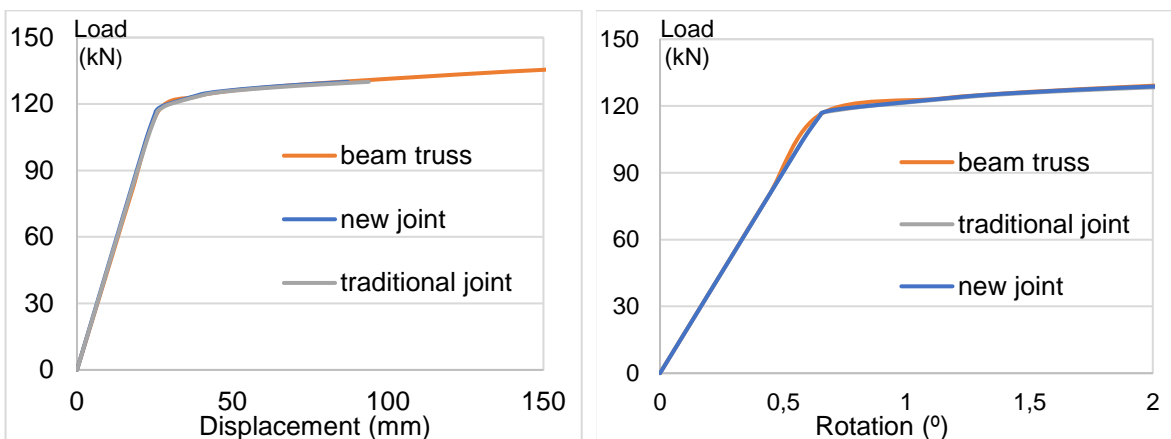
Starting by analysing the global behaviour of different 3D joints models and comparing them with previous pre-design results, Figure 5.9 and Figure 5.10 show the development of displacements and rotations for each section profile, respectively, on the truss extremity node.



a) Load - displacement

b) Load - rotation

Figure 5.9: Global behaviour of CHS models - substructure type I.



c) Load - displacement

d) Load - rotation

Figure 5.10: Global behaviour of OPEN section models - substructure type I.

From these four diagrams, it is very clear that global behaviour of truss specimens is not being affected by different joint's typologies, neither in displacements or rotation in-plane. This result was not expected from an initial perspective on the influence of innovative connections.

As it was already introduced, the rise of new joints' stiffness might not only affect joints strength but also truss members' resistance. On the other hand, by adopting the global model as a combination of beam and solid elements where only two joints are being specified, a big simplification is being done and this might explain the non-existence of differences in these analyses. Additionally, it should also be noted that the structures in cause represent specimens from truss girders and their smaller dimension as well as boundary conditions may not provide the best description of real truss girder behaviour. In that situation, perhaps the influence of these joints could be better noticed.

Hereinafter, looking from a local perspective, the following Figure 5.11 and Figure 5.12 present the graphics of the deformation on chord's face during load application.

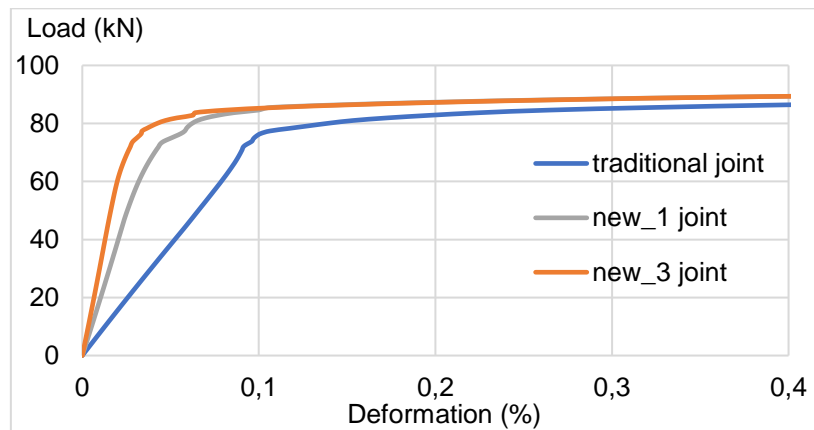


Figure 5.11: Chord surface deformation on CHS N-joints (A).

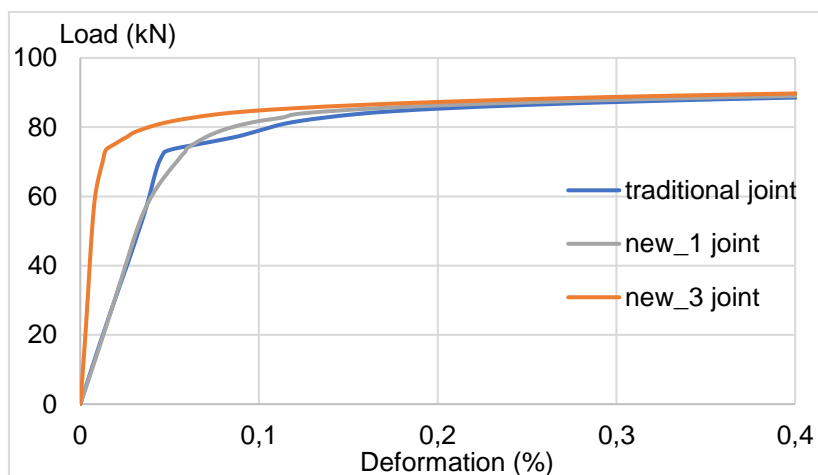


Figure 5.12: Chord surface deformation on CHS N-joints (B).

The previous graphics can primarily conclude that joint "new\_3" (with both braces embedded inside the chord in half cane) represent an advantageous solution in terms of chord's strength by presenting less deformation comparing to others. Concerning to joint new\_1, the difference to the traditional solution was expected to be more significant.



In fact, variations between joints are not much expressive and the advantages of LASTEICON solutions are not clearly denoted. Moreover, despite the traditional connection (A), any of the other joints reached the ultimate failure deformation (set at approximately 0,82% or the theoretical value of  $3\% \cdot d_0$ ), which means that chord's face failure mode is not being critical on joints resistance.

The representation of effective plastic strains (PEEQ) in joints deformed shape (which is qualitatively alike to all CHS N-joints solutions), comes to testify the previous statement (Figure 5.13). It can be observed that the deformation on brace members is considerably higher than in the rest of the joint. At a first stage, it might be disregarded that chords are oversized and their strength is preventing the expected failure modes to occur.

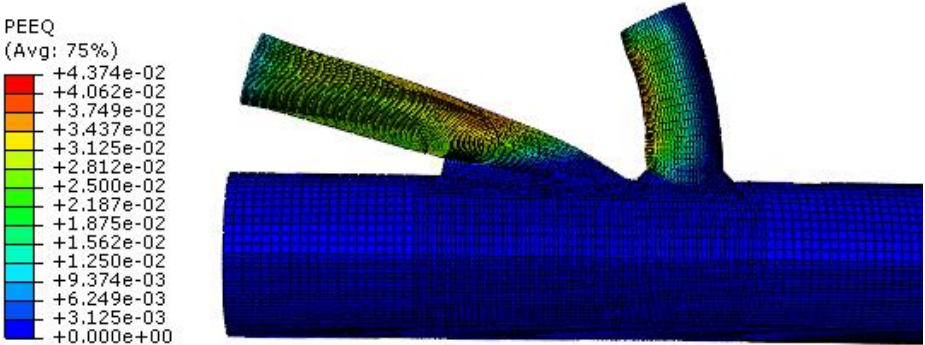


Figure 5.13: Effective plastic strain on traditional connection (A), truss type I.

Additionally, from the graphics of Figure 5.11 and Figure 5.12, a closer look on deformation values enables us to conclude that when comparing connections A and B (compression and tension chords) the deformation on A is bigger, for a specified load. This result is in relation with the forces applied on the chord once compression will positively influence this deformation.

Figure 5.14 shows the second deformation parameter calculated on the vertical brace member, in compression, for the connection A (for connection B is identical). The curves on the diagram clearly show that the indicated deformation is not affected by the typology of the joint. Additionally, it is observed that deformation magnitude is bigger in this member and inclusively exceed the ultimate limit, which means that local failure is going to occur in braces' member and not in the chord.

Figure 5.15 shows Von Mises stresses distribution for "traditional" and "new\_1" joints where it is seen that maximum stresses and deformations are very similar in both models whereas, in the embedded region, stresses are much smaller and almost insignificant. In fact, when comparing this deformed shape with other results obtained from previous research in this field (Figure A.2, from Appendix) it can be concluded that chord's dimensions are oversized and therefore affecting the study of these solutions.

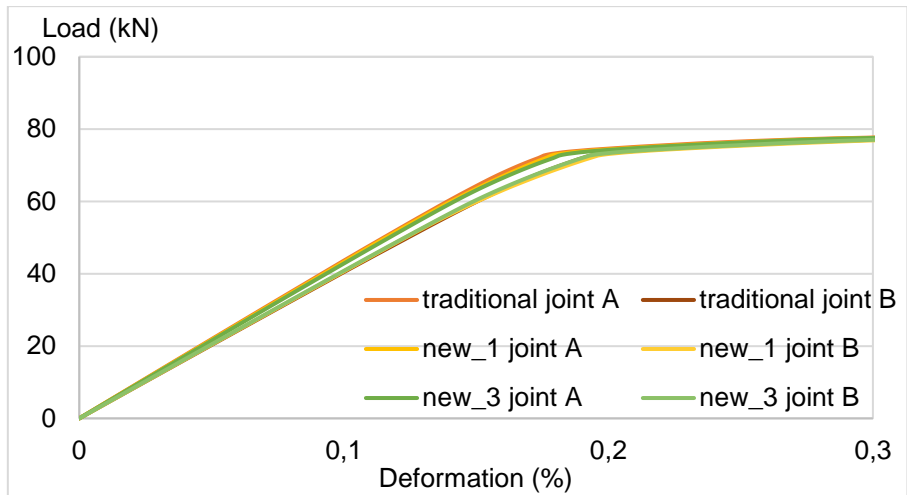


Figure 5.14: Vertical brace deformation of CHS N-joints (A & B).

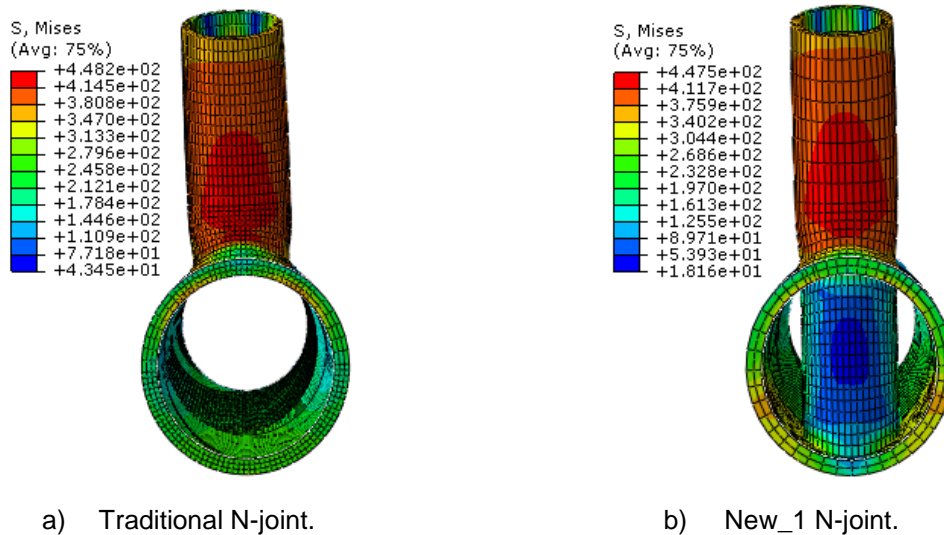
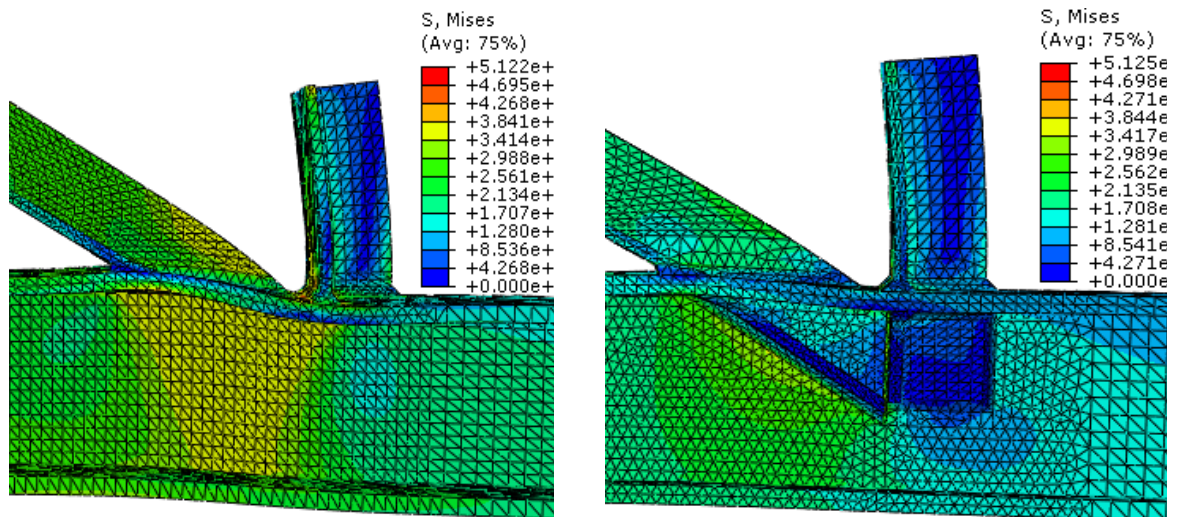


Figure 5.15: Von Mises stresses on CHS N-joints (A) (units in MPa).

Finally, it's time to analyse the OPEN section joints. The geometry of this typology of joints is much different from CHS and in this case the deformations calculated previously were inconclusive once braces forces are going to induce larger deformations in chord's flanges than in the web (Figure 5.16, (a)), because it has higher moment of inertia. Thus, the analyses on OPEN section joints deformation were conducted on the upper flanges (Figure 5.16). This deformation corresponds in fact to an angular distortion caused by the relative flange displacements.

Additionally, by comparing both solutions bellow (Figure 5.16) it is perceptible that the "New" solution reduces the distortion induced by brace forces although with very small gains. The graphic in Figure 5.17 comes to verify the same conclusion: the intersection of bracing members through the chord has reduced flanges' distortion.



a) Traditional N-joint.

b) New N-joint.

Figure 5.16: Von Mises stresses on OPEN section N-joints (A) (units in MPa).

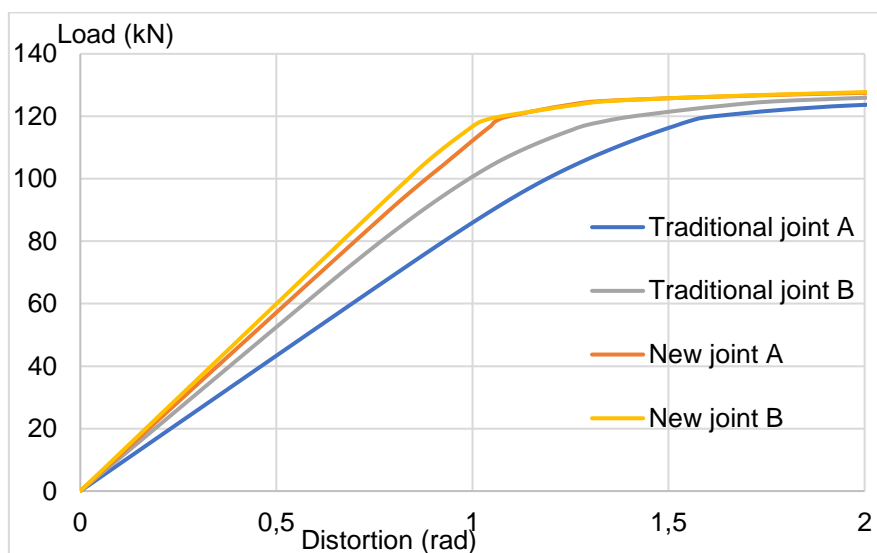


Figure 5.17: Vertical deformation of the upper flange of OPEN sections N-joints (A & B).

Similarly to what has been done with CHS joints, the deformation on vertical brace members of OPEN section N-joints was determined (according to Figure 4.23). From the results on Figure 5.18, no significant differences were observed between innovative and conventional solutions. However, when comparing both connections (A and B) a large difference was obtained, which is in contrast with initial expectations as well as with the results of the same parameter in CHS profiles (Figure 5.14).

In fact, this difference is resultant from the compatibility problem related to the use of angle profiles in these types of connections, described already in section 4.3.2.. In Figure A.1 (Appendix), this problem is also described through a 3D image, so it can be easily understood.

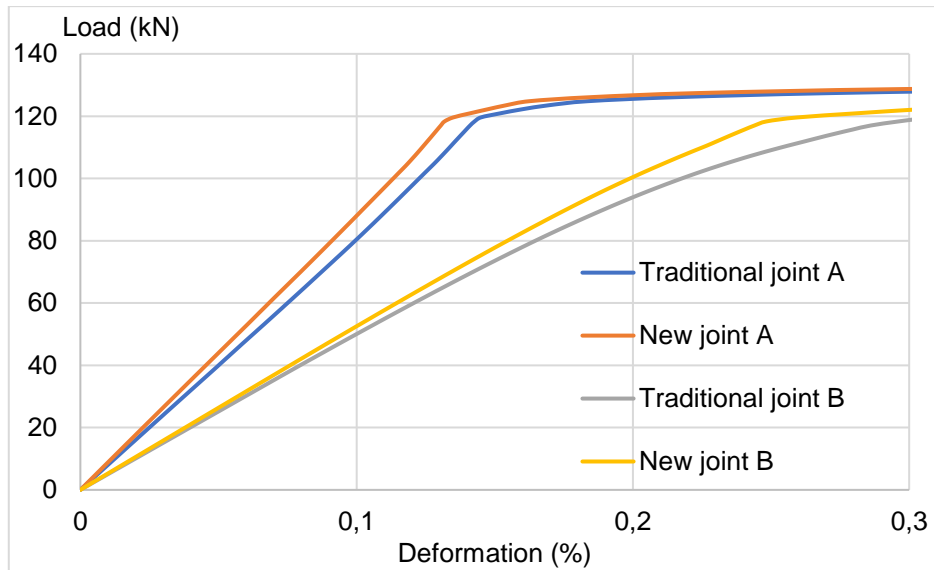


Figure 5.18: Vertical brace deformation of OPEN sections N-joints (A & B).

#### 5.1.4.2. Substructure Type II

Shifting the analyses to substructure type II, where K-joints are going to be studied, Figure 5.19 and Figure 5.21 start by presenting the global behaviour of different models, for CHS and OPEN section profiles.

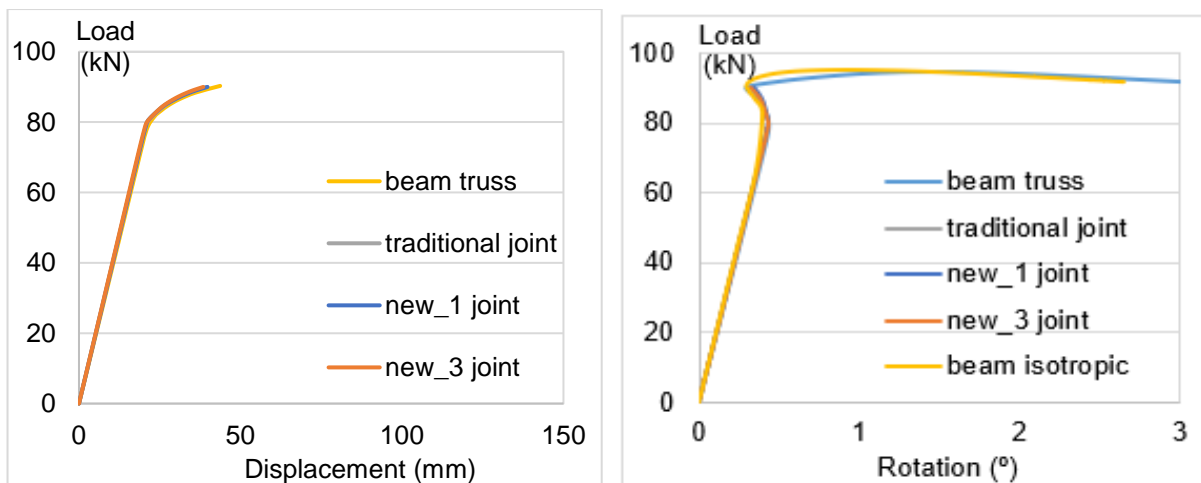


Figure 5.19: Global behaviour of CHS models – substructure type II.

The rotation diagram on CHS, truss type II, shows an anomaly when load passes upon 80kN, as it continues to increase while rotation reduces. From different model's comparison, it is concluded that neither solid joint, mesh quality nor material properties ("beam isotropic" model) are causing this behaviour once the results are identical in all of them.

However, the lower chord is in compression and failure will occur due to buckling near the lower support. Due to chord's bigger stiffness, it is going to respond like a continuous beam that is being tensioned by two bracing diagonals in the opposite direction of the deformation. Therefore, the chord is prone to have a small bend, qualitatively represented in Figure 5.20, which might be creating this inversion of rotation (in the extremity node).

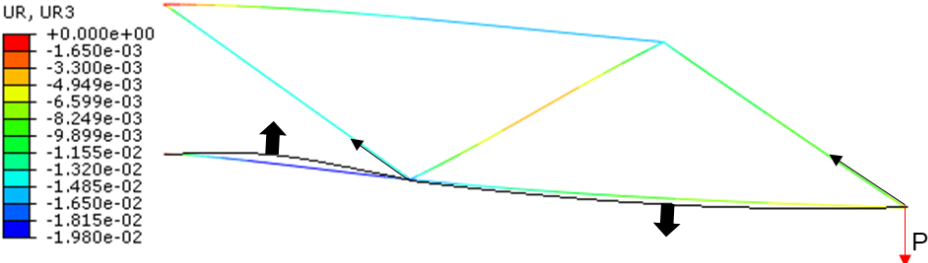


Figure 5.20: Rotation deformation of CHS truss specimen type II (units in rad).

In Figure 5.21, the global behaviour for OPEN sections in substructure type II is represented.

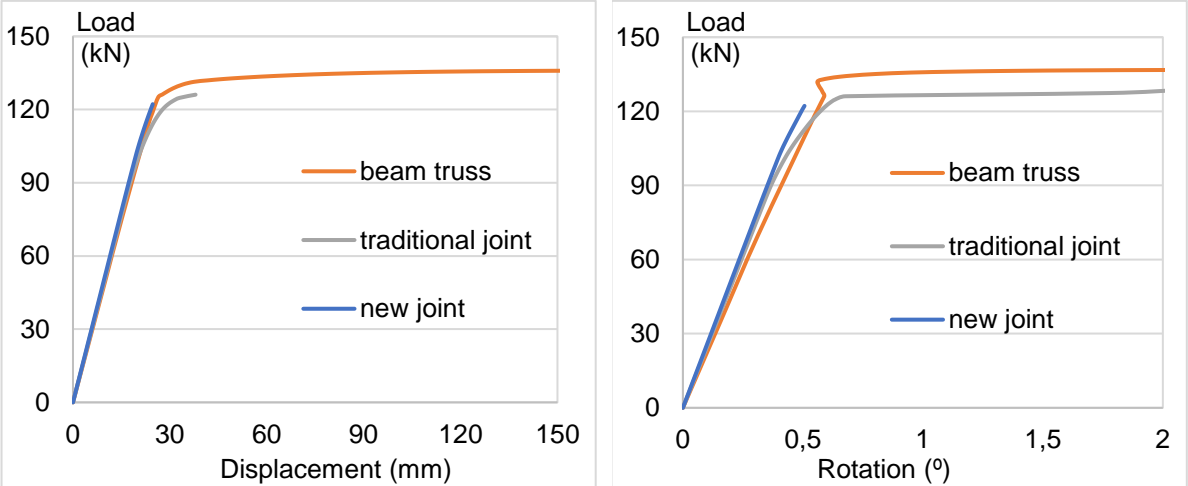


Figure 5.21: Global behaviour of OPEN section models - substructure type II.

Similarly to truss specimen type I, the influence of different joints' typologies in the global behaviour of the truss was not observed.

It is noted that the slope of the curves suddenly decreases in the end of the simulations presented so far. This situation refers to inherent non-linearity problems in which models, after some deformation, start to diverge. In addition, it is seen that for some 3D joints models the simulation stops right before that big variation in the slope of the diagrams whereas for beam element models that does not happen. In fact, when that stage is reached, the deformations may distort the elements (tet and hex) and the FEM is not able to solve the equilibrium equations, even if the time step is reduced. Therefore, convergence is not achieved and the simulation is "aborted". To overcome this issue and achieve

convergence, a more refined mesh should have been used adopting automatic stabilization mechanisms.

In sum, for the following analyses the numerical results above the load of 80kN won't be considered.

Proceeding with the determination of chord's deformation, a representation of the lateral displacement (U3) on connections A and B (Figure 5.22), is firstly shown which from a qualitative point of view is similar in all three joint solutions.

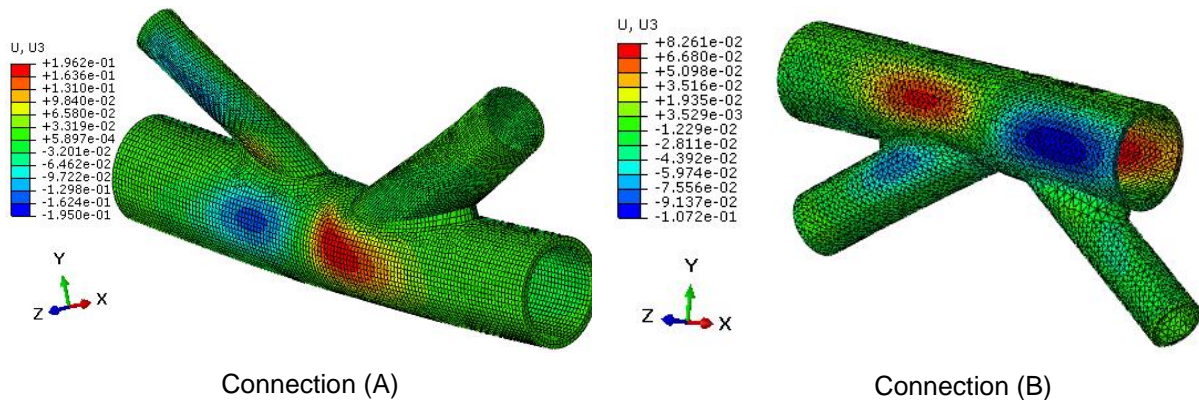


Figure 5.22: Lateral displacements variation on CHS K-joints (z-direction) (units in mm).

According to U3 (displacements in the z-direction) colour's legend, the lateral chord's face expansion corresponds to positive values (in red) and the lateral tightening corresponds to negative U3 values (in blue), which is in accordance with the direction of the applied forces (see Figure 4.12).

The calculation of the vertical deformation on chord's face was neglected once it was placed in the middle of the two highlighted regions, represented in Figure 5.22, which represent the maximum lateral displacements of the chord's wall. To accurately estimate these phenomena, the calculation of chord's face deformation was performed in the centre of those crucial regions.

The results are represented in Figure 5.23 and Figure 5.24 through a load vs deformation diagram. The signal of deformation was settled as equal to the initial displacement (U3) to differentiate both behaviours (wall expansion and tightening).

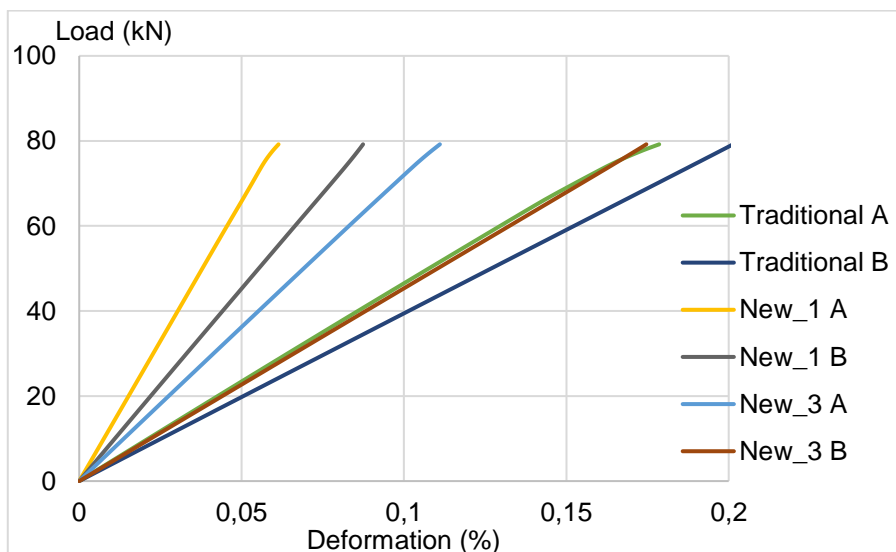


Figure 5.23: Lateral expansion deformation on chord's face of CHS K-joints (A & B).



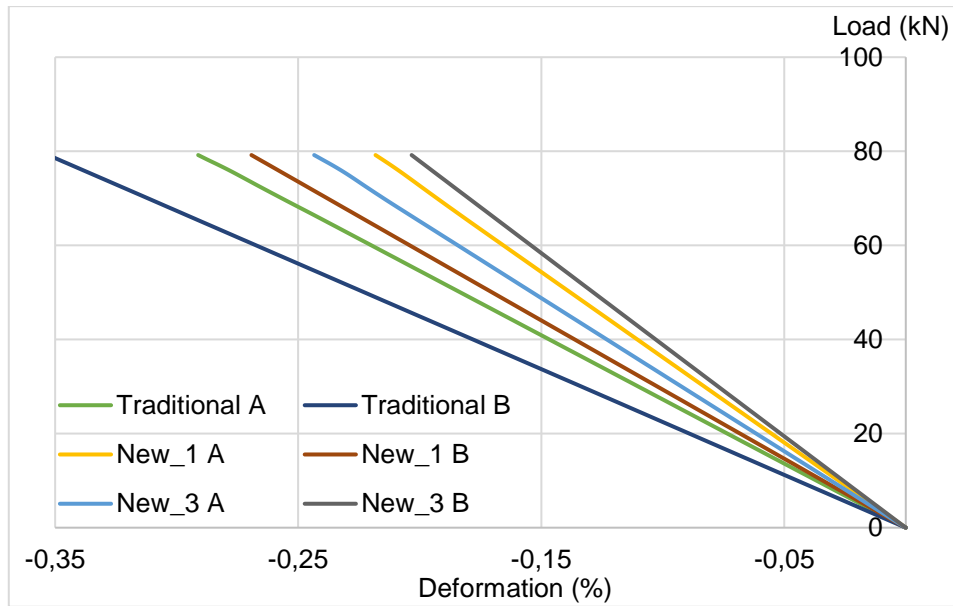


Figure 5.24: Lateral tightening deformation on chord's face for CHS K-joints (A & B).

The sequence of slopes for each of the joint models is being preserved in both diagrams and in agreement with the previous deformation models presented.

It is verified that both “New\_1 joint” and “New\_3 joint” contemplate less deformation than “Traditional joint”, giving a good prospect for LASTEICON solutions. Moreover, between both innovative joints, “New\_1 joint” gets the better performance in both analysis of connection (A), and in the first analysis (lateral expansion) of connection (B). This result reflects that when total brace member is embedded inside the chord, the chord's wall becomes more resistant and deformations are minimized. This can be explained by the distribution on stresses through the brace member, up to both top and bottom faces of the chord.

For the case where “New\_3 joint” is favourite (Figure 5.24), it is noted that the geometry of the joint is characterised by a reduction in the chord's length because it's located in an extremity node (see Figure 5.22, connection (B)). This aspect probably influences the result.

On the other hand, the solution “New\_1 joint” is reducing a large part of chord's surface and that effect should have caused a loss of strength, making solution “New\_3 joint” the most efficient, as expected. The reason why this is not being observed may be related to the fact that chord's stiffness is considerably higher than brace's and so the reduction of the walls surface might not cause the effect expected.

In Figure 5.23, the differences between connection (A) and (B) are well denoted which validates the previous conclusion that the compression in the chord member has big influence in the joint's behaviour.

Finally, Figure 5.25 and Figure 5.26 present the deformation analyses performed on substructure type II, adopting OPEN sections profiles. Starting by the determination of the distortion induced in the chord's flange, it is seen that no significant results exist to differentiate both solutions. Subsequently, the deformation on diagonal compression members was also estimated for both connections A and B. In contrast with the results derived for truss type I, in this case, no significant strength is observed for the innovative connections, when comparing to the traditional solution.

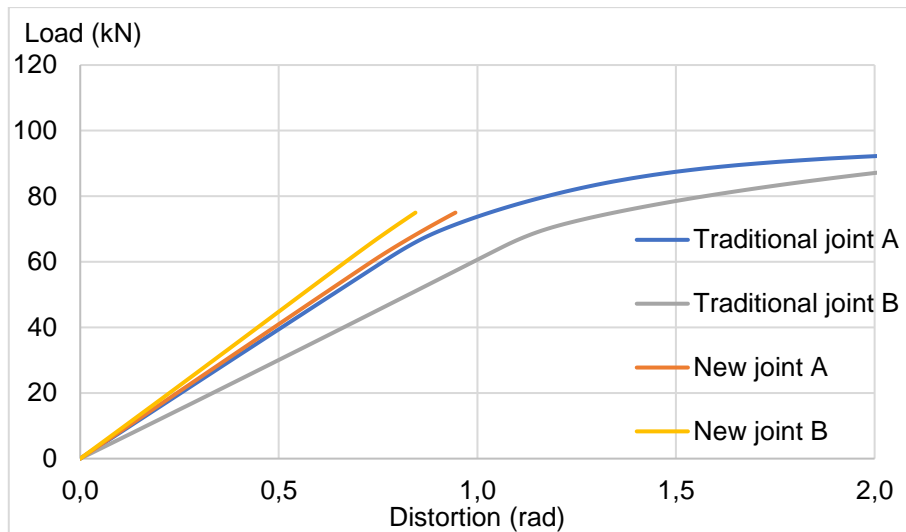


Figure 5.25: Vertical distortion in the upper flange of the chord for OPEN section K-joints (A & B).

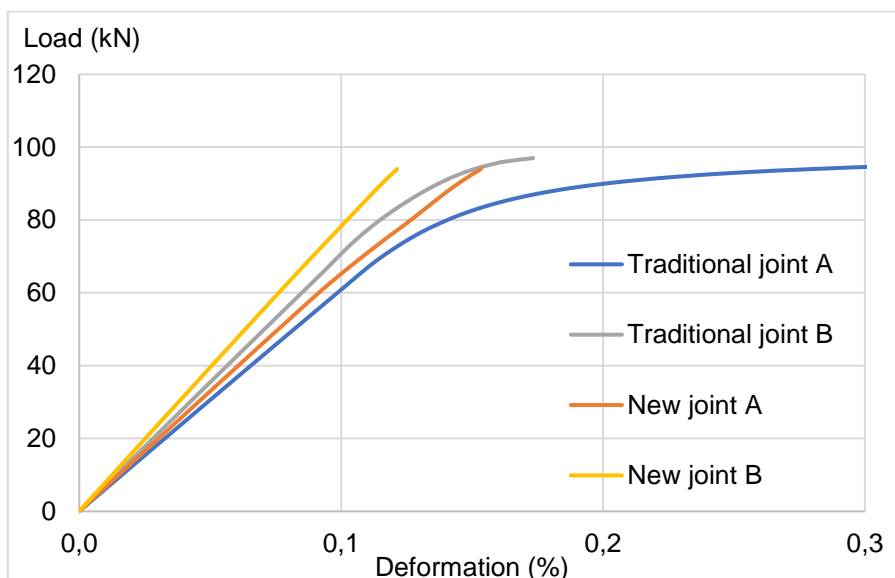


Figure 5.26: Longitudinal deformation in diagonal members for OPEN section K-joints (A & B).

In conclusion, the last analysis pretends to perform the comparison between both truss specimens' results. This comparison is based on the previous deformation parameters applied on the regions where maximum expansion deformation occurs. Therefore, Figure 5.27 collects all lateral deformations of CHS chord's face on connection (A), for truss type I and II, under the brace member in compression.

Before looking at the results, the evidence that the compression brace members in truss type II (K-joint) have bigger sections dimensions (CHS - 60,3x4,0mm) than the similar one in truss type I (N-joint, CHS - 42,2x3,2mm) may predict that the joints tested for truss type II will be stiffer and thus, deformations should be lower. However, truss type II also represents a more economical truss where the number of profiles is inferior and therefore forces on the brace members will be larger, which will consequently induce more deformation on the chord.



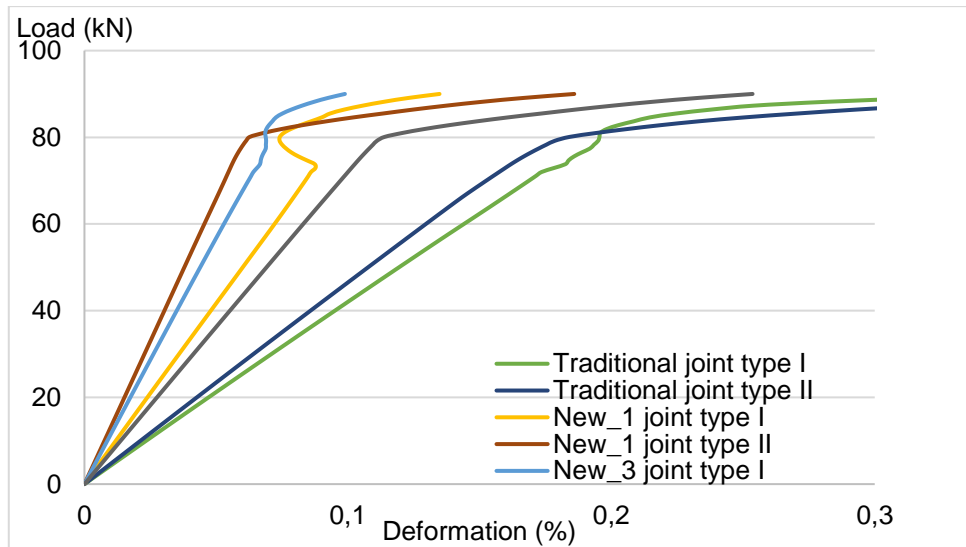


Figure 5.27: Lateral expansion of chord's face on CHS connection (A), for trusses type I & II.

The results from the previous diagram point out that both traditional models represent the weaker performance. On the other hand, the remaining models, corresponding to the innovative joints, show a better deformation performance, proving the advantages of LASTEICON solutions. As expected, the solution “New\_1 joint type II” has the smallest deformation due to bigger brace member’ section. Concerning “New\_3 joint”, it was also expected that type II solution would be better than type I, however, this wasn’t verified.

Regarding the OPEN sections truss specimens, the comparison will be made based on the distortion of the upper flanges due to bracing compression (Figure 5.28).

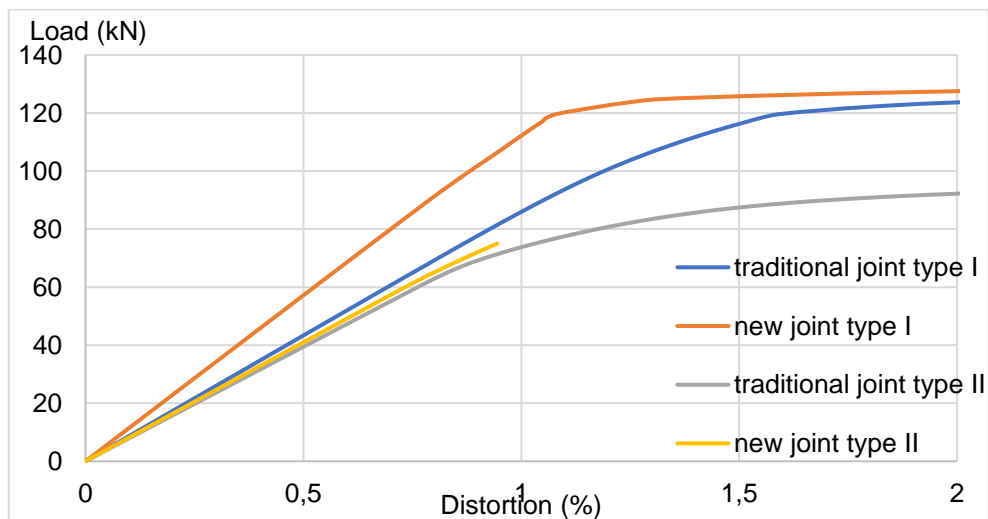


Figure 5.28: Vertical distortion in the upper flange of the chord for OPEN section connection (A), truss type I & II.

The comparison between OPEN sections summarizes that truss type II has more deformation on the chord’s flange in addition to a decrease in the load capacity. Again, both “new” connections represent a strengthened performance. Figure A.3, in Appendix, shows the Von Mises stresses distribution where previous conclusions can be verified.



# 6. Parametric analyses

From the previous studies on CHS profile truss specimens, results proved that the chord was too stiff and neither of the expected failure modes or deformation shape were being observed. In fact, the objective when designing truss specimens in section 5.1.3 was not correctly accomplished once the focus was taken only on brace members optimisation, disregarding the chords pre-design. In this way, it was decided to reduce the thickness of the chord from 6,3 mm to 4 mm (second lower dimension available in Vallourec).

From research it is stated that joint resistance increases as the diameter to thickness ratio decreases, which means that in this case, by reducing the thickness in 2,3mm, joint's resistance will decrease. This way, chord's stiffness will also decrease and more deformations will take place in this element. With this effect, it is expected that the difference between joint's behaviour is clearer and more objective conclusions can be drafted about LASTEICON solutions.

Starting by analysing the respective difference in the global behaviour of both trusses, Figure 6.1 and Figure 6.7 present the global displacements and rotations during simulation, for CHS truss type I and II, respectively.

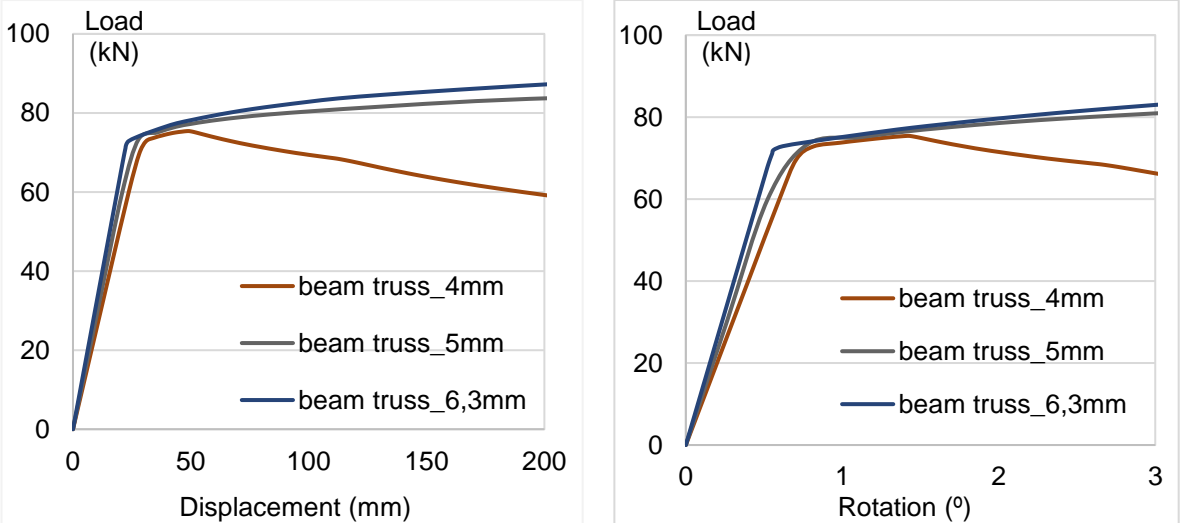


Figure 6.1: Global deformation of CHS profiles for different thicknesses, truss type I.

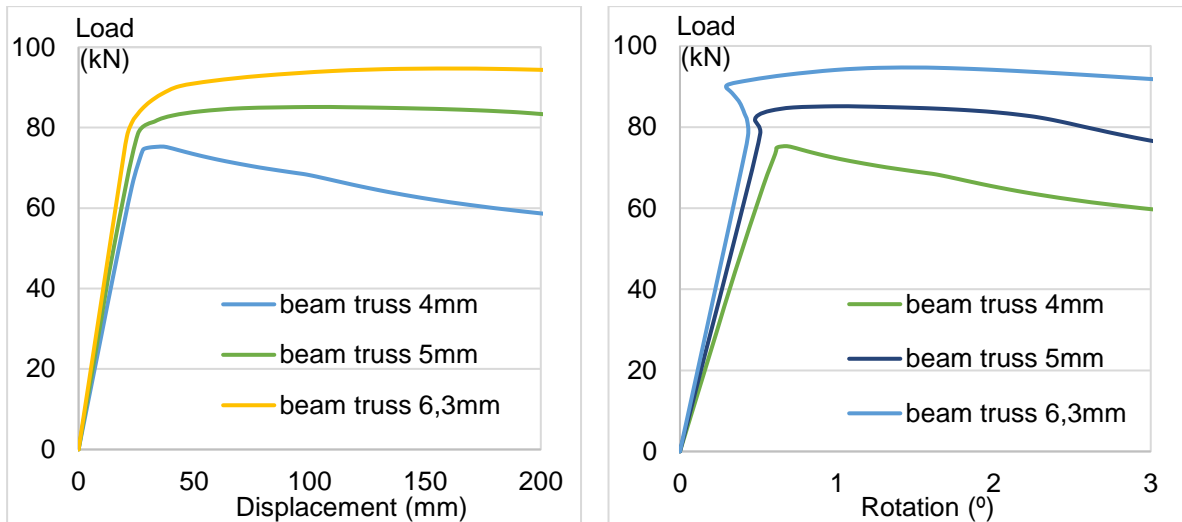


Figure 6.2: Global behaviour of CHS profiles for different thicknesses, truss type II.

The first important conclusion besides the loss of load capacity with thickness reduction is that for this new dimension, very small steel hardening capacity exists after achieving the yield stress (around a load of 74kN). In fact, the loss of inertia in the chord led to premature buckling.

The analyses on local joints behaviour were performed following the same procedure, where the deformation of the chord's face and brace member was determined. Accordingly, Figure 6.3 shows the respective deformed shape of a N-joint with 4mm chord thickness. For comparison, it is also represented the same connection with the initial dimensions in Figure 6.4 (thickness of 6,3mm).

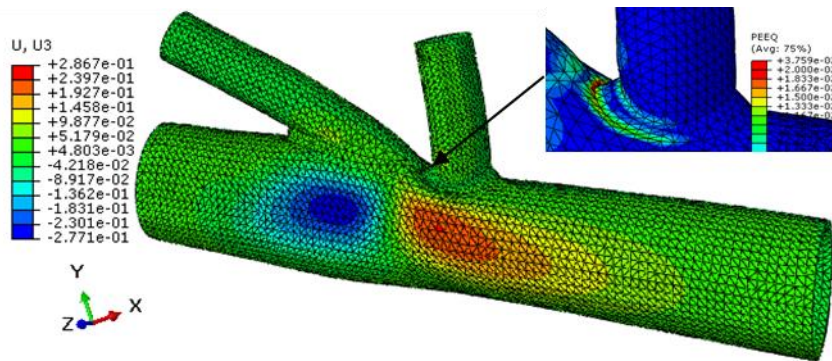


Figure 6.3: Lateral displacements in CHS N-joint (A) with 4mm thickness, truss type I (units in mm).

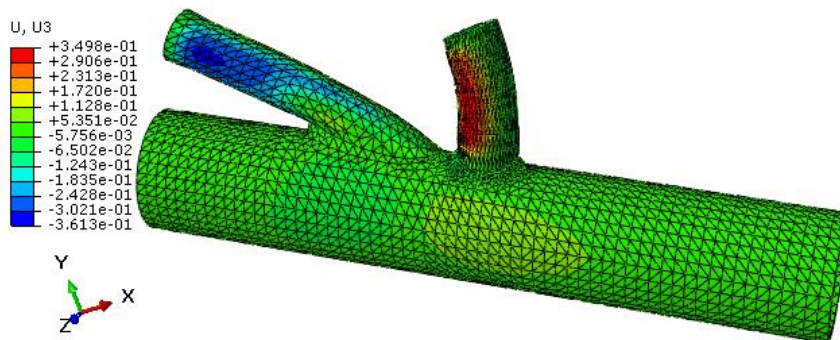


Figure 6.4: Lateral displacements in CHS N-joint (A) with 6,3mm thickness, truss type I (units in mm).

In Figure 6.3, besides the expected highlighted regions showing where large lateral chord's deformation occurs, it is denoted the detail between the vertical brace member and the chord, where it is located the maximum stresses and plastic strains (PEEQ). This region becomes a critical point of the connection once it is related with chord face failure mode, which was not occurring in the initial model. Additionally, the big tension in the diagonal brace member is inducing the possibility to occur punching shear failure.

Comparing both models, it is clear how regions with maximum displacements change from one model to the other. As prove, the reduction of stiffness from the chord increased substantially the stresses and the deformation in the element, where before were placed on the bracing members.

Replacing the graphic of "Figure 5.11: Chord surface deformation on CHS N-joints (A)" and overlapping it with the parametric results from 4mm chord's thickness (Figure 6.5) it is possible to compare this parameter's influence. Additionally, it is represented in Figure A.4 (Appendix) the Von Mises stress distribution for all the studied connections with a cutting view perpendicular to longitudinal chord's axis located where the deformation measurement was done.

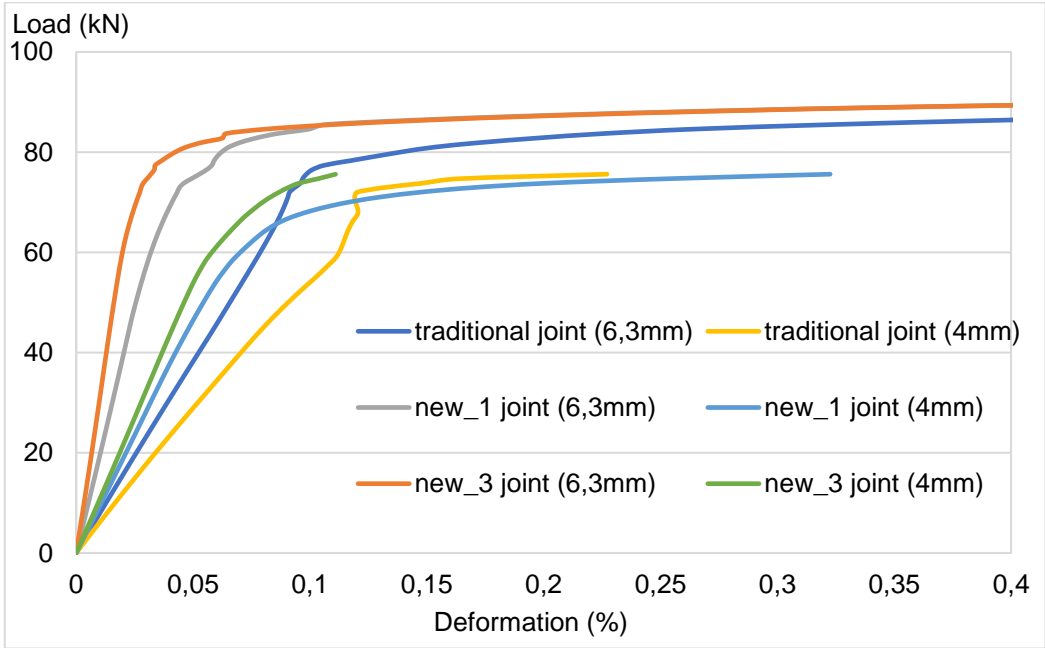


Figure 6.5: Vertical chord surface deformation on CHS N-joints (connection A) for both chord thicknesses, truss type I.

By looking for models "traditional joint (6,3mm)", "new\_3 joint (4mm)" and "new\_1 joint (4mm)" it is revealed that by applying LASTEICON solutions the performance of a model with smaller thickness profile is identical to the conventional solution with bigger thickness chord dimension. This important result means that steel wasting material can be saved, structural weight and costs can be reduced and laser cutting technology has potential to enhance the structural performance of trusses.

The same application was performed for connection (B), as shown in Figure 6.6, and where it can also be verified the advantages of connection "new\_3 joint (4mm)" in relation to the conventional one.

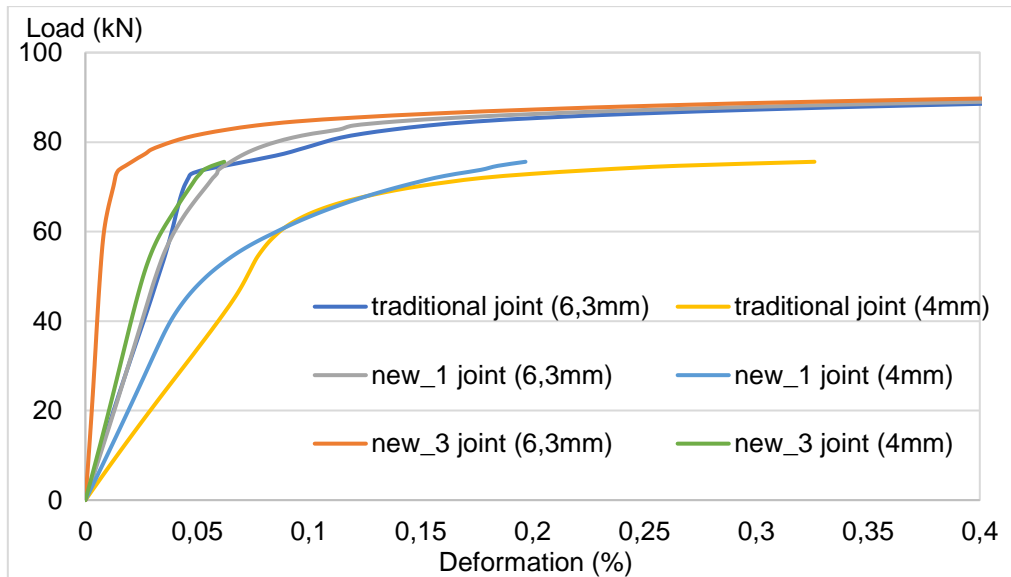


Figure 6.6: Vertical chord deformation on CHS N-joints (connection B) for both chord thicknesses, truss type I.

For truss type II, the new thickness dimension was also simulated and following analyses were performed (Figure 6.9 and Figure 6.10). Figure 6.7 represent the solution “new\_1 (4mm)” for connection A and Figure 6.8 represents the solution “new\_3 (4mm)” for connection A.

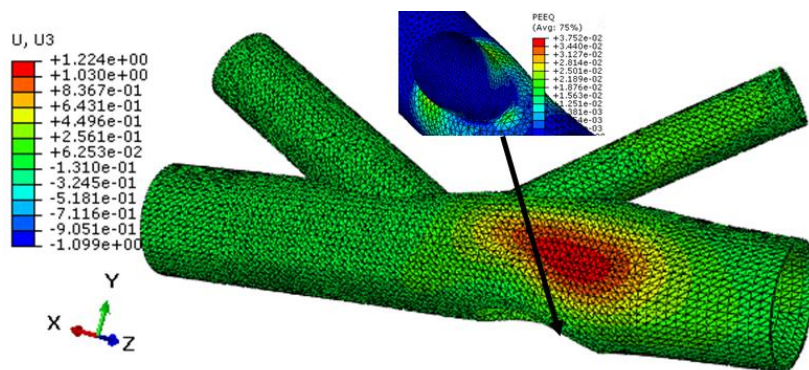


Figure 6.7: Displacement diagram “New\_1 (4mm)” (connection A), truss type II (units in mm).

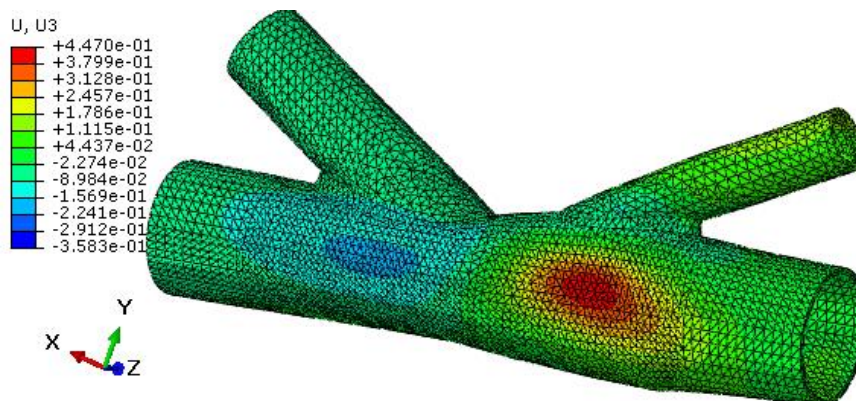


Figure 6.8: Displacement diagram “New\_3 (4mm)” (connection A), truss type II (units in mm).

From Fig. 6.7 the embedded brace diagonal, with larger section, is causing the occurrence of larger plastic strains near the opening hole on the bottom face of the chord. Additionally, it is possible to see that the tightening deformation region (in red) from “New\_1 (4mm)” has moved in result of the hole created.

In both cases, the presence of embedded members is causing compression in the bottom surface of the chord whereas, on the top, the other brace is in tension. Therefore, two opposite forces are going to be applied in the same vertical plane, resulting in the increment of tightening deformation.

Figure A.5, in Appendix, gives a good perspective of the results explained above by showing the Von Mises stresses distribution of different joints on their deformed shape.

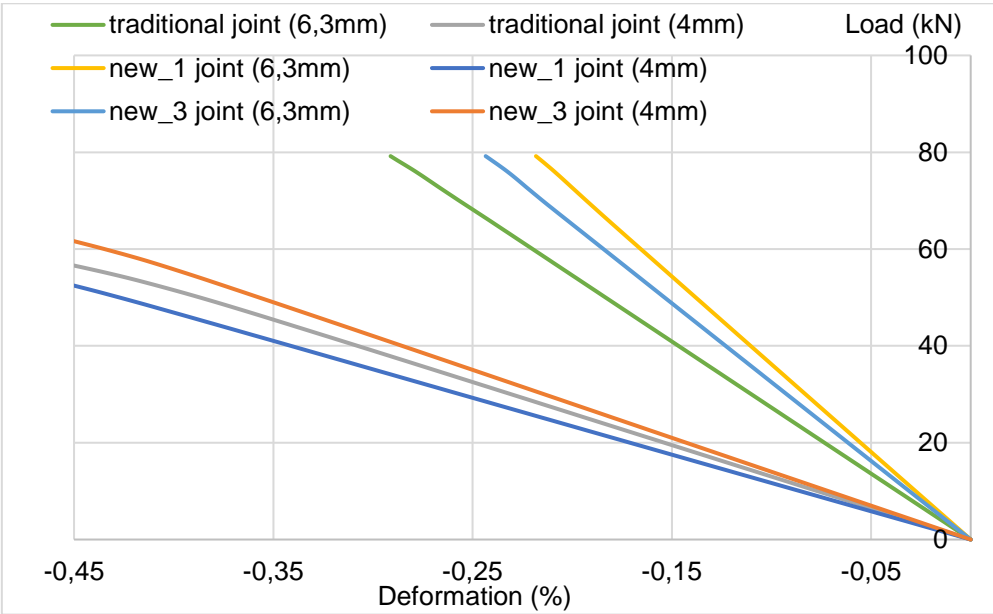


Figure 6.9: Lateral tightening deformation of CHS K-joints (connection A) for different chord thicknesses, truss type II.

In agreement with the results from previous deformed shapes, Figure 6.9 shows how the connection “new\_1 joint (6,3mm)” had the best performance and “new\_1 joint (4mm)” had the worst.

Additionally, the results from both design dimensions are detached which means that in this case the first chord thickness solution cannot be replaced by an economical solution.

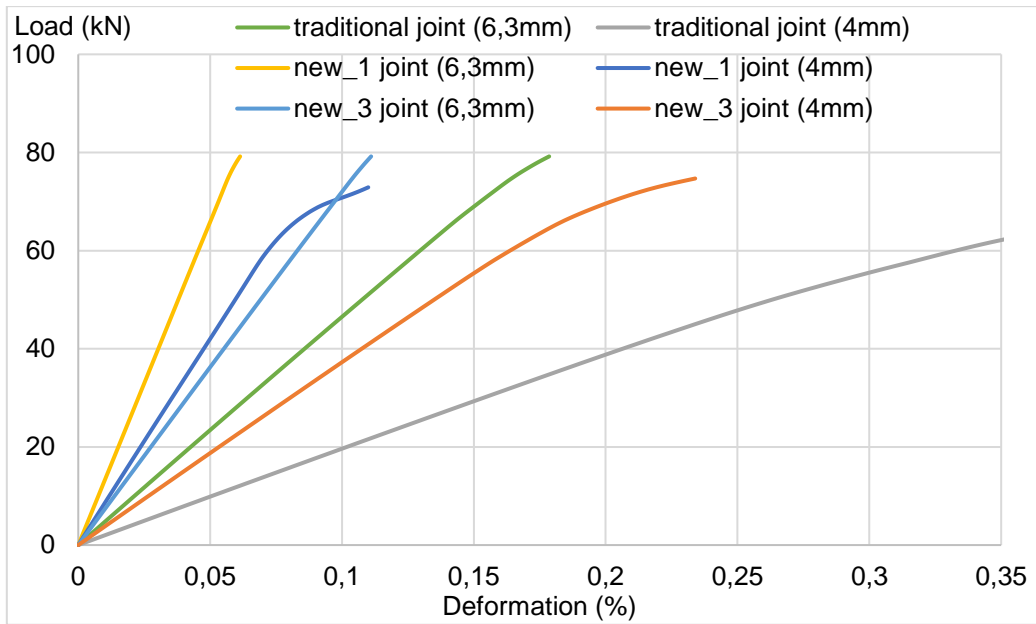


Figure 6.10: Lateral expansion of chord's face on CHS K-joints (connection A), for truss type II.

In contrast with Figure 6.9, in Figure 6.10 it is concluded that to optimize lateral deformation due to bracing compression, the connection “traditional joint (6,3mm)” can be replaced by “new\_1 joint (4mm)”, achieving more strength. The deformation shape of these connections is represented in Figure A.6 where it can be observed the Von Mises stresses distribution.



## 7. Conclusions and future developments

### 7.1. General conclusions

In the present work, a study on the static behaviour of steel truss specimens' connections, created through laser cutting technology, was developed. These connections consist in creation laser cut slots in the chord's face, so that brace members can pass through and be welded both on bottom and top surfaces.

The study was based on the results provided by a numerical analysis performed on two different truss specimens' connections, where a combination between solid and beam elements was adopted.

Overall, joints' structural performance was enhanced in comparison to conventional connections which proves the viability to proceed with these new joints typologies through more advance analyses, such as experimental tests.

From global behaviour analyses performed on truss specimens, significant differences were not found between the different models studied. This result was not expected and might be related to the model approach adopted.

Particularly for CHS truss specimen type I, joint "New\_3", which considers both braces members passing through the chord, was the solution with better performance in terms of chord deformation. Additionally, for OPEN sections, the "new joint" typology has also exhibited the better performance in terms of deformation. From the two connections studied for each truss model (connections A & B), some differences were observed, with respect to the influence of chord's axial force (compression and tension).

In what concerns to CHS truss type II, the results are not so clear once they differ for different parameters studied, however, both innovative solutions represented advantages when compared to conventional ones.

Moreover, a parametric analysis was performed based on the initial numerical results, where the thickness of truss type I chords was decreased. The analysis of "New\_3 joint" deformations, considering with 4mm of chord's thickness, revealed to have an identical performance to the initial "traditional joint" (with 6,3mm of chord's thickness). These results show how the application of LASTEICON solutions can optimize structural design and consequently reduce wasted steel material, weight and costs of the structure.

Finally, the investigation upon issues like sustainability, economy and fabrication processes demonstrate how this technology, when applied on steel structures, can have a remarkable impact on the technological development of construction industry.

## 7.2. Numerical tests

Numerical models were developed using Abaqus FEM. The simulations comprised a pre-design of truss specimens under monotonic action with displacement control followed by a study on joints behaviour. To accomplish this, a set of parameters like displacements, rotation, stresses and action load were used to compare joint's resistance, strength, deformation and rotational stiffness on joints.

Several modelling difficulties were found, starting by the design of joints using a 3D modelling software (SW) and subsequently transfer to Abaqus. The choice to perform the 3D designs on another software revealed to be challenging once the initial effort on trying to represent all joints' details, like welding, tolerances and angle of cut, resulted in too complex geometries with serious problems in mesh refinement and model simulations. In fact, numerical convergence was an obstacle to the analyses due to the high computational demands, inherent of the non-linearity of the problem. One of the solutions could have passed by the simplification of model characteristics, as for example, symmetry properties or the adoption of shell elements, instead of solid.

In general, the conclusions achieved from the several models tested agreed with the initial expectations present in the beginning of this project.

## 7.3. Future developments

The research work on the LASTEICON project is still in its early stage and these results pretend to serve as recommendations and guidelines for future experimental tests where accurate results will be obtained upon the behaviour of these connections.

Furthermore, in terms of numerical analyses it is expected that upcoming results on experimental tests can help calibrating and validate 3D models.

Regarding to following upcoming tests on numerical models, other parameters likely to influence the performance of the joints or analyses' approach could be tested. Those numerical models could contemplate:

- The thickness of bracing and chord members. According to research investigation made, the  $\beta$  parameter, correspondent to brace and chord diameters ratio, has influence on joint's strength and therefore, it should be taken into analysis;
- The cutting tolerances. As already referred in this work (section 2.6), a tolerance study pretends to minimize welding waste material by performing more precise cuts making use of laser technology. In this work no tolerances were considered but in upcoming LASTEICON tests this issue will become relevant.
- The test on real truss girders. In fact, as an extension of the work performed on truss specimens, it is pretended to analyse joints behaviour under real conditions set by a real truss structure;

- The relative rotation between joint's members. By analysing this parameter, it should be possible to understand how the rotational stiffness classification of each type of joint is affecting the structure;
- The adoption of a channel section (U-section) profile for the bracing members of OPEN section truss specimens. This way, the higher moment of inertia in the out-of-plane direction (which restrains buckling in-plane), will create a stiffer joint solution and avoid compatibility problems (see Figure A.1, Appendix).
- The test of other joints' typologies. In fact, all joints studied in this work are characterised by having two brace members, one in compression and one in tension, which in reality is the most common solution. However, to study the influence of LASTEICON connections on the resistance against common joint's failure modes, the analysis of a T-joint may come out to be the most efficient approach.



## Bibliography

- ABAQUS. v.6.13 *Documentation*. Dassault Systèmes, Simulia, 2013.
- B2Bmetal.eu. 2014.
- BOERAEVE, Ph., ERNOTTE, B., DEHARD, J., BORTOLOTTI, E., ZIELEMAN, Ph., and BABIN, J.M. *A joints solution by laser cutting in the chords of CHS structures*. IIW International Conference "Tubular Structures", 2006.
- BUEHLER, M. M. *Presentation "Committed to Improving the State of the World", Lisbon. BCG analysis in World Economic Forum*. IST, Lisbon, 2017.
- BURSI, O. S., and A. KUMAR. *Design and integrity assessment of high strength tubular structures for extreme loading conditions (Hitubes)*. Research Fund for Coal and Steel, European Commission, EUR 25903 EN, 2013.
- BURSI, O.S., M. D'INCAU, G. ZANON, S. RASO, and P. SCARDI. *Laser and mechanical cutting effects on the cut-edge properties of steel S355N*. Journal of Constructional Steel Research 133, 181–191, 2017.
- CASTIGLIONI, C., et al. *LASTEICON project proposal 709807*. Participant Portal Submission Service, 2015.
- EN1993-1-8. *Eurocode 3: Design of steel structures - Part 1-8: Design of joints*. Brussels: Comité Européen de Normalisation (CEN), 2005.
- ESPINHA, M. *Hysteretic behaviour of dissipative welded devices for earthquake resistant steel frames*. Master Thesis, Instituto Superior Técnico, Universidade Técnica de Lisboa, 2011.
- FELDMAN, M. *Stahlbau Leichtmetallbau*. 2016. <http://www.stb.rwth-aachen.de/projekte/2016/LASTEICON/LASTEICON.html>.
- FINCON, Consulting Italia. *T.1.2 Pre-design of main joint typologies*. Project LASTEICON 709807, Research Fund for Coal and Steel, 2016.
- HALE, S. CAE Associates. 2014. <https://caeai.com/blog/how-do-i-know-if-my-mesh-good-enough>.
- IVARSON, A., J. POWELL, and J. SILTANEN. *Influence of alloying elements on the laser cutting process*. 15th Nordic Laser Materials Processing Conference, Physics Procedia 78 84 – 88, 2015.
- KELLENS, K., G.C. RODRIGUES, W. DEWULF, and J.R. DUFLOU. *Energy and Resource Efficiency of Laser Cutting Processes*. 8th International Conference on Photonic Technologies LANE, 854 – 864, 2014.
- KHODAIE, S., M. R. MOHAMADI-SHOOREH, and M. MOFID . *Parametric analyses on the initial stiffness of the SHS column base plate connections using FEM*. Engineering Structures 34, 363-370, 2012.
- KIRSCH, U. *Optimal topologies of structures*. Applied Mechanics Reviews 42, 1989.
- LASTEICON. *Website*. 2016. <http://www.lasteicon.eu/>.
- LI, L., M. SOBIH, and P. L. CROUSE. *Striation-free Laser Cutting of Mild Steel Sheets*. CIRP Annals Vol. – Manufacturing Technology, 193-196, 2007.

- MADIĆ, M., J. ANTUCHEVICIENE, M. RADOVANOVIĆ, and D. PETKOVIĆ. *Determination of laser cutting process conditions using the preference selection index method*. Optics & Laser Technology 89, 214–220, 2017.
- RADIĆ, I., D. MARKULAK, and M. MIKOLIN. *Design and FEM Modelling of Steel Truss Girder Joints*. Republic of Croatia: Strojarstvo 52 (2) 125-135, 2010.
- SAIDANI, M. "The effect of joint eccentricity on the distribution of forces in RHS lattice girders." Coventry University, Warwickshire, UK, 1998.
- SILVA, L. S., SANTIAGO, A., L. S. SILVA, and A. SANTIAGO. *Manual de ligações metálicas*. Coimbra: Associação Portuguesa de Construção Metálica (CMM), 2003.
- SMITH, J., J. HODGINS, I. OPPENHEIM, and A. WITKIN. *Creating Models of Truss Structures with Optimization*,. 295-301, (n.d.).
- SOLIDWORKS. *3D mechanical CAD Student Edition 2017/18*. 1995-2017 Dassaul Systèmes, n.d.
- SZLENDAK, J.K., and P.L. OPONOWICZ. *Experimental Tests and Numerical Models of Double Side Non-Welded T RHS Truss Joints*. 11th International Conference on Modern Building Materials, Structures and Techniques (MBMST), 1109-1120, 2013.
- VALLOUREC. "MSH - Structural Hollow Sections." 2011. [http://www.vallourec.com/constructionsolutions/EN/E-Library/Publications/Lists/Publications/V\\_D01B0008B-GB.pdf](http://www.vallourec.com/constructionsolutions/EN/E-Library/Publications/Lists/Publications/V_D01B0008B-GB.pdf).
- WARDENIER, J. *Construction with Hollow Steel Sections*. Comité International pour le Développement et l'Etude de la Construction Tubulaire (CIDECT), 2000.
- ZANON, G., S. RASO, O. BURSI, M. D'INCAU, and N. TONDINI. *Laser cutting performance for structural steel*. Naples, Italy: Eurosteel 2014, 2014.
- ZHU, L., Q. SONG, Y. BAI, Y. WEI, and L. MA. *Capacity of steel CHS T-Joints strengthened with external stiffeners under axial compression*. Thin-walled Structures 113, 39-46, 2017.

## A. Appendix

Table A.1: Design of axial resistance of welded joints between CHS brace members and CHS chords (EN1993-1-8 2005).

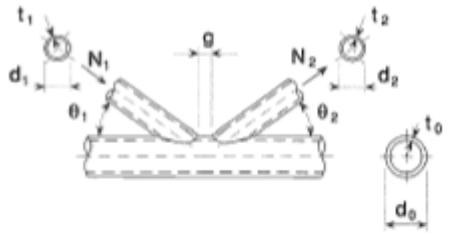
Chord face failure - K and N gap or overlap joints	
	$N_{1,Rd} = \frac{k_g k_p f_{t0} t_0^2}{\sin \theta_1} \left( 1,8 + 10,2 \frac{d_1}{d_0} \right) / \gamma_{M5}$ $N_{2,Rd} = \frac{\sin \theta_1}{\sin \theta_2} N_{1,Rd}$
<b>AC2</b> Punching shear failure for K, N and KT gap joints and T, Y and X joints <span style="float: right;">[i = 1, 2 or 3] <b>AC2</b></span>	
When $d_i \leq d_0 - 2t_0$ : $N_{i,Rd} = \frac{f_{t0}}{\sqrt{3}} t_0 \pi d_i \frac{1 + \sin \theta_i}{2 \sin^2 \theta_i} / \gamma_{M5}$	
Factors $k_g$ and $k_p$	
$k_g = \gamma^{0,2} \left( 1 + \frac{0,024 \gamma^{1,2}}{1 + \exp(0,5g/t_0 - 1,33)} \right)$ <span style="float: right;">(see Figure 7.6)</span>	
For $n_p > 0$ (compression): $k_p = 1 - 0,3 n_p (1 + n_p)$ but $k_p \leq 1,0$ For $n_p \leq 0$ (tension): $k_p = 1,0$	

Table A.2: Range of validity for welded joints between CHS brace members and CHS chords (EN1993-1-8 2005, 108).

Diameter ratio		$0,2 \leq d_i/d_0 \leq 1,0$
Chords	tension	$10 \leq d_0/t_0 \leq 50$ (generally), but:
	compression	Class 1 or 2 and $10 \leq d_0/t_0 \leq 50$ (generally), but:
Braces	tension	$d_i/t_i \leq 50$
	compression	Class 1 or 2
Overlap		$25\% \leq \lambda_{ov} \leq \lambda_{ov,lim}$ , see 7.1.2 (6)
Gap		$g \geq t_1 + t_2$

Table A.3: Description of numerical tests performed for CHS and Open section profiles.

Test N°	Truss Type	Section Type	Joint Name
1	I	CHS	Traditional
2	I	CHS	New_1
3	I	CHS	New_3
4	I	OPEN	Traditional
5	I	OPEN	New
6	II	CHS	Traditional
7	II	CHS	New_1
8	II	CHS	New_3
9	II	OPEN	Traditional
10	II	OPEN	New

Table A.4: Truss type I – profile dimensions and number of tests.

Truss Type I					
Profile type		Section type (mm)	Length/ truss (m)	n° tests	Total length (m)
<b>CHS</b>	Chord	88,9 x 6,3	5	3	15
	Vertical web	42,4 x 3,2	1,2		3,6
	Diagonal web	42,4 x 3,2	3,6		10,8
<b>OPEN</b>	Chord	HEA 100	5	2	10
	Vertical web	L 40 x 40 x 5	2,4		4,8
	Diagonal web	L 40 x 40 x 5	7,2		14,4

Table A.5: Truss type II - profile dimensions and number of tests.

Truss Type II					
Profile type		Section type (mm)	Length/ truss (m)	n° tests	Total length (m)
<b>CHS</b>	Chord	88,9 x 6,3	5	3	15
	Web 1	48,3 x 3,6	1,2		3,6
	Web 2	60,3 x 4,0	1,2		3,6
	Web 3	42,4 x 3,2	1,2		3,6
<b>Open section</b>	Chord	HEA 100	5	2	10
	Web 1	L 40 x 40 x 6	2,4		4,8
	Web 2	L 60 x 40 x 6	2,4		4,8
	Web 3	L 40 x 40 x 5	2,4		4,8



Table A.6: Failure modes for joints between CHS members (EN1993-1-8 2005).

Mode	Axial loading	Bending moment
a		
b		
c		
d		
e		
f		

Table A.7: Geometrical properties of OPEN section profiles.

	L section properties			2*L section properties			┴ section properties		
	$I_{xx}$ (cm <sup>4</sup> )	$I_{yy}$ (cm <sup>4</sup> )	A (cm <sup>2</sup> )	$I_{xx}$ (cm <sup>4</sup> )	$I_{yy}$ (cm <sup>4</sup> )	A (cm <sup>2</sup> )	$I_{xx}$ (cm <sup>4</sup> )	$I_{yy}$ (cm <sup>4</sup> )	A (cm <sup>2</sup> )
L 40x40x5	5,56	5,56	3,75	11,12	26,52	7,50	10,94	25,63	6,35
L 40x40x6	6,45	6,45	4,44	12,90	32,06	8,88	13,60	30,80	7,62
L 40x60x6	20,35	7,28	5,64	40,71	32,84	11,28	41,60	34,20	9,00

Table A.8: Profiles dimensions adopted for each test on truss specimens design (the highlighted dimensions denote the sections that were changed from the previous test).

<b>CHS - Substructure Type I</b>					
Test:	initial	case 1	case 2	case 3	case 4
CHORD	88,9x6,3	88,9x6,3	88,9x6,3	88,9x6,3	-
VERTICAL	42,4x3,2	42,4x4,5	48,3x3,2	48,3x5,0	-
DIAGONAL	42,4x3,2	42,4x4,5	48,3x3,2	48,3x5,0	-
<b>OPEN - Substructure Type I</b>					
Test:	initial	case 1	case 2	case 3	case 4
CHORD	HEA 100	HEA 100	HEA 100	HEA 100	-
VERTICAL	L 40x40x5	L 40x40x5	L 40x40x4	L 40x40x4	-
DIAGONAL	L 40x40x5	L 40x40x6	L 40x40x5	L 40x40x6	-
<b>CHS - Substructure Type II</b>					
Test:	initial	case 1	case 2	case 3	case 4
CHORD	88,9x6,3	88,9x6,3	88,9x6,3	88,9x6,3	-
BAR 1	42,4x3,2	42,4x3,2	42,4x3,2	48,3x3,6	-
BAR 2	42,4x3,2	48,3x3,2	60,3x4,0	60,3x4,0	-
BAR 3	42,4x3,2	42,4x3,2	42,4x3,2	42,4x3,2	-
<b>Open section - Substructure Type II</b>					
Test:	initial	case 1	case 2	case 3	case 4
CHORD	HEA 100	HEA 100	HEA 100	HEA 100	HEA 100
BAR 1	L 40x40x5	L 40x40x5	L 40x40x5	L 40x40x5	L 40x40x6
BAR 2	L 40x40x5	L 30x60x5	L 40x60x5	L 40x60x6	L 40x60x6
BAR 3	L 40x40x5	L 40x40x5	L 40x40x5	L 40x40x5	L 40x40x5

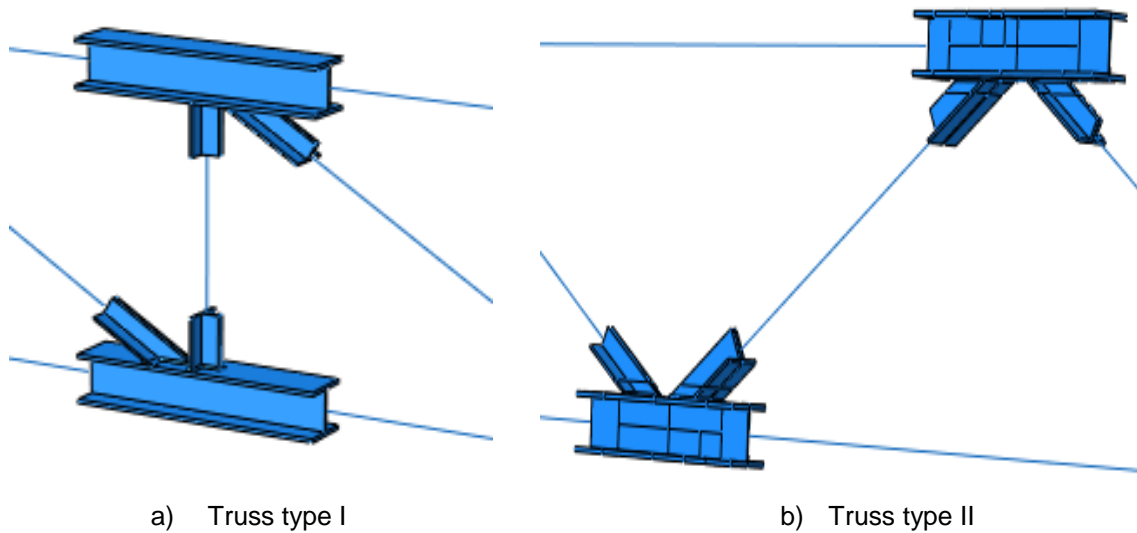


Figure A.1: Detail to understand the compatibility in the positioning of angle profiles.

In order to better understand the results obtained from the first analyses performed on truss type I, a comparison with an article found from research investigation in this field (ZHU, et al. 2017) is represented in Figure A.2.. The following model of a T-joint shows clearly how vertical brace compression induces plasticity in chord's face.

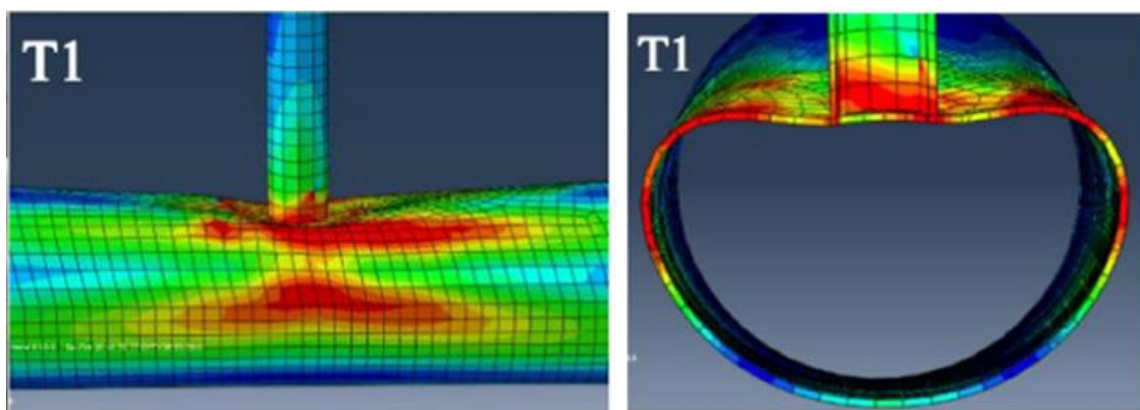
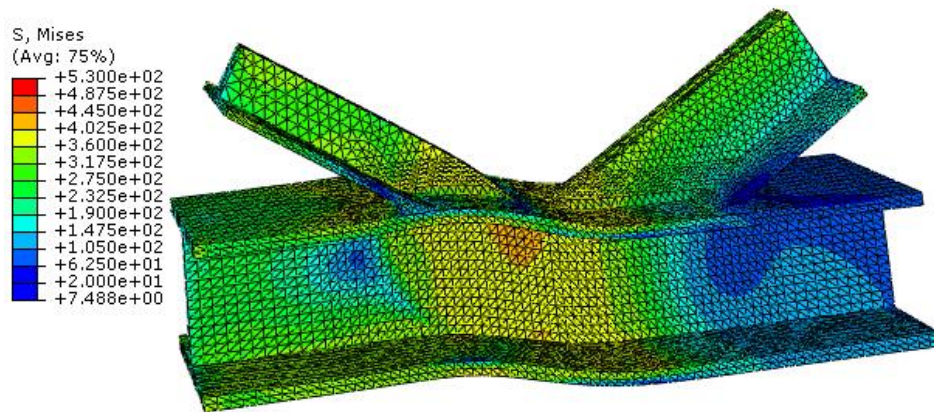
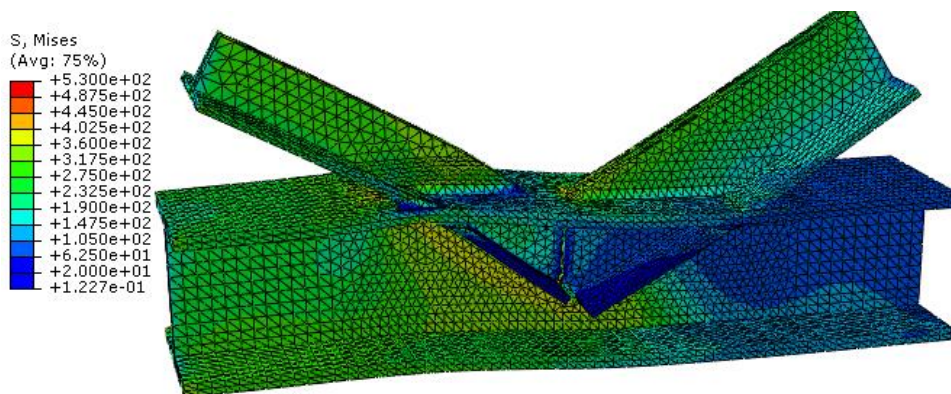


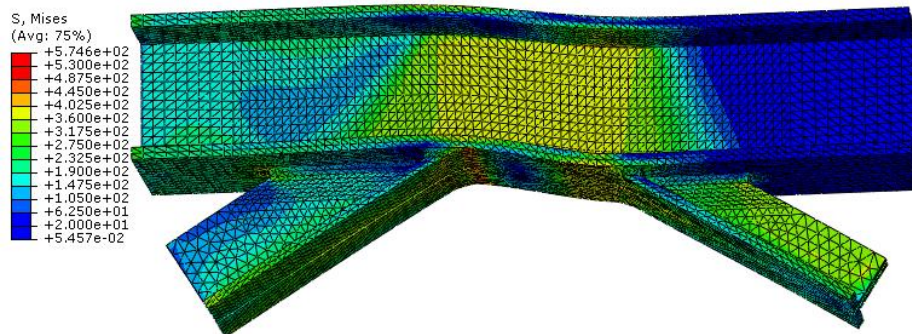
Figure A.2: Deformed shape of a CHS T-joint without external stiffeners.



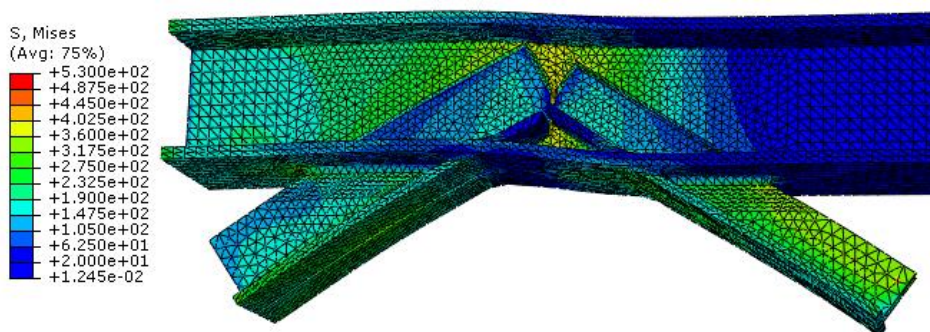
a) Traditional K-joint, connection A



b) New K-joint, connection A



c) Traditional K-joint, connection B



d) New K-joint, connection B.

Figure A.3: Von Mises stresses for OPEN section K-joints, truss type II (units in MPa).



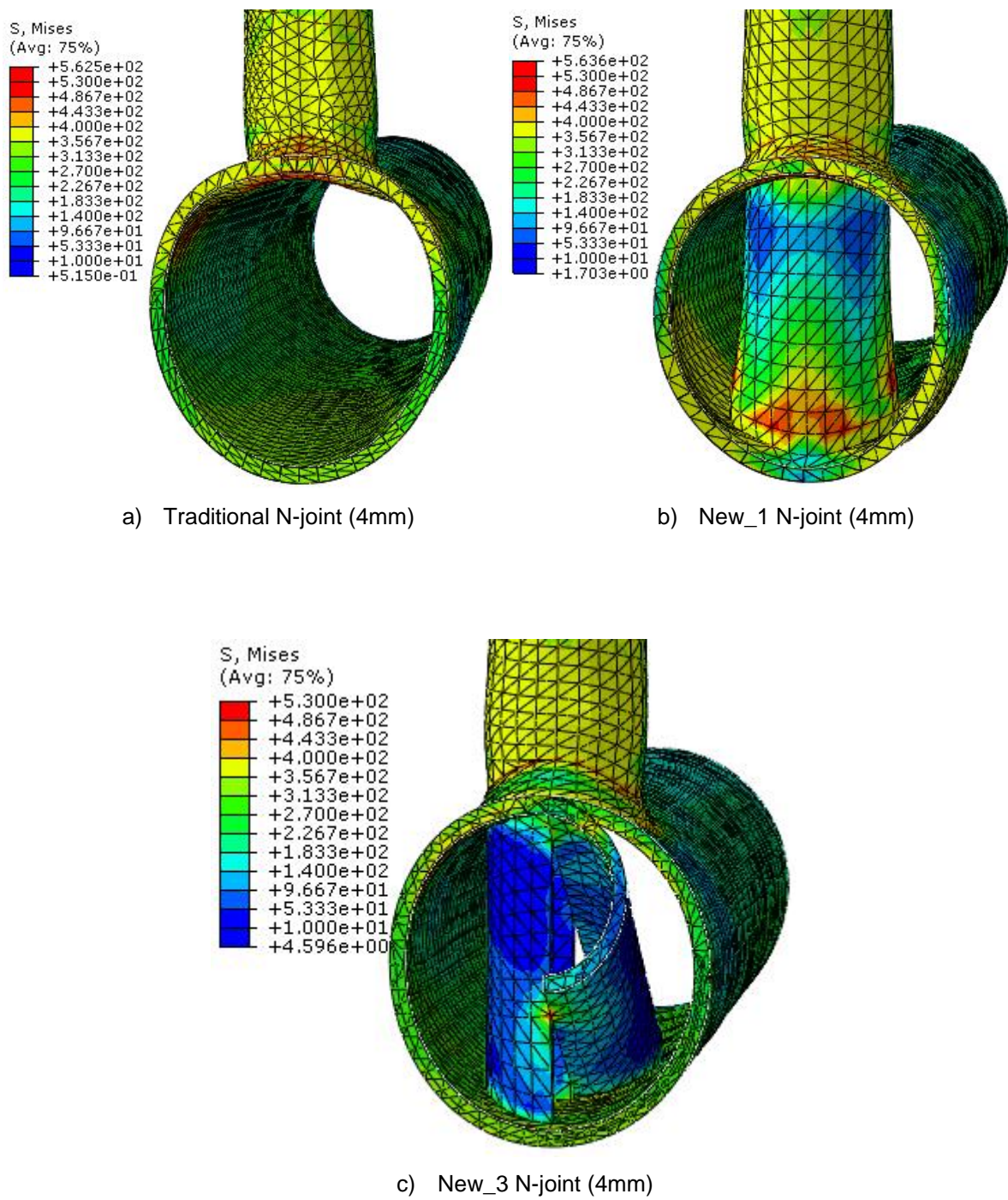
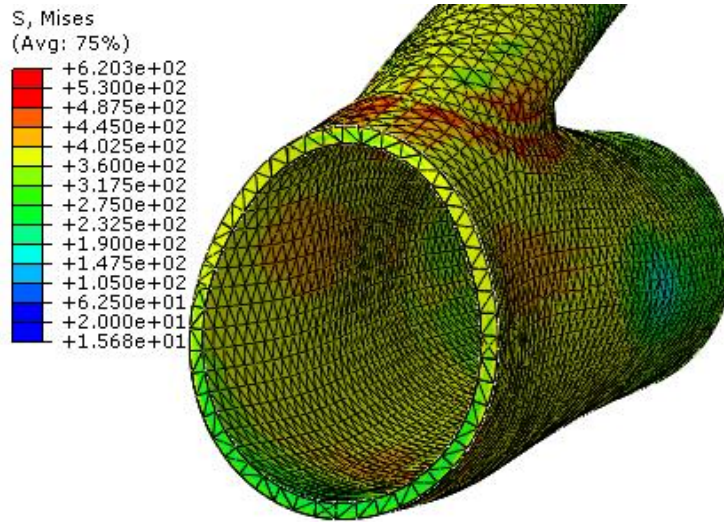
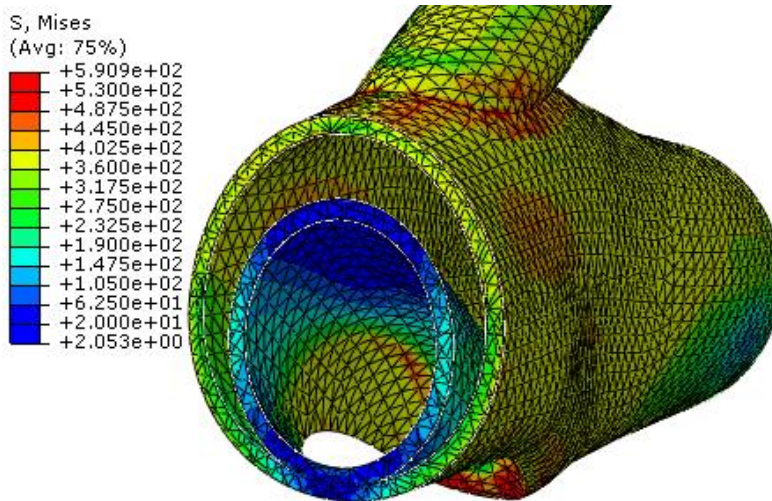


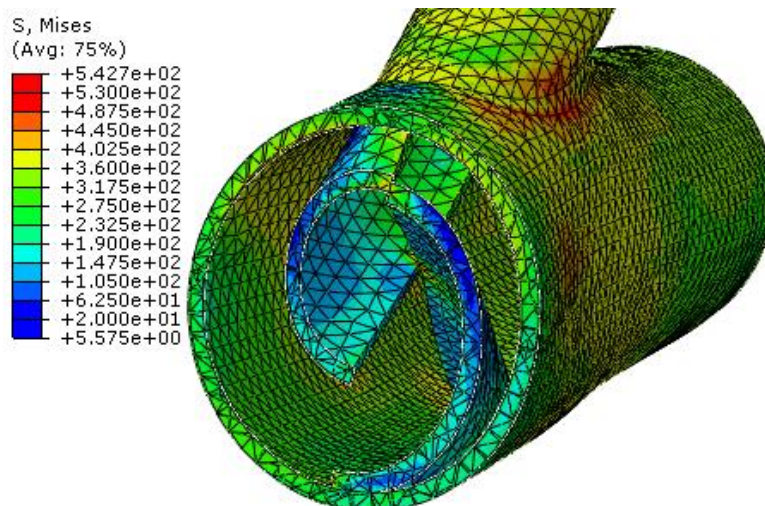
Figure A.4: Von Mises Stresses for CHS N-joints with 4mm chord thickness (region under the compression brace), truss type I (units in MPa).



a) Traditional K-joint A (4mm)



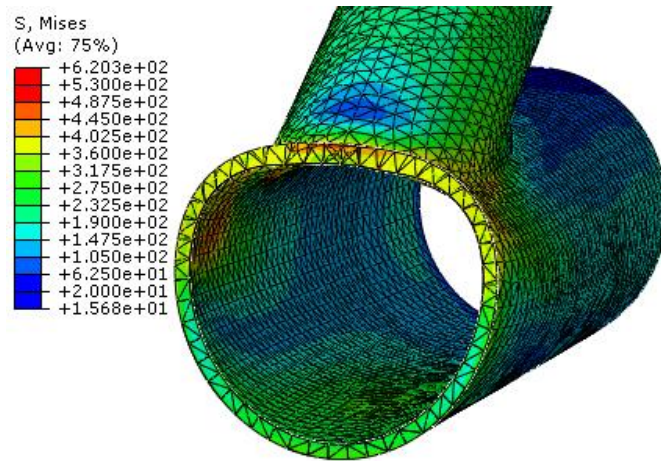
a) New\_1 K-joint A (4mm)



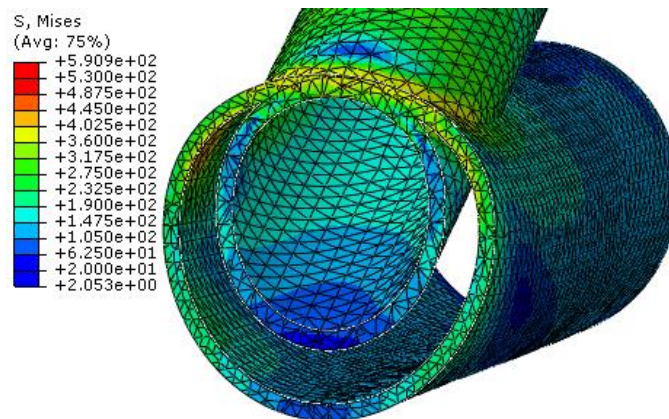
b) New\_3 K-joint A (4mm)

Figure A.5: Von Mises stresses for CHS K-joints with 4mm chord thickness (region under diagonal tension member), truss type II (units in MPa).

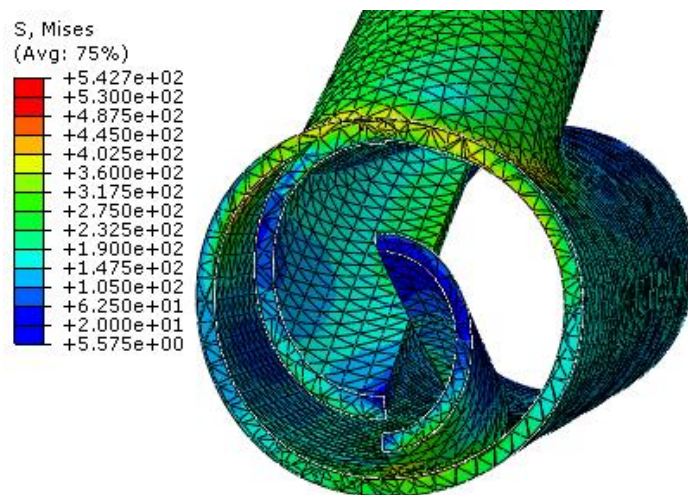




a) Traditional K-joint A (4mm)



b) New\_1 K-joint A (4mm)



c) New\_3 K-joint A (4mm)

Figure A.6: Von Mises Stresses for CHS K-joints with 4mm chord thickness (region under the compression brace), truss type II (units in MPa).